Dissertation

Characterization of Genomic Changes in Different Tumor Types by Array-CGH

submitted at the

Medical University of Graz

Institute of Human Genetics

by

DI$_{(FH)}$ Karin FLICKER

for the academic degree of

Doctor of Philosophy (Ph.D.)

under supervision of

Prof. Dr. Michael R. Speicher

Dezember 2012

The great tragedy of science is the slaying of a beautiful hypothesis by an ugly fact.

Thomas H Huxley

.

ACKNOWLEDGEMENTS

Though only my name will appear on the first page of this dissertation there are so many people I have to thank, all those people who made the dissertation possible and who were inspiring and supporting me throughout the last years.

My deepest gratitude goes to my supervisor Prof. Michael Speicher who gave me the opportunity to do my PhD. Many thanks for his support and guidance during the last years. Through him I got a deep insight into the field of science. His great knowledge about things fascinates me anew every day. I am especially thankful to him for his big support with the manuscript. He put a lot of work into the paper in order to get it published. I really appreciate it a lot. I also would like to thank him for his support with my dissertation.

A very special 'thank you' goes to Prof. Roswitha Pfragner. She was one of the initiators of my MTC project, and without her it would not have been possible to do the project. Many thanks for her help with the manuscript and for being a member of my thesis committee as well as my final committee. Thank you for all the discussions we had and especially for all the support throughout the last years.

I am also very grateful to Prof. Farid Moinfar and to Doz. Bernadette Liegl from the Pathology Graz for our collaboration.

I also would like to thank Prof. Ernst Malle, who was a member of my thesis committee, for critical discussions and for his time.

I do not want to let the opportunity slip to thank all the people at the Institute of Human Genetics. I owe my gratitude to everyone who helped me and gave me practical advice in the last years. I really liked working with all of you.

Many thanks are going to the 'office girls': the PhD girls Anna, Kristina, and Ivana and Eva, but also Christine and Martina. With some of you I was sharing my experiences from the first day the beginning in the last years. We all had many interesting, amusing, stimulating, and critical discussions, not only about science, but also about private things. It was not always easy to work in the office (I am sure you know what I mean),

nevertheless, I really enjoyed it. It was certainly a great time and I can be glad that I had so nice colleagues during my PhD. Special thanks are of course going to Anna. She helped me a lot, especially at the beginning of my PhD, but also later on. Many thanks for all the practical advice. It is hard to imagine how hard things would have been without her.

At last I have to thank my family, my parents and my partner Kurt who shared my joy and my frustration during the last years. Their belief in me was a big support throughout the years and without them things would have been much harder. I want to thank my parents for giving me the opportunity to experience such a good education and for supporting all the decisions I made. Many thanks go to my partner Kurt who always supported my decisions.

Thank you to everyone for inspiring my scientific as well as my personal life!

STATUTORY DECLARATION

I hereby declare that this thesis is my own original work and that I have fully acknowledged by name all of those individuals and organizations that have contributed to the research for this thesis. Due acknowledgement has been made in the text to all other material used. Throughout this thesis and in all related publications I followed the guidelines of “Good Scientific Practice”.

Date: ……. Signature: ……

TABLE OF CONTENTS

LIST OF FIGURES

LIST OF TABLES

SUMMARY

Copy number alterations are frequently seen in tumor genomes and they are considered as potentially important in tumor evolution. Copy number alterations also may act as a driving force for tumorigenesis and for tumor progression, moreover, an altered gene expression may determine the fate of a cell or the phenotype of an organism. This thesis provides information regarding copy number changes in three different tumor entities.

Part I of this dissertation describes the characterization of the MTC genome by array-CGH (comparative genomic hybridization) and M-FISH (multiplex fluorescent in situ hybridization). Hereditary and sporadic medullary thyroid carcinoma (MTC) are closely associated with *RET* proto-oncogene mutations. However, the role of additional changes in the tumor genomes remains unclear. The objective of the project was the identification of chromosomal regions involved in MTC tumorigenesis and to assess their significance by using MTC derived cell lines. Array-CGH was employed to map chromosomal imbalances in 52 primary tumors and 10 metastases. Furthermore, 5 MTC cell lines were characterized by M-FISH in detail and the tumorigenicity of three cell lines was evaluated by severe combined immunodeficiency (SCID)-mouse experiments. The MTC data suggest that - in contrast to most other tumor entities – this tumor entity does not acquire a multitude of genomic imbalances.

Part II of this dissertation describes copy number changes in uterine smooth muscle tumors as assessed by array-CGH. In section I array-CGH was employed to map copy number changes in 4 endometrial stromal nodules (ESN) cases, 22 endometrial stromal sarcomas (ESS) cases and 4 undifferentiated endometrial sarcomas (UES) cases. The results indicate a low number of copy number variations in ESN and a high number of gains and losses in ESS and UES. The number of aberrations directly correlates with their histological grading and clinical behavior. In section II 20 leiomyoma (LM) cases, 14 atypical leiomyoma (at-LM) and 13 leiomyosarcoma (LMS) were analyzed for their presence of gains and losses in their genome. The results show that LM harbor a low number of copy number variations followed by an increase in gains and losses in at-LM and LMS. Atypical LM and LMS share several copy number variations in their genome which may propose a similar genetic pathway involved in their evolvement.

ZUSAMMENFASSUNG

In Tumorgenomen wird häufig eine Änderung in der Kopienzahl beobachtet. Diese genomischen Aberrationen werden in der Tumorpathogenese als potentiell wichtig betrachtet. Kopienzahlveränderungen im Genom können die Genexpression beeinflussen und zelluläre Prozesse stören, beziehungsweise sogar Auswirkungen auf den Phänotyp eines gesamten Organismus haben. In dieser Dissertation werden Veränderungen in der Kopienzahl in drei verschiedenen Tumorentitäten beschrieben.

In **Teil I** wird das Medulläre Schilddrüsenkarzinom (MTC) mit Hilfe von Array-CGH (vergleichende genomische Hybridisierung) und M-FISH (Multiplex-Fluoreszenz in situ Hybridisierung) behandelt. Hereditäre und sporadische MTC stehen eng im Zusammenhang mit Mutationen im *RET* Proto-Onkogen, jedoch bleibt die Rolle von zusätzlichen Veränderungen im Tumorgenom unklar. Das Ziel dieses Projektes war es, bestimmte chromosomale Regionen im MTC Genom zu identifizieren und deren pathogenetischen Stellenwert mit Hilfe von MTC stammenden Zelllinien zu beurteilen. Array-CGH wurde angewandt, um in insgesamt 52 Primärtumoren und 10 Metastasen Kopienzahlveränderungen darzustellen. Des Weiteren wurden 5 MTC-Zelllinien mit Hilfe von M-FISH charakterisiert. Die tumorigene Eigenschaft von 3 Zelllinien wurde in SCID-Maus-Experimenten (schwerer kombinierter Immundefekt) getestet. Die MTC Daten indizieren, dass im Gegenteil zu vielen anderen Tumorentitäten, diese Tumorentität keine Vielzahl von genomischen Ungleichgewichten aufweist.

In **Teil II** dieser Dissertation werden Kopienzahlveränderungen in Uterustumoren mit Hilfe von array-CGH beschrieben. Im Abschnitt I wurde array-CGH bei 4 endometrialen Knoten (ESN), 22 Stromasarkomen (ESS) und 4 undifferenzierten endometrialen Sarkomen (UES) angewandt. Die Ergebnisse zeigen eine kleine Anzahl von Aberrationen in ESN gefolgt von einer hohen Anzahl von Gewinnen und Verlusten in UES und ESS. Die Anzahl der auftretenden Aberrationen steht in Proportionalität zu der pathologisch-histologischen Einteilung der Malignität der Tumoren sowie dem Schweregrad des klinischen Verlaufs. Im Abschnitt II wurden 20 Leiomyome (LM), 14 atypische Leiomyome (at-LM) und 13 Leiomyosarkome (LMS) auf genomische Aberrationen untersucht. Die Ergebnisse zeigen, dass LM die geringste Anzahl von Veränderungen aufweisen, gefolgt von einem Anstieg genomischer Veränderungen in at-LM und LMS.

Atypische LM und LMS zeigen einige gleiche Veränderungen, wodurch ein ähnlicher genetischer Signalweg in deren Pathogenese vorschlagen werden könnte.

LIST OF ABBREVIATIONS

°C	Grad Celsius
µg	microgram
array-CGH	comparative genomic hybridization
at-LM	atypical leiomyoma
CGH	comparative genomic hybridization
CNC	copy number change(s)
CNV	copy number variation
DNA	deoxyribonucleic acid
ESN	endometrial stromal nodule
ESS	endometrial stromal sarcoma
FMTC	familial medullary thyroid carcinoma
hMTC	hereditary medullary thyroid carcinoma
hpf	high power field
Hyst	hysterectomy
LM	leiomyoma
LMS	leimyosarcoma
MEN2-A, B	multiple endocrine neoplasia type 2A, B
M-FISH	multiplex-fluorescent in situ hybridization
MTC	medullary thyroid carcinoma
Myomct	myomectomy
NF-H_2O	nuclease free water
ng	nanogram
PCR	polymerase chain reaction
RET	rearranged during transfection proto-oncogene
RT	room temperature
sMTC	sporadic medullary thyroid carcinoma
t(7;17)	translocation between chromosomes 7 and 17
UES	undifferentiated endometrial stromal sarcoma
unk	unknown

Part I:

HIGH-RESOLUTION ANALYSIS OF ALTERATIONS IN MEDULLARY THYROID CARCINOMA GENOMES

1. HIGH-RESOLUTION ANALYSIS OF ALTERATIONS IN MEDULLARY THYROID CARCINOMA GENOMES

Karin Flicker[1], Peter Ulz[1], Harald Höger[2], Petra Zeitlhofer[3], Oskar A. Haas[3], Annemarie Behmel[1], Wolfgang Buchinger[4], Christian Scheuba[5], Bruno Niederle[5], Roswitha Pfragner[6], Michael R. Speicher[1]

[1]Institute of Human Genetics, Medical University of Graz, 8010 Graz, Austria

[2]Department of Laboratory Animal Science and Genetics, Medical University of Vienna, 2325 Himberg, Austria

[3]medgen.at GmbH, 1150 Vienna, Austria

[4]Department of Internal Medicine, Hospital Barmherzige Brüder Eggenberg, 8020 Graz, Austria

[5]Section of Endocrine Surgery, Division of General Surgery, Department of Surgery, Medical University of Vienna, 1090 Vienna, Austria

[6]Institute of Pathophysiology and Immunology, Medical University of Graz, 8010 Graz, Austria

This paper was published in the International Journal of Cancer.

1.1. ABSTRACT

Hereditary and sporadic medullary thyroid carcinoma (MTC) are closely associated with *RET* proto-oncogene mutations. However, the role of additional changes in the tumor genomes remains unclear. Our objective was the identification of chromosomal regions involved in MTC tumorigenesis and to assess their significance by using MTC derived cell lines. We employed array-CGH (comparative genomic hybridization) to map chromosomal imbalances in 52 primary tumors and 10 metastases. Eleven tumors (11/52, 21%) were hereditary and 41 (41/52; 79%) were sporadic. Among the latter, 15 tumors (15/41, 37%) harbored *RET* mutations. Furthermore, we characterized 5 MTC cell lines in detail and evaluated the tumorigenicity of three cell lines by severe combined immunodeficiency (SCID)-mouse experiments. Most MTCs had only few copy number changes and losses of chromosomes 1p, 4q, 19p, and 22q were observed most frequently. The number of chromosomal aberrations increased in metastases. Twenty-three percent (12/52) of the primary tumors did not even show any chromosomal gains and losses. We injected three cell lines (two of these were without chromosomal changes and pathogenic *RET* mutations) into immune deficient SCID mice and in each case we observed rapid tumor growth at the injection sites. Our data suggest that MTCs - in contrast to most other tumor entities - do not acquire a multitude of genomic imbalances. SCID mouse experiments performed with chromosomally normal cell lines and without *RET* mutations suggest that presently unknown submicroscopic genomic changes are sufficient in MTC tumorigenesis.

1.2. INTRODUCTION

1.2.1. General background thyroid cancer

The genetic changes leading to thyroid cancer are poorly characterized. The great majority of all thyroid cancers are either papillary, follicular, or anaplastic carcinomas, which are thought to be derived from follicular cells. Only 5% to 10% are medullary thyroid carcinomas which originate from the C-cells (Hemmer *et al.*, 1999). This histopathological classification of thyroid carcinomas into four major subtypes has been considered as established, and each of the four entities have typical clinical features.

1.2.2. Clinical background of medullary thyroid carcinoma

Human medullary thyroid carcinoma (MTC) is a calcitonin-producing tumor originating from the parafollicular C-cells of the thyroid. It constitutes about 5-8% of all thyroid cancers and may occur sporadic (70–80% of cases) or hereditary (20-30%) (Schlumberger *et al.*, 2008). Hereditary MTC is inherited in an autosomal-dominant pattern, either as familial MTC (FMTC) without other endocrinopathies, or as part of multiple endocrine neoplasia syndrome type 2A (MEN-2A), or in multiple endocrine neoplasia type 2B (MEN-2B) (Ponder, 1999).

As the disease may develop over many years without clinical signs, lymph node metastasis are documented in more than 50% of patients and distant metastasis are found in at least in one quarter of patients at the time of diagnosis. With 5- and 10-year survival reported at 86% and 78%, respectively, prognosis is less favorable than for differentiated thyroid cancer. Patients with distant metastases have only a 35% survival after 5 years. MTC, both in patients and in preclinical models, is resistant to chemotherapy and radiation therapy. Surgical removal of all malignant tissue is the only potentially curative treatment in localized disease (Schlumberger *et al.*, 2008). Management guidelines for treatment of MTC were recently published by the American Thyroid Association (American Thyroid Association Guidelines Task Force *et al.*, 2009).

1.2.3. RET proto-oncogene

MTC is closely associated with mutations in the *REarranged during Transfection* (*RET*) proto-oncogene in chromosome 10q11.2. The *RET* gene has 21 exons. It encodes a membrane tyrosine kinase receptor. This membrane associated receptor is composed of an extracellular domain with a distal cadherin-like region and a cystein-rich region just outside the membrane, a single transmembrane region and an intracellular tyrosine kinase domain (Manie *et al.*, 2001). RET is an example how different mutations of a single gene can lead to different neoplastic phenotypes: Specific mutations have been identified for each of the MTC variants and mutations analysis is used in diagnosis and management of MEN2-patients and their families (Figure 1). As a consequence there is a close relationship between the genotype and phenotype (Eng *et al.*, 1996, Santarpia *et al.*, 2009). The hereditary variants MEN-2/FMTC are associated with activating germline point mutations in the *RET* proto-oncogene and nearly 100% of carriers develop MTC (Hofstra *et al.*, 1994, Mulligan *et al.*, 1993, Santoro *et al.*, 1995). In addition, *RET* mutations are also found in roughly 50% of sporadic tumors.

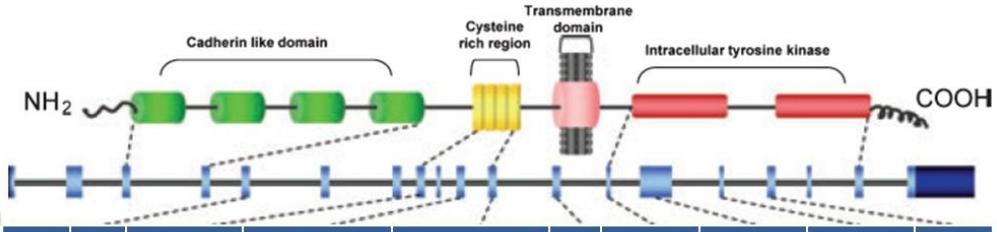

	Exon5	Exon8	Exon10	Exon11	Exon12	Exon13	Exon14	Exon15	Exon16
MEN2A		G533C	C609G/R/S/Y/W/F 611G/F/R/S/Y C618G/F/R/S/Y C620G/F/R/S/W/Y	C630F/S/Y/R C634F/G/R/S/W/Y/T/A E632D/L633V/C634R S649L		L790F			
MEN2B							V804M E805K Y806C	A883F/T S904C	M918T
FMTC	G321R	C515S G533C Dupl E529-C531	D603N Y606C C509G/R/S/Y/W/F 611G/F/R/S/Y C618G/F/R/S/Y C620G/F/R/S/W/Y	C634F/G/R/S/W/Y/T/A S649L		E768D N777S L790F Y791F V778I/V804M	V804L/M E819K R844L/Q	A876V A883F/T R886W S891A	R912P
sMTC			V591I Dupl G592-G507 K603N C609G/R/S/Y/W 611G/F/R/S/Y del F612-C620 C618G/F/R/S/Y C620G/F/R/S/W/Y	D631G C634F/G/R/S/W/Y/T/A del L629-D631 del D631-L633 del E632-C634 del C630-D631 del E632-L633 E632S (del L633-R635) T636S del E632-A640/ins VRP A639G/A641R	G748C	P766S E768D	R833C	A883F/T E884K delD898-E902	G911D M918T E921K S922F/P T930M

Figure 1. Schematic representation of the RET tyrosine kinase receptor. Nearly all mutations (intra-extracellular and transmembrane domains) which are described for MTC are summarized (modified after **(Santarpia *et al.*, 2009)**).

1.2.3.1. SNPs of the RET proto-oncogene

Several single nucleotide polymorphisms (SNPs) of the RET proto-oncogene have been described in the general population as well as for other endocrine tumours. The direct association of single SNPs in the RET gene and predisposition or modifying roles in the pathogenesis of MTC are not known yet. Exonic RET SNPs have been more extensively studied than intronic RET SNPs, however, data are still controversial for both (Baumgartner-Parzer *et al.*, 2005).

It is still a matter of debate to which extent neutral sequence variants (polymorphisms) could have interacting, predisposing, or modifying roles in the pathogenesis of MEN2 or sporadic MEN2-related tumors. The use of a detected somatic mutation as a marker of prognosis has been questioned. Its value has been debated with inconclusive results in different studies, some studies have shown a significant difference in the clinical outcome of sporadic MTC based (Frisk *et al.*, 2001, Romei *et al.*, 1996, Zedenius *et al.*, 1994, Dvorakova *et al.*, 2008).

RET			
IVIS1-126 c>a (rs2565206)[f]	60	240	63
A45A g>a (rs1800858)	77	268	45
A432A g>a (rs1800860)	75	256	39
G691S g>a (rs1799939)[h]	63	360	49
L769L t>g (rs1800861)	76	302	39
S836S g>a (rs1800862)[i]	114	481	11
S904S g>c (rs1800863)[h]	66	359	51
IVS19+47 c>t (rs2075912)	94	354	34
STOP+95bp a>g (rs2075914)[j]	78	304	44
STOP+388bp g>a (rs3026782)[j]	66	357	49

Figure 2. Overview of the reported SNPs in the RET proto-oncogene. The table summarises the exonic as well as intronic RET SNPs. The 4 exonic SNPs in the red frame are occuring most often and have been investigated in most studies. A45A and A432A are less often occuring RET SNPs. Table modified after **(Cebrian *et al.*, 2005)**.

No other genes have been consistently implicated yet in MTC tumorigenesis, however, components of the *RB1* and *TP53* tumor suppressor pathways have been discussed to possibly contribute to MTC formation (Cerrato *et al.*, 2009).

1.2.4. Cytogenetics

The cytogenetics of MTC has been studied sparsely, because the cells are difficult to grow in culture (Herrmann, 2003). At present the Mitelman database has 327 karyotypes of cases with thyroid cancer (http://cgap.nci.nih.gov/Chromosomes/Mitelman) (Status: Oct 06, 2010). However, none of these cases relate to MTC. The few published cases have not identified recurrent structural rearrangements yet (Wurster-Hill *et al.*, 1986, Scappaticci *et al.*, 1992). MTC has also not been extensively analyzed by comparative genomic hybridization (CGH). Older studies employing chromosome CGH with a poor resolution described alterations involving chromosomes 1p, 3q, 3p, 4, 9q13-22, 11c-q12, 13q, 19, and 22q(Hemmer *et al.*, 1999, Frisk *et al.*, 2001, Marsh *et al.*, 2003). A more recent study used array-CGH and found frequent allelic loss in 7q36.1, 12p13.31, 13q12.11, and 19p13.3-11 (Ye *et al.*, 2008).

Thus, 25 years after identification of the role of *RET* mutations and their association with MTC, no other genetic lesion has been consistently associated with MTC formation. Therefore, the aim of this study was a more detailed analysis of MTC-genomes by array-based approaches of primary tumors, their respective metastases, and MTC-derived cell lines. In addition, the tumorigenicity of the MTC cell lines with various genomic changes was tested.

1.3. MATERIALS AND METHODS

1.3.1. Patient and tumor samples

All MTCs were examined immunohistochemically for calcitonin, carcinoembryonic antigen, and neuroendocrine markers (chromogranin A, synaptophysin). One part of the tumor tissue was cultivated to generate cell lines; the other part was stored in liquid nitrogen and used for our analyses. The study was approved by the ethical committee of the Medical University of Graz (# 18-182 ex 06/07). Written informed consent was obtained from all patients. The patients were treated and material was kindly provided by B. Niederle, C. Scheuba (Section of Endocrine Surgery, Division of General Surgery, Department of Surgery, Medical University Vienna; n=49), R. Roka and N. Neuhold (Department of Surgery and Department of Pathology, Kaiserin Elisabeth Spital, Vienna; n=3), D. Depisch (Department of Surgery, General Hospital, Wr. Neustadt; n=3), W. Buchinger (Division of Nuclear Medicine, Hospital Barmherzige Brüder, Graz; n=3), G. Wolf (Division of General Surgery, Department of Surgery, Medical University Graz; n=2), W. Pimpl (Department of Surgery, Hospital Bad Aussee; n=1), H-J. Böhmig (Department of Surgery, Hospital Elisabethinen, Linz; n=1).

1.3.2. DNA extraction

DNA was extracted after proteinase K (#19133, Qiagen, Hilden, Germany) digestion employing conventional phenol chloroform extraction (according to standard protocols). In brief, digestion was performed in a thermo mixer at 56°C, shaking at ~600 rpm until the tissue was completely lysed. Afterwards an RNA digestion step was performed by addition of 5µl RNAse A (100mg/ml; #19101, Qiagen, Hilden, Germany) for 2-5 min at 37°C. DNA extraction was performed by adding one volume of phenol/chloroform/isoamylalcohol (#A156, Lactan, Austria) and one volume chloroform/isoamylalcohol 24:1 (#X984, Lactan, Austria) to the DNA. To precipitate the DNA 4M NaCl and 100% ethanol was added and centrifugation was performed for 10 min at full speed. The DNA was washed with 70% ethanol and after drying the pellet the DNA was dissolved in nuclease free water (NF-H_2O).

For tumors with a diameter less than ~3 mm the QIAamp DNA Micro Kit (#56304, Qiagen, Hilden, Germany) was used according to the manufacturer's protocol 'Isolation of

genomic DNA from tissue'. Proteinase K digestion was performed in a thermo mixer at 56°C shaking at ~600 rpm until the tissue was completely lysed. RNA digestion was performed by adding 4µl RNAse A (100mg/ml; #19101, Qiagen, Hilden, Germany) to the DNA for 2 min at RT. DNA was eluted in NF-H_2O.

1.3.2.1. Evaluation of DNA quality

DNA quantity and quality was assessed by a Nanodrop measurement (Peqlab, Polling, Austria) and by a multiplex PCR approach (van Beers *et al.*, 2006). A 1.5% agarose gel (#840004, Biozyme, Vienna, Austria) was run at 130V for 40 min to evaluate the multiplex PCR.

Table 1. Pipetting scheme for the multiplex PCR mix.

Reagent	Volume [µl]
Hotstar Polymerase Mix (#203445, Qiagen, Germany)	6
Primermix [100 mM]	0.5
NF-H_2O	4.5
DNA Template	1.0

Table 2. Primers used for Multiplex PCR. The respective primer pair with size and sequence is summarized in the table.

Pair	Size of Primer [bp]	Primer Sequence 5'-3'
1	100	F: gtt cca ata tga ttc cac cc R: ctc ctg gaa gat ggt gat gg
2	200	F: agg tgg agc gag gct agc R: ttt tgc ggt gga aat gtc ct
3	300	F: agg tga gac att ctt gct gg R: tcc act aac cag tca gcg tc
4	400	F aca gtc cat gcc atc act gc R: gct tga caa agt ggt cgt tg

Table 3. Program used for Multiplex PCR.

Step	Temperature [°C]	Time [min]
1	95	15
2	94	1
3	56	1
4	72	1'30
5	go to 2 for 34 cycles	
6	72	7
7	8	forever

1.3.3. RET mutations status

The *RET* proto-oncogene consists in total of 21 exons. For both familial and sporadic cases we sequenced exons 10, 11, 13, 14, 15, 16, for familial cases additionally exon 8 was sequenced. Mutation screening for all relevant exons was carried out using high resolution melting (HRM) real-time PCR. Sequencing was carried out at the Institute of Human Genetics, Medical University of Graz, by Karin Flicker and Peter Ulz and at medgen.at Gmbh, Vienna, by Petra Zeitlhofer and Oskar Haas. RET sequencing data on peripheral blood were kindly provided by Oskar Haas, medgen.at GmbH, Vienna.

Table 4. Primers used for Sequencing at the Institute of Human Genetics. The primers were M13 tagged to be able to use the same primers for the PCR and the sequencing reaction.

RET Exon	Primer Sequence
Exon 8	F: gtgctgttccctgtccttg R: ctatgctggcatcgagagc
Exon 9	F: gatctgcctaggaggtggtg R: actctggctgaagtgcctgt
Exon 10	F: tatgcttgcgacaccagttg R: gagggagggaagtttcatgg
Exon 11	F:gcatacgcagcctgtaccc R: cacaggatggcctctgtctc
Exon 13	F: ctgacctggtatggtcatgg R: agggagaacagggctgtatg
Exon 14	F: gtccacccccttactcattg R: atggtgggctagagtgtgg
Exon 15	F: ctggtcacaccaggctgag R: tcggtatctttcctaggcttcc

RET Exon	Primer Sequence
Exon 16	F: gagtgtctacagcactcctctgg R: aattccctggccaagctg

Table 5. Primers used for *RET* sequencing medgen.at GmbH.

RET Sequencing Primer	Primer Sequence 5'-3'
Exon 5	F: tggttttgggggtctg R: aggtgtgcatgtgtgtaggg
Exon 8	F: ctgtccttgggcactagctgga R: ggctgatgcagacaatgagtcc
Exon 10	F: gcgccccaggaggctgagtg R: ggtggtggtcccggccgcc
Exon 11	F: ccagtggtgccgagcctct R: ctggcctccctccctggaa
Exon 13	F: gcaggcctctctgtctgaactt R: ggagaacagggctgtatgga
Exon 14	F: gcagagagcaagtggttcaag R: gtggtgggtcagggtgtgg
Exon 15	F: gactcgtgctatttttcctc R: atggtgcacctgggatc
Exon 16	F: agggatagggcctggccttc R: taacctccaccccaagagag

Table 6. Primers used for HRM *RET* analysis at medgen.at GmbH.

HRM Primer	5'-3'
Exon 5	F: actgaccaacgccctctg R: cccatgaagagcgagcac
Exon 8	F: tgtgaccctgcttgtctgc R: ggcgtttccagggcttac
Exon 10	F: caggaggctgagtgggctac R: tgggaggtggtggtggtc
Exon 11	F: ccagtggtgccgagcctct R: ctggcctccctccctggaa
SNP K691S im Exon 11	F: gctgagatgaccttccggag R: catccacggagacctggttc
Exon 13	F: atcgtttgcaacctgctctg R: ccctgcagctggccttac
SNP L769L im Exon 13	F: atcgtttgcaacctgctctg R: gttgaactctgacagcaggtctc
Exon 14	F: agggccccctctctcc R: tgcagagccatatgcacg

HRM Primer	5'-3'
SNP S836S im Exon 14	F: tgggcagtggaggcag R: tcatccgggtggtccag
Exon 15	F: gactcgtgctatttttcctc R: atggtgcacctgggatc
SNP S904S im Exon 15	F: cggcttgtcccgagatg R: gactgggcacctggctc
Exon 16	F: agggatagggcctggccttc R: agagcaacacccacacttacac

1.3.4. Array-comparative genomic hybridization (array-CGH)

We used 44k and 60k arrays from Agilent Technologies. Samples were labeled with the Bioprime Array-CGH Genomic Labeling System (#18095-12, Invitrogen, Carlsberg, CA) according to the manufacturer's instructions. In brief, 500 ng test DNA and reference DNA (#G147A and #G152A, Promega, Germany) were differentially labeled with dCTP-Cy5 or dCTP-Cy3 (#PA53021 and #PA55021, GE Healthcare, Piscataway, NJ). Slides were scanned using a microarray scanner (#G2505B; Agilent Technologies, Santa Clara, CA). Data normalization and calculation of ratio values were conducted employing Feature Extraction software from Agilent Technologies. Data analysis was performed using the software Genomic Workbench 5.0.14 (statistical algorithm: ADM-2; aberration threshold: 8.0; moving average window: 2MB; Fuzzy zero: off; consecutive clone filter: 10) from Agilent Technologies. Log ratios higher/lower 0.22 were considered as copy number change.

1.3.5. Cell culture

We established several continuous MTC cell lines with the designations BOJO, HEVE-II, SHER-I, SINJ, and OEE-III (Table 1). Some of the cell lines together with the respective cultivation methods have been published previously (Pfragner *et al.*, 1990, Pfragner *et al.*, 1993, Pfragner *et al.*, 2002, Pfragner *et al.*, 2004). The cell lines were provided and cell culture was performed by Roswitha Pfragner, Institute of Pathophysiology and Immunology, Medical University of Graz.

1.3.6. Preparation of metaphase spreads

To arrest cells at metaphase, 10 µl colcemid [10 µg/ml; #J01-003, PAA Laboratories, Austria] were added per 1 ml medium. The colcemid incubation time was adjusted to the growth characteristics of each cell line, ranging from 3 h to 8 h. The hypotonic treatment was conducted with pre-warmed 0.8% Sodium Citrate (#1.06448.0500, Merck, Darmstadt, Germany) at 37°C for 20 min. Cells were fixed three times with fixative (acetic acid:methanol, ratio 3:1).

1.3.7. Multiplex-FISH (M-FISH)

M-FISH was performed according to a previously published protocol (Geigl *et al.*, 2006). A commercially available M-FISH Probe (#33-100099, Abbot/Vysis, Germany) was used. Briefly, pepsin digestion was carried out for ~3 -10 seconds in a 1 M HCl solution at 37°C. Denaturation was performed in 70% formamide/2x SSC at 70°C for 1 min 30 sec. The M-FISH probe was denatured at 78°C for 7 min and pre-annealed at 42°C for 20 min. Hybridization was carried out in a dark, moist chamber at 37°C for 48 h. Images were taken with a Leica microscope. Data analysis was carried out with the software 'Leica QFISH'.

1.3.8. Tumor xenotransplants in severe combined immunodeficiency (SCID) mice

In order to prove their malignancy, cells from cell lines OEE-III, SHER-I, and HEVE-II were suspended in phosphate buffered saline (PBS) and injected subcutaneously into the flanks of female SCID mice, aged 7-8 weeks. The mice were observed for a maximum of twelve weeks. The study protocol was approved by the Ministry of Science and Research, Vienna (BMWF-66.009/0142-II/10b/2010 and BMWF-66.009/0110-C/GT/2007). All mouse experiments were performed by Harald Höger, Department of Laboratory Animal Science and Genetics, Medical University of Vienna, 2325 Himberg, Austria. The cells for mouse experiments were provided by Roswitha Pfragner, Institute of Pathophysiology and Immunology, Medical University of Graz.

1.3.9. Statistical analysis

Descriptive statistical analysis was performed to compare the hereditary and sporadic subgroups. The two-sided Fisher Exact test was used for 2x2 table analysis. Statistical analysis was performed by Michael Speicher, Institute of Human Genetics, Medical University of Graz.

1.4. RESULTS

1.4.1. *RET* mutation status in germline and in primary tumors

Of the 52 tumors 11 (11/52, 21%) were hereditary (designated as H1-H11; Table 7) and 41 cases were sporadic. In the sporadic cases we found *RET* mutations in 15 tumors (15/41, 37%) (designated as S1-S15; Table 2), i.e. 26 (26/41, 63%) sporadic tumors occurred without *RET* mutations (designated as S16-S41).

Table 7. Overview of the germline *RET* Mutation carrier patients (n=11). The exon with the corresponding *RET* mutation is listed.

Patient ID	Exon	Germline Mutation	Mutation Tumor
H1	8	G533C GGC>TGC het	G533C GGC>TGC het
H2	14	V804M GTG>ATG het	V804M GTG>ATG het
H3	11	C634R TGC>CGC het	C634R TGC>CGC het
H4	11	C634Y TGC>TAC het	C634Y TGC>TAC het
H5	11	C634R TGC>CGC het	C634R TGC>CGC het
H6	11	*	C634W TGC>TGG het
H7	11	*	C634Y TGC>TAC het
H8	15	K907M AAG>ATG het	K907M AAG>ATG het
H9	13	Codon 782 and 769	Codon 782 and 769
H10	14	*	V804M GTG>ATG het
H11	10	C620Y TGC>TAC het	C620Y TGC>TAC het

het: heterozygous

*These cases are hereditary cases based on the respective family history. However, in these cases we could only sequence DNA from the tumor tissue.

Table 8. Overview of *RET* mutations found in sporadic MTC tumors (n=15). The exon with the corresponding *RET* mutation is listed.

Patient ID	Exon	Mutation
S1	10	C618R TGC>CGC het
S2	16	M918T ATG>ACG het
S3	16	M918T ATG>ACG het
S4	16	M918T ATG>ACG het
S5	11	C634Y TGC>TAC het
S6	16	M918T ATG>ACG het
S7	15	A883S GCT>TCT het
S8	15	A883S GCT>TCT het
S9	16	M918T ATG>ACG het
S10	16	M918T ATG>ACG het
S11	16	M918T ATG>ACG het
S12	16	M918T ATG>ACG het
S13	15	A883F or A883S or A883V het*
S14	16	M918T ATG>ACG het
S15	16	M918T ATG>ACG het

het: heterozygous

*change of amino acid depending on haplotype.

1.4.2. Array-CGH of primary tumors

In total 52 MTCs were hybridized. The most frequent changes observed in the 52 MTCs were losses of chromosomes 1p (19/52, 37%), 22q (18/52, 35%), 19p (12/52, 23%), 19q (9/52, 17%), and 4q (8/52, 15%) (Figure 3).

Figure 3. Array-CGH results of all MTC primary tumors (n=52). The penetrance plot shows the percentages of losses (green; to the left of each chromosome) and gains (red; to the right of each chromosome). The percentages refer to all cases including the balanced tumors (12/52 or 23% were balanced). The frequent gains and losses at the X- and Y-chromosomes merely reflect sex differences between the tumor and the reference DNA and therefore do not represent true copy number changes.

To check whether the frequency of chromosomal changes correlated with the RET mutation status we defined three groups, i.e. hereditary tumors, sporadic tumors with RET mutations, and sporadic tumors without RET mutations. In hereditary tumors (n=11) only a few changes, such as losses of chromosomes 1p, 4q, 19p, and 19q, were recurrent, i.e. appeared in 2 of the 11 cases (18%) (Figure 4). Five (5/11; 45%) of these tumors were balanced, i.e. no chromosomal gains or losses were observed. In sporadic MTCs with a RET mutation (n=15), the most frequent changes were losses of chromosomes 1p (7/15, 47%), 22 (6/15, 40%), 3q (3/15, 20%), and 4q (3/15, 20%) (Figure 6). Three tumors (3/15, 20%) were balanced. In sporadic MTCs without RET mutation (n=26) the most frequent changes were losses of chromosomes 22 (11/26, 42%), 1p (10/26, 39%), 19p (8/26, 31%),

19q (5/26, 19%), and 21q (5/26, 19%) (Figure 5). Four tumors (4/26, 15%) were balanced. Supporting information is given in the Appendix in supplementary tables 1 and 2.

Figure 4. Array-CGH results of all hereditary MTC cases (n=11). The penetrance plot shows the percentages of losses (green; to the left of each chromosome) and gains (red; to the right of each chromosome). The percentages refer to all cases including the balanced tumors (5/11 or 45% were balanced). The frequent gains and losses at the X- and Y-chromosomes merely reflect sex differences between the tumor and the reference DNA and therefore do not represent true copy number changes.

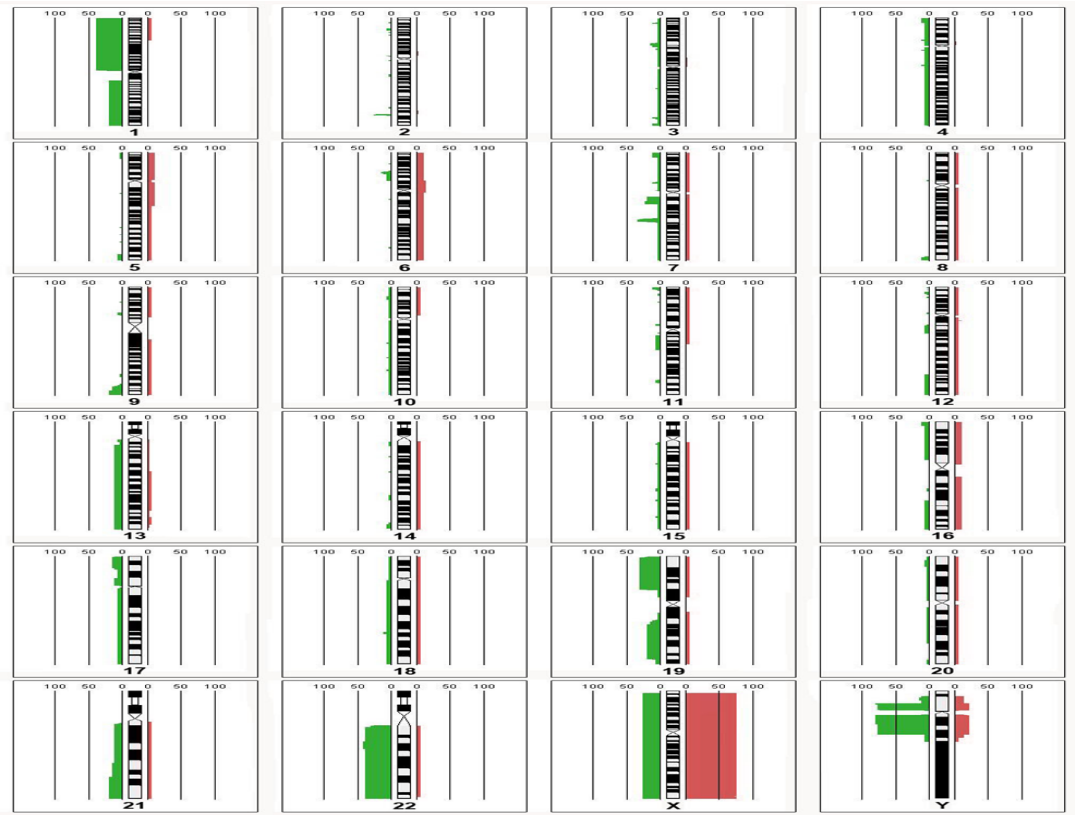

Figure 5. Array-CGH results of sporadic MTCs without *RET* mutations (n=26). The penetrance plot shows the percentages of losses (green; to the left of each chromosome) and gains (red; to the right of each chromosome). The percentages refer to all cases including the balanced tumors (4/26 or 15% were balanced). The frequent gains and losses at the X- and Y-chromosomes merely reflect sex differences between the tumor and the reference DNA and therefore do not represent true copy number changes.

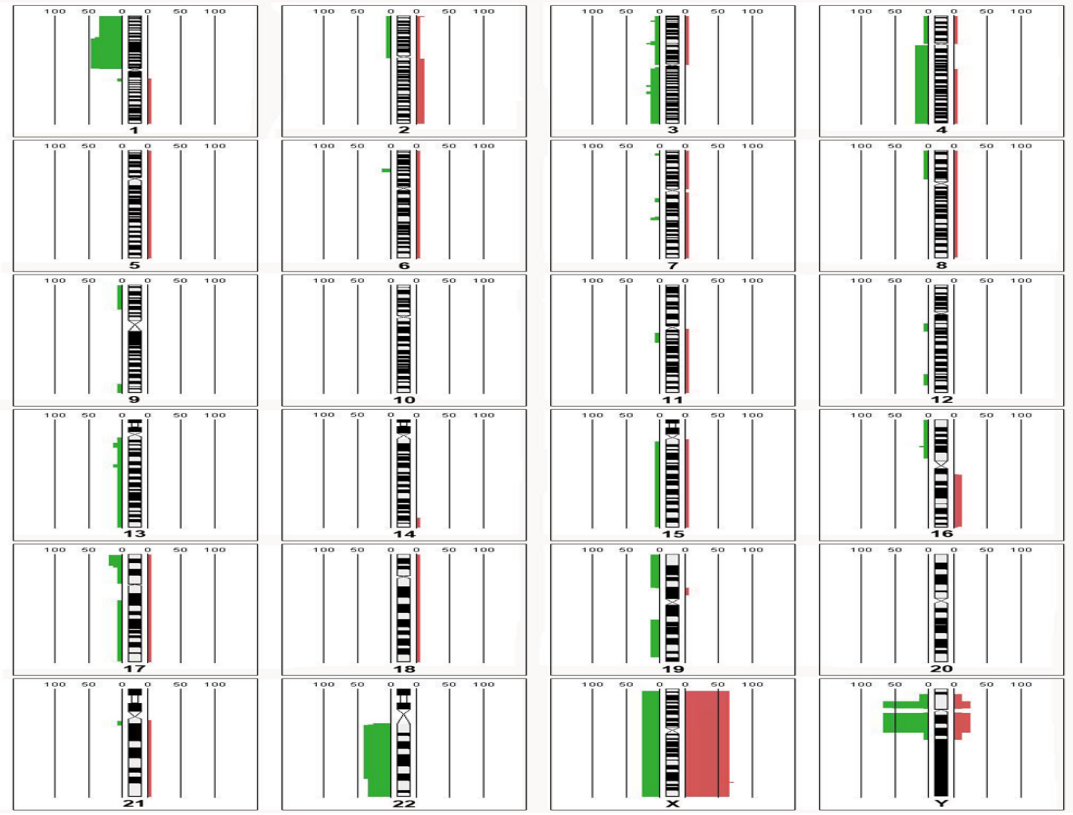

Figure 6. Array-CGH results of sporadic MTCs with *RET* mutations (n=15). The penetrance plot shows the percentages of losses (green; to the left of each chromosome) and gains (red; to the right of each chromosome). The percentages refer to all cases including the balanced tumors (3/15 or 20% were balanced). The frequent gains and losses at the X- and Y-chromosomes merely reflect sex differences between the tumor and the reference DNA and therefore do not represent true copy number changes.

Thus, in the two groups of sporadic tumors the pattern of chromosomal gains and losses was similar. The most frequent difference between hereditary and sporadic tumors (with or without RET mutation) was loss of chromosome 22 material, which was observed in 41% (17/41) of sporadic MTCs, but only in 9% (1/11) of hereditary tumors. This was statistically significant ($p = 0.009$). All chromosomal aberrations found together with the boundaries of the deletions/duplications per tumor are listed in the appendix in supplementary table1. In addition, supplementary table 2 summarizes the shortest regions of overlap (SROs) of lost and gained regions. We also compared our array-CGH findings with previously published studies. An overview is given in Table 9.

Table 9. Detailed comparison of our CGH findings with previously published studies.

	Frisk et al. 2001	Hemmer et al. 2003	Marsh et al. 2003	Ye et al. 2008 (*)	This study
No. of cases	24	10	37	30	52
hereditary (%)	NA	NA	22	10	21
sporadic (%)	NA	NA	78	20	79
balanced (%)	40	50	35		23
1p		L: 10%	L: 19%		L: 37%
1q		G: 10%	G: 5%		
3		L: 10%	L: 13.5%		
3q23~26-qter	L: 12.5%	L: 10%	L: 11%		
4q			L: 13.5%		L: 15%
5q			L: 8% G: 5%		
5q13.2				L: 33%	
5q31.1				L: 33%	
6		G: 10%	G: 5%		
6q13				L: 33%	
7p		G: 10%			
7q36.1				L: 37%	
9p22.1				L: 30%	
9q			L: 11%		
9q31.2				L: 33%	
11c-q12	G: 12.5%				
11q		G: 10%			
12p			G: 5%		
12p13.31				L: 43%	
13q		L: 20%	L: 19%		
13q12.11				L: 37%	
13q21	L: 21%				
14q			G: 5%		
16p			L: 5%		

	Frisk et al. 2001	Hemmer et al. 2003	Marsh et al. 2003	Ye et al. 2008 (*)	This study
17			L: 8%		
17q11.2				L: 30%	
18p		L: 10%			
18q21-qter		L: 10%			
19p	G: 21%		L: 3% G: 11%	L: 37%	L: 23%
19q	G: 29%		L: 3% G: 11%		L: 17%
21q		G: 10%			
22q	G: 12.5%	L: 20%	L: 13.5%	L: 30-33%	L: 35%

NA: not available; G: gain; L: loss

(*) Only copy number changes with 30% or greater frequency in all MTCs were listed.

Overall, compared to other tumor entities (Pinkel and Albertson, 2005), copy number changes in MTC are relatively rare. This is further supported by the interesting observation of the large number of balanced tumors without any chromosomal changes (12/52, 23%), which occurred more frequently in the hereditary cases (5/11, 45%) than in sporadic tumors (7/41, 17%).

1.4.3. Array-CGH of metastases

To check whether the number of genomic alterations increases with advanced tumor stages, we included metastases into our analyses. Altogether we had nine lymph node and one liver metastasis for analysis. Five of these metastases were derived from the aforementioned primary tumors. One of these five cases was from a hereditary case (H5), two from sporadic cases with a RET mutation (S3, S12), and two from sporadic cases without RET mutations (S25, S40). The other 5 metastases without genetically characterized primary tumors had all the same somatic M918T ATG>ACG RET mutation.

Of these 10 metastases only 1 (10%) was balanced. The other 9 cases showed more imbalances than the primary tumors (Figure 7). Although gains were rarely observed in

primary tumors, they were frequent in metastases. The most common gains were observed for chromosomes 6 (5/10, 50%), 16 (5/10, 50%), 19q (4/10, 40%), 19p (3/10, 30%), 7 (3/10, 30%), and 15 (3/10, 30%). Chromosomes 13q (4/10, 40%) and 22q (4/10, 40%) were most frequently lost (Figure 7). All chromosomal aberrations found together with the boundaries of the deletions/duplications per tumor are listed in the appendix in supplementary table1. In addition, supplementary table 2 summarizes the shortest regions of overlap (SROs) of lost and gained regions.

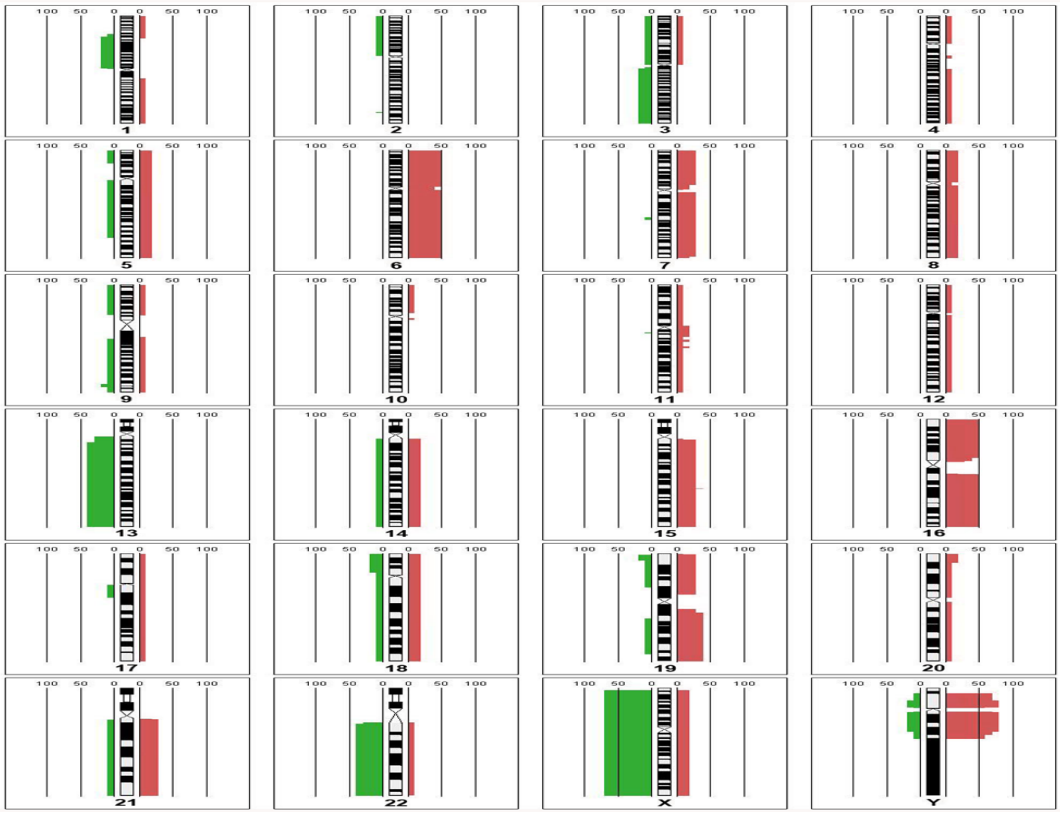

Figure 7. Array-CGH findings for all metastases (n=10). The penetrance plot shows the percentages of losses (green; to the left of each chromosome) and gains (red; to the right of each chromosome). 1 of the 10 cases was balanced. Gains and losses at the sex chromosomes indicate different sexes between tumor and reference DNA and therefore do not reflect true copy number changes (compare Figure 3).

We found many similarities and few differences between the array-CGH profiles of primary tumors and their respective metastases (Figure 8a – 8e).

In three sporadic cases (i.e. one without RET mutation [S40], and two with RET mutations [S3, S12]) the vast majority of imbalances observed in the primary tumor were also found in the respective metastases (Figure 8 a-c). The metastasis of S40 had a gain of chromosome 15, which was not present in the primary tumor (Figure 8 a). The primary tumor of S3 had a gain of chromosome 2, which was not observed in the metastasis, whereas only the metastasis had a gain of chromosome 19. Remarkably, the primary tumors of these two cases (i.e. S40 and S3) had a surprisingly high number of gains and losses for this tumor entity (Figure 8 a-b). A gain of chromosome 19q was the only difference between primary tumor and its metastasis in case S12. In addition, we analyzed two metastases with balanced primary tumors (i.e. one sporadic without RET mutation [S25] and one hereditary case [H5]). In both cases the metastases were not balanced but had losses of material from chromosomes 1, 5, and 13 in one case (S25) (Figure 8d) and gain of chromosome 6 and losses of chromosomes 13 and 14 in the other case (H5) (Figure 8e).

The data suggest that advanced MTCs are associated with an increased number of chromosomal gains and losses.

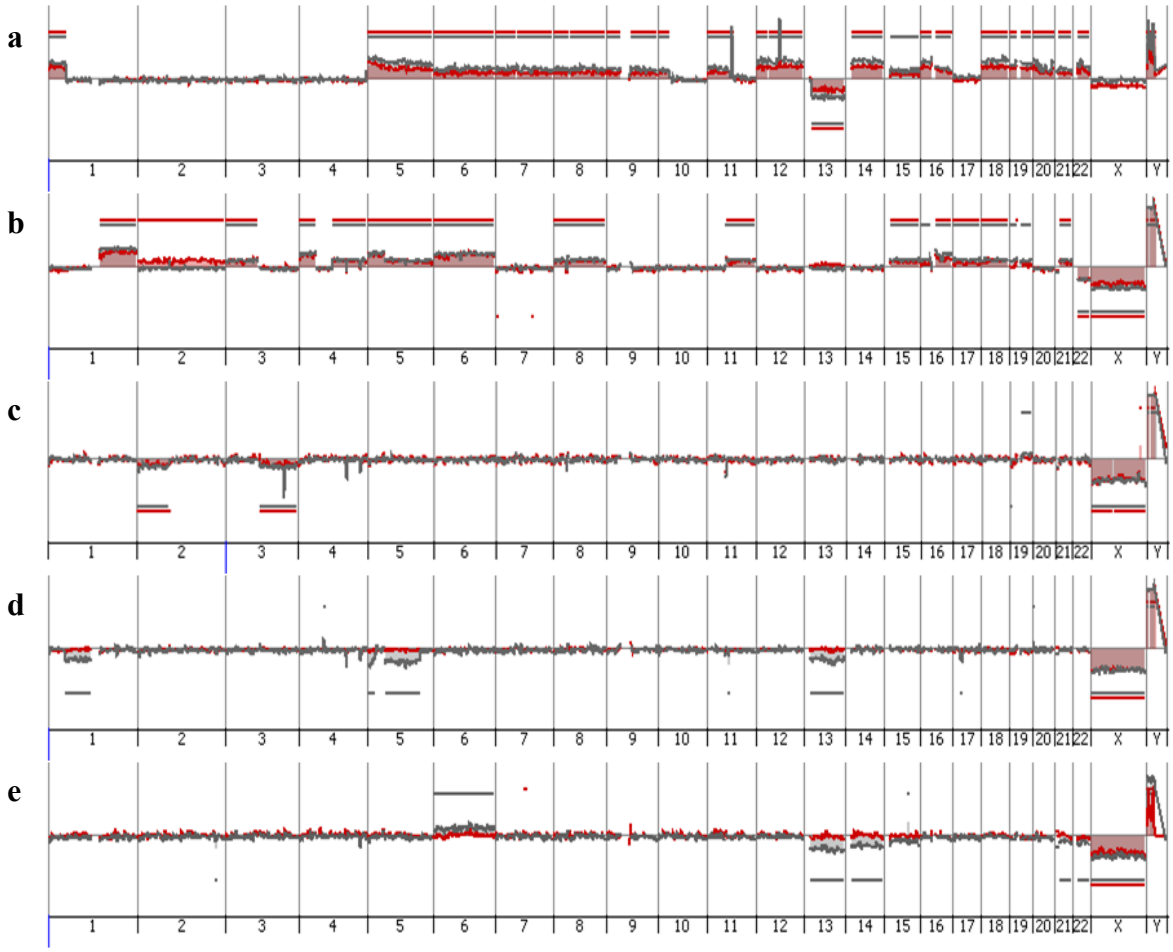

Figure 8 a-e. Simultaneous representations of genome-wide array-CGH profiles obtained for primary tumors (displayed in red) and their respective metastases (grey) for (a) S40 STUR; **(b)** S3 DIJO; **(c)** S12 STAA; **(d)** S25 HOKA; and **(e)** H5 LAWO.

1.4.4. Determination of SNPs in MTC genomes

We obtained the SNP status within the *RET* gene for 45 (45/52, 87%) patients. Thereof 25 patients (25/45, 57%) were identified to carry one or more SNPs (hereditary cases: 4/11, 36%; sporadic cases with somatic *RET* mutations: 7/15, 47%; sporadic cases without RET mutations: 14/26, 54% (Table 10). For 10 patients the SNP status could not be determined (4 hereditary cases; 3 sporadic cases with somatic *RET* mutations; 3 sporadic cases without *RET* mutations). In total 17 patients (17/45, 38%) did not carry a SNP. The SNP status was determined also for 5 metastases. Thereof 2 (2/5, 40%) carry a SNP (Table 10).

No correlation was observed between the number of SNPs and the number of aberrations detected in the samples. There was no difference observed between patients that carry heterozygous or homozygous *RET* SNPs or in patients that did not carry a SNP.

Table 10. Summary of SNPs identified. The table summarizes the *RET* SNPs for 25 MTC patients and 2 MTC metastasis.

Patient ID	Exon	SNP
hereditary MTC		
H1	11 15	G691S het S904S het
H2	13	L769L het
H4	13	L769L het
H8	15	S904S het
MTC without RET mutation		
S2	13	L769L hom
S3	11 13 15	G691S het L769L het S904S het
S6	13	L769L het
S7	15	S904S het
S8	11 15	S904S het S904S het
S9	13	L769L het
S11	13	L769L het
MTC with RET mutation		
S16	11 13 15	G691S het L769L het S904S het
S20	15	S904S het
S21	13	L769L het
S23	15	S904S het
S24	13	L769L het
S25	13	L769L het
S27	13	L769L het

Patient ID	Exon	SNP
S28	11 13 15	G691S het L769L het S904S het
S29	13	L769L hom
S34	13	L769L het
S35	13	L769L het
S36	13	L769L hom
S37	13 15	L769L het S904S het
S39	15	S904S het
Metastasis		
M2	13 14	L769L het S836S het
M5	13	L769L het

het: heterozygous; hom: homozygous

1.4.5. Correlation of array-CGH results with clinical data

We obtained detailed clinical data from 35 (35/52, 67%) patients (hereditary cases: 7/11, 64%; sporadic cases with somatic RET mutations: 9/15, 60%; sporadic cases without RET mutations: 19/26, 73%) (Table 11).

Table 11. Summary of clinical data. For 35/52, 67% of patients the clinical data are summarized below.

	sex	Age (years)	size MTC left lobe (mm)	size MTC right lobe (mm)	# of positive lymph nodes	# of resected lymph nodes	UICC TNM 2002	Total gains (bp)	Total losses (bp)	Total gains and losses (bp)
H1	F	29.5	10	35	3	39	T2N1a	0	0	0
H2	F	77.1	7	20	6	101	T3bN1b	42519235	0	42519235
H3	F	24.2	12	5	26	103	T1bN1b	0	713419730	713419730
H4	F	47.6	30	30	10	120	T3bN1b	0	0	0
H5	M	33.9	7	5	23	101	T1aN1b	0	0	0
H8	F	29.6	9	2	3	65	T1aN1b	0	0	0
H11	M	21.7	18	9	24	171	T2bN1b	2465986	0	2465986
S1	F	68.1	35	0	1	64	T2N1b	0	66716015	66716015
S2	F	51.7	0	22	0	32	T2N0	0	374863236	374863236
S3	M	43.4	20	5	108	155	T4bN1b	1540840070	39360140	1580200210
S5	F	53.9	0	32	7	47	T2N1b	0	258640314	258640314
S6	F	80.0	0	25	0	57	T2bN0	0	332767102	332767102
S7	M	64.1	0	25	1	68	T2N1b	321350311	182670994	504021305
S8	F	75.2	19	0	1	71	T1bN1	0	0	0
S11	F	47.6	0	30	12	.	T2N1	0	105315856	105315856
S14	F	79.6	13	0	0	35	T1bN0	0	0	0
S16	F	38.5	42	0	0	83	T3aN0	0	509970291	509970291
S17	F	75.9	35	0	1	12	T2N1	0	256855267	256855267
S18	F	72.9	3	20	0	27	T2N0	0	23770008	23770008
S20	M	45.4	0	13	0	83	T1bN0	0	119697739	119697739
S21	F	32.2	0	8	0	119	T1aN0	0	223680807	223680807
S23	F	60.6	0	3	0	159	T1aN0	223423808	961208106	1184631914
S24	F	72.5	0	6	0	106	T1aN0	0	0	0

	sex	Age (years)	size MTC left lobe (mm)	size MTC right lobe (mm)	# of positive lymph nodes	# of resected lymph nodes	UICC TNM 2002	Total gains (bp)	Total losses (bp)	Total gains and losses (bp)
S25	M	56.6	35	0	21	108	T3bN1b	0	0	0
S28	F	56.7	0	12	2	94	T1bN1a	84891404	59645084	144536488
S29	F	73.2	37	0	0	77	T2N0	0	231706980	231706980
S30	F	70.8	0	12	0	41	T1bN0	0	35419710	35419710
S31	F	48.9	0	24	0	43	T2N0	0	71391196	71391196
S32	F	61.5	50	0	4	59	T3bN1b	0	193379986	193379986
S33	F	82.7	0	13	1	140	T1bN1a	0	0	0
S34	F	52.5	28	0	0	131	T2N0	0	39085716	39085716
S35	F	27.5	7	0	0	99	T1aN0	0	932710173	932710173
S36	F	51.8	0	0.6	0	88	T1aN0	0	66670219	66670219
S38	F	72.3	14	0	0	89	T1bN0	18203537	326517490	344721027
S40	M	75	50	0	16	91	T4aN1b	1587868114	89716147	1677584261

To address the question whether an increased number of aberrations is correlated with advanced stage of MTC, we calculated for each patient the size of all regions involved in gains and losses as detailed in Table 11 and correlated it with the size of the respective MTCs at time of diagnosis. However, linear regression clearly revealed that no relationship existed between these two parameters (Figure 9). We repeated the analysis with the number of positive lymph nodes, which yielded almost identical results (Figure 10).

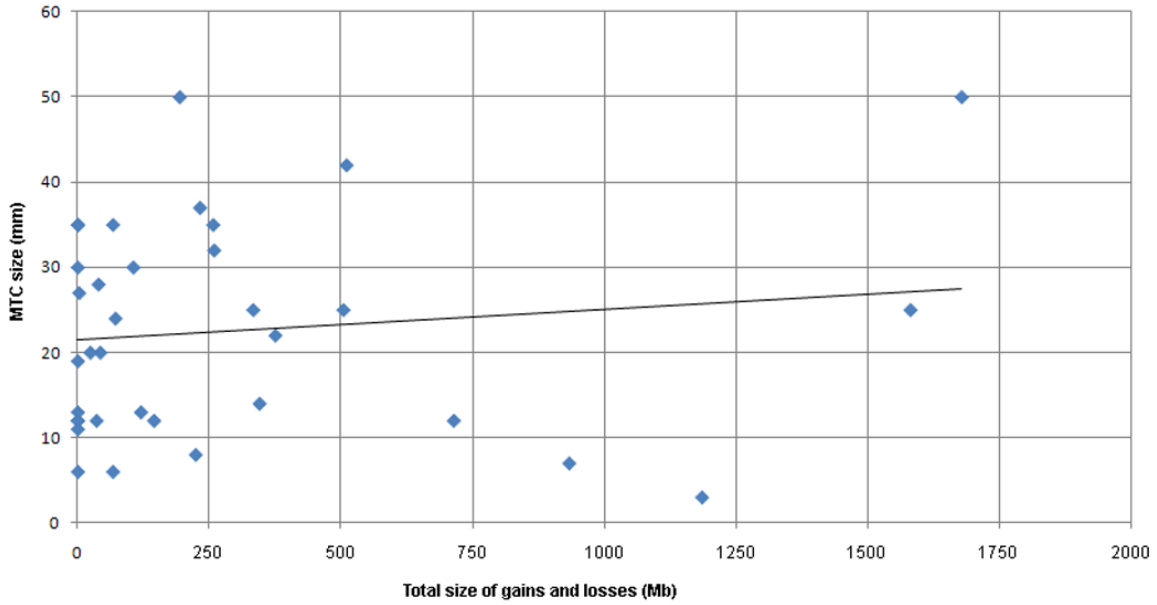

Figure 9. Correlation of MTC size and total size of gains and losses.

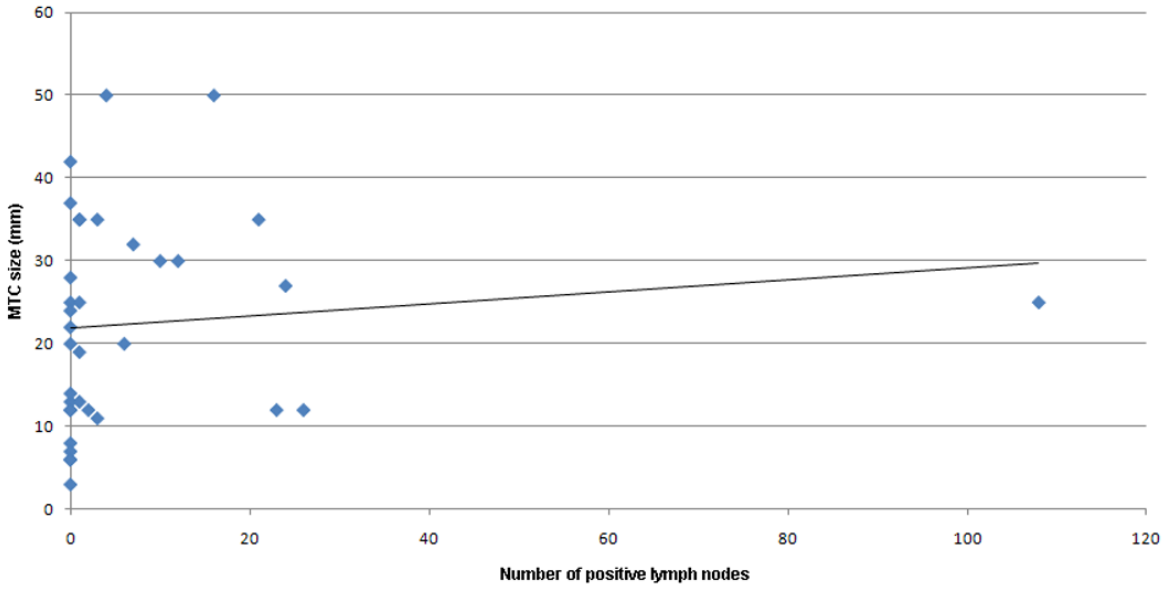

Figure 10. Correlation of MTC size and number of positive lymph nodes.

Recently, it had been reported that loss of CDKN2C (INK4C, p18) correlates with higher proliferation rates and with larger MTCs (van Veelen *et al.*, 2008). In our cohort, there were six patients with loss of the CDKN2C region (i.e., chromosome 1: 51.426.417-51.440.305), and for five of these patients (i.e., S2, S5, S6, S7 and S11), we could obtain detailed data about the MTC size at time of diagnosis. The mean MTC size for these five patients was 26.8 mm (median: 25 mm; range: 22–32 mm). In contrast, the mean MTC size in the group without loss of the CDKN2C locus was 21.8 mm (n = 30; median: 19.5 mm; range: 3–50 mm). Although this difference was not statistically significant (p = 0.11), it

suggests that synergistic effects of RET and CDKN2C may indeed be possible in MTCs as previously suggested (van Veelen *et al.*, 2008).

Because of the frequent loss of chromosome 22, we also checked its impact on tumor size. The mean MTC size in the group without chromosome 22 loss was 21.25 mm (n = 24; median: 19.5 mm; range: 6–50 mm), whereas the mean MTC size was 25.2 mm (n = 11; median: 25 mm; range: 3–42 mm) in the group with chromosome 22 loss. This difference was statistically not significant (p = 0.39).

1.4.6. Characterization of cell lines

To further elucidate the significance of gains and losses, we evaluated five MTC cell lines (BOJO, HEVE-II, OEE-III, SHER-I, SINJ). All five cell lines were derived from sporadic cases. One cell line (SHER-I) was derived from a primary tumor, the other four cell lines from lymph node metastases (Table 12).

Table 12. Characteristics of MTC cell lines. All cell lines were derived from sporadic cases.

Cell line	Tumor stage* at time of surgery	Sex	*Somatic RET* status	Primary tumor/ metastasis	Passage number at time of analysis
BOJO	pT4aN1M1	M	∅ mutation	Lymphnode-metastasis	24
HEVE-II	pTxN1bMX	F	∅ mutation	Lymphnode-metastasis	9
SHER-I	pT4aN1MX	M	∅ mutation	Primary tumor	25
SINJ	pT2aN1M0	M	∅ mutation	Lymphnode-metastasis	21
OEE-III	pT2aN1bM1	F	M918T	Lymphnode-metastasis	15

* UICC TNM 1997

Four of them had no RET mutation, whereas one cell line (OEE-III) had a M918T RET mutation (Table 12). All MTC cell lines were stained for calcitonin, carcinoembryonic

antigen, and neuroendocrine markers, such as chromogranin A, and synaptophysin, to confirm the C-cell origin. We prepared metaphase spreads and analyzed them with M-FISH in order to assess also structural rearrangements. The respective passage numbers of the cell lines are listed in Table 12.

Array-CGH identified a gain of chromosome 5q and a loss of chromosome 9p material in the BOJO cell line. This correlated excellently with the M-FISH result, which had identified an unbalanced translocation between chromosomes 5 and 9 (Figure 11). Cell line OEE-III showed multiple rearrangements with M-FISH and many gains and losses with array-CGH (Figure 12).

Three cell lines (i.e. HEVE-II, SHER-I and SINJ) had a balanced array-CGH profile. In two of these cases (i.e. HEVE-II; Figure 13 and SHER-I; Figure 14) we could exclude the existence of balanced structural chromosomal rearrangements, such as translocations, by M-FISH. For one cell line (SINJ; Figure 15) we did not succeed in the preparation of metaphases with a quality sufficient for a detailed analysis.

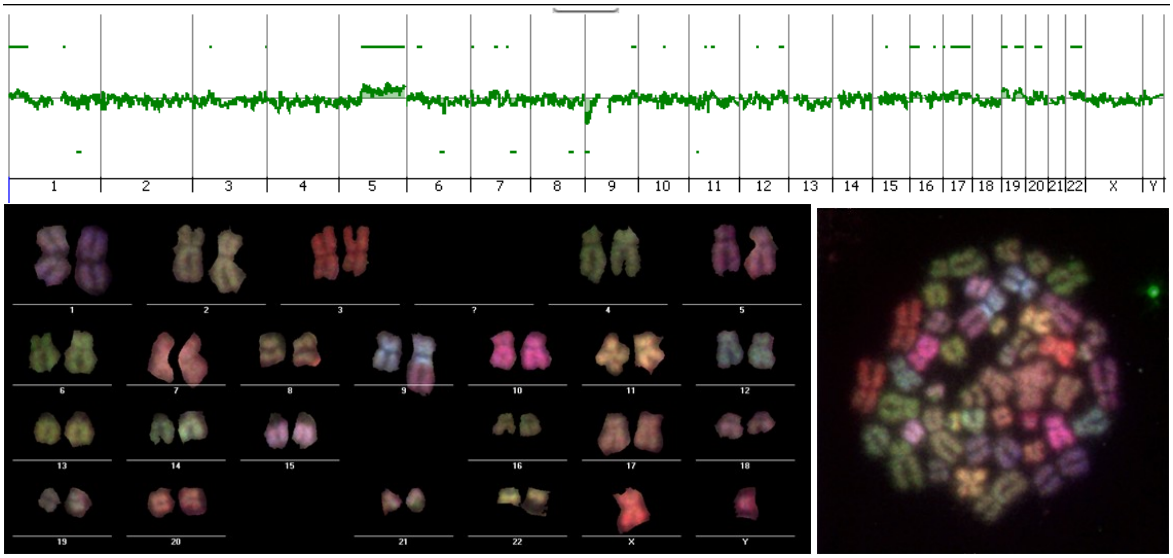

Figure 11. Characterization of the cell line BOJO. The upper panel shows the genome-wide array-CGH profile, the lower panel illustrates a representative metaphase and the respective karyotype after M-FISH.

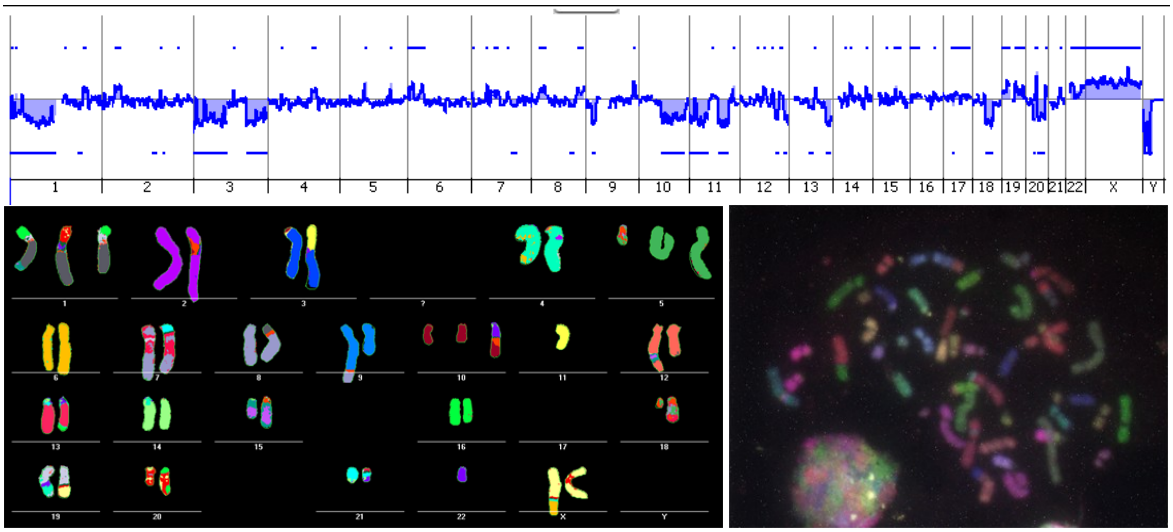

Figure 12. Characterization of the cell line OEE-III. The upper panel shows the genome-wide array-CGH profile, the lower panel illustrates a representative metaphase and the respective karyotype after M-FISH.

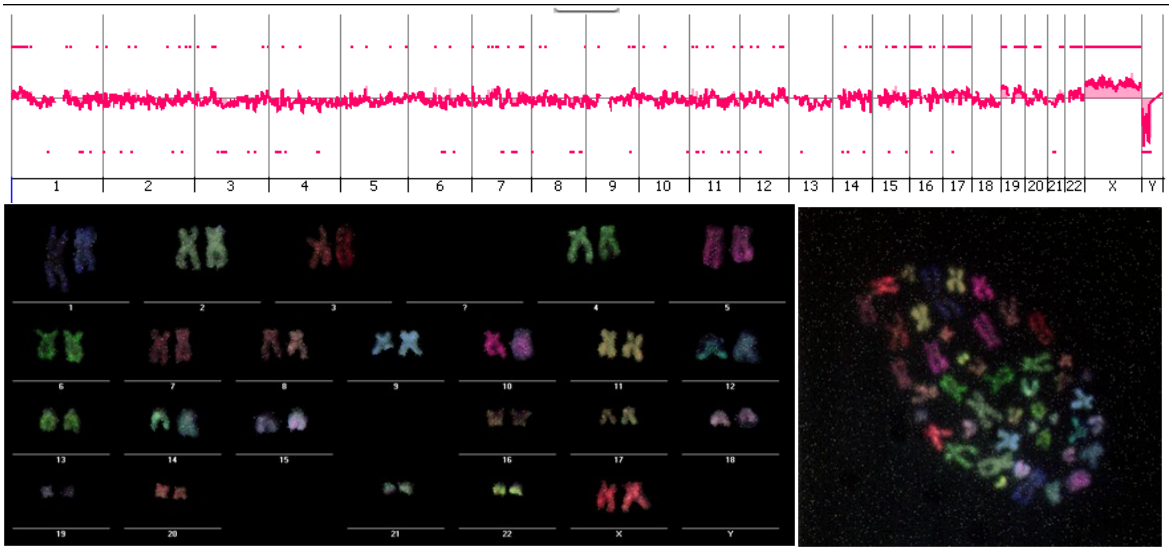

Figure 13. Characterization of the cell line HEVE-II. The upper panel shows the genome-wide array-CGH profile, the lower panel illustrates a representative metaphase and the respective karyotype after M-FISH.

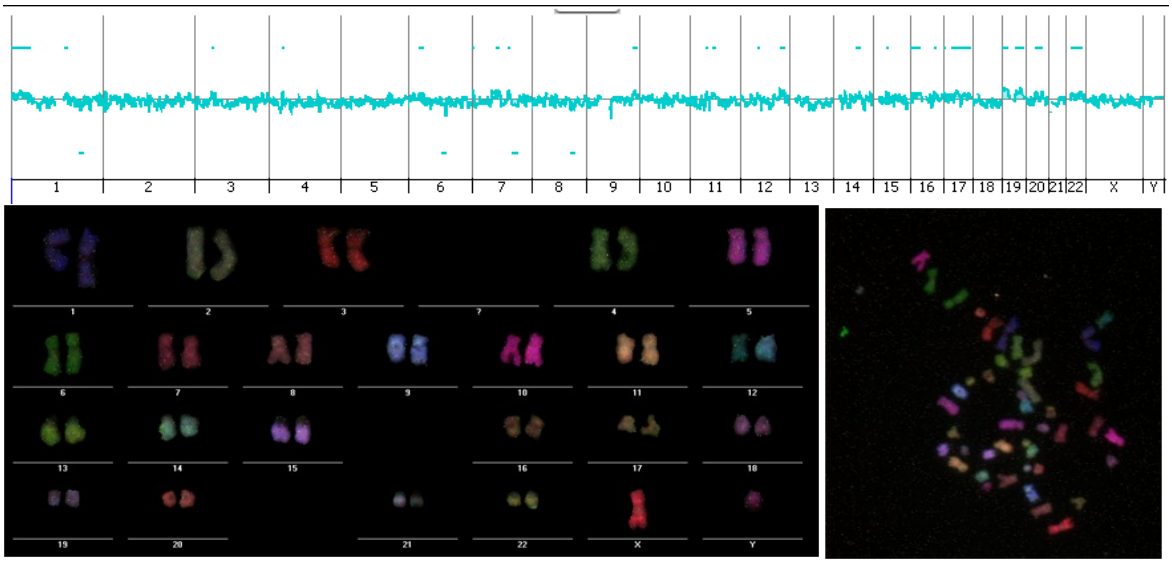

Figure 14. Characterization of the cell line SHER-I. The upper panel shows the genome-wide array-CGH profile, the lower panel illustrates a representative metaphase and the respective karyotype after M-FISH.

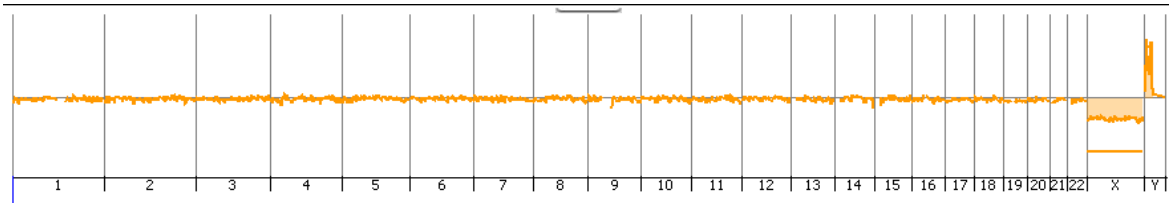

Figure 15. Genome wide array-CGH profile of the cell line SINJ.

1.4.7. Severe combined immunodeficiency (SCID) mouse experiments

To confirm the tumorigenicity of our cell lines we injected cells (3 x 10^7 per mouse) from cell lines OEE-III, SHER-I, and HEVE-II subcutaneously into SCID-mice. In all cases we observed tumor growth at the injection site, which was visible about one month after injection. Figure 16a and Figure 16b illustrate a tumor four weeks after injection of SHER-I cells into a SCID mouse. Tumors did not metastasize and exulcerated when reaching diameters of >10 mm. To evaluate whether the tumor genome changed in the xenotransplants, we assessed copy number changes in tumors from xenotransplants from the cell line with multiple changes (OEE-III) and from a balanced (HEVE-II) cell line.

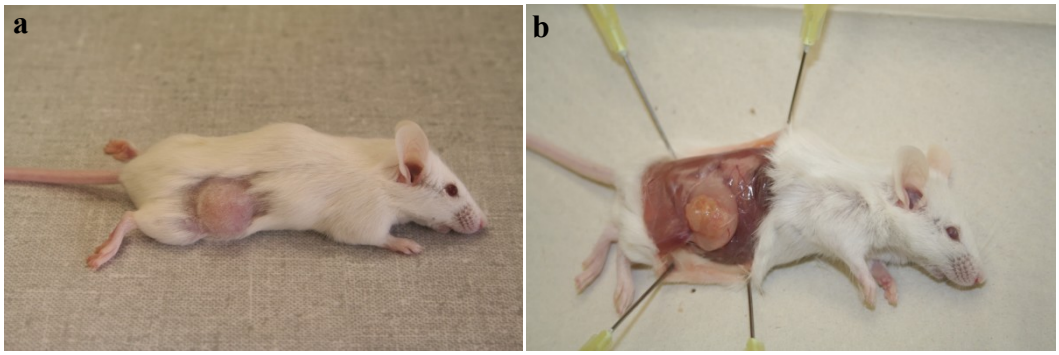

Figure 16 (a-b). Tumor growth in SCID mouse and analysis of xenotransplants. (a) Tumorigenicity of SHER-I cell line: Tumor four weeks after subcutaneous injection of 3 x 10^7 cells. **(b)** Subcutaneous tumor at the site of injection. No metastases were found.

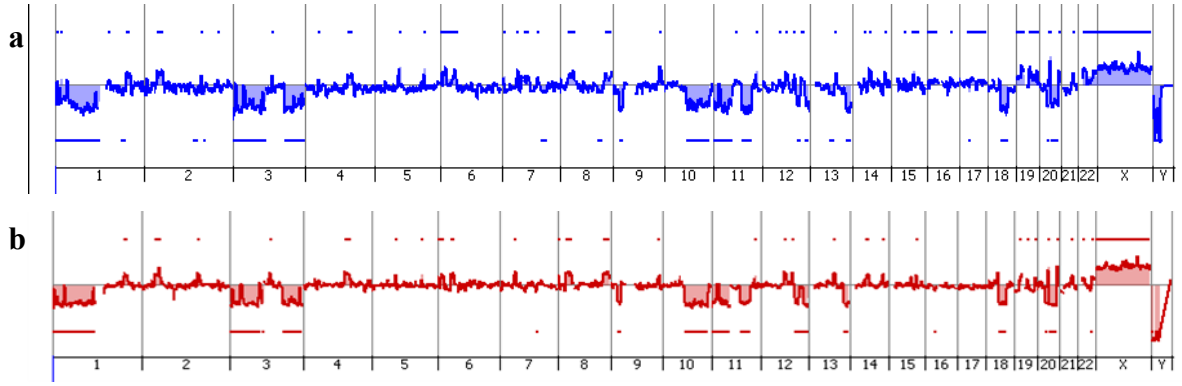

Figure 17 (a-b). Array-CGH profiles from the cell line OEE-III. (a) Array-CGH profiles obtained with DNA from the cell line; **(b)** profile with DNA from the respective mouse xenotransplant.

With cell line OEE-III we obtained an almost identical array-CGH profile with DNA from the mouse tumor as compared to the original cell line profile (Figure 17).

For the balanced HEVE-II cell line we performed additional experiments. We cultivated cells from the xenotransplant and repeated the experiment, i.e. we injected cells from the first mouse xenotransplant into another mouse to generate a second xenotransplant. Cells from this second transplant induced tumor growth with the same speed as the first transplant. DNA from both the first and second xenotransplants was subjected to array-CGH and demonstrated that the array-CGH profiles remained balanced (Figure 18 b).

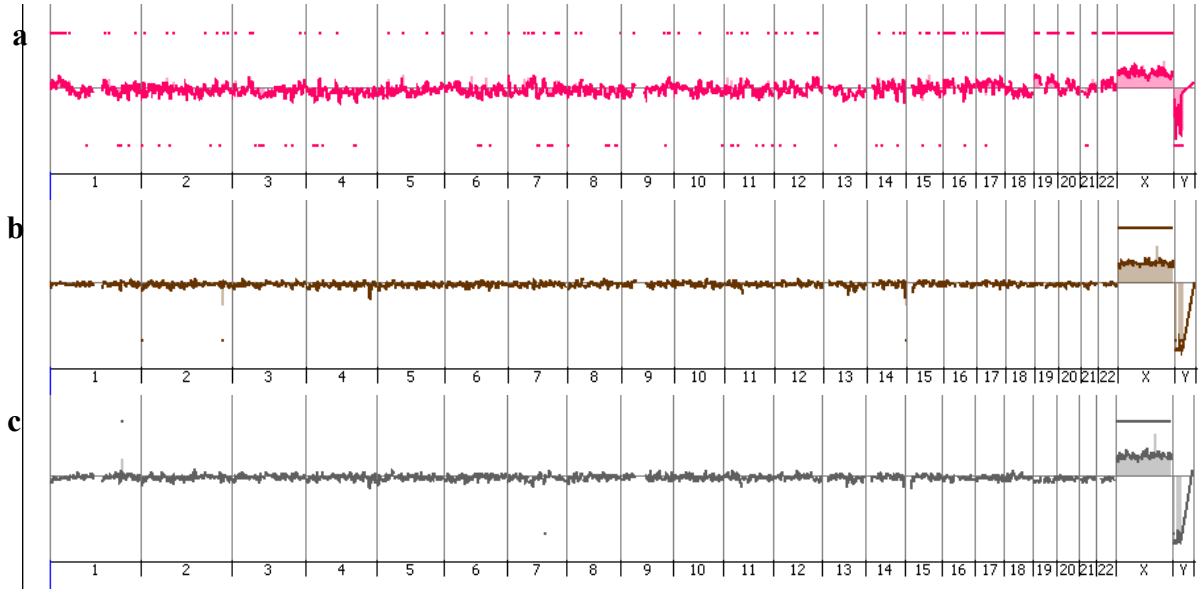

Figure 18. Array-CGH profiles from cell line HEVE-II. (a) profile obtained with the cell line DNA; **(b)** profile obtained from the first mouse xenotransplant; **(c)** profile obtained from the second mouse xenotransplant.

This suggests that MTC can arise in the absence of chromosomal changes and without RET mutation.

1.5. DISCUSSION

Activating mutations of *RET* proto-oncogene have been reported in roughly 50% of sporadic MTC and in more than 95% of MEN-2 families (Schlumberger *et al.*, 2008, Ponder, 1999). The role of *RET* and *RET* pathway in MTC pathogenesis is well documented (Drosten and Putzer, 2006, Messina and Robinson, 2007). However, tumor phenotype and progression is influenced by the genetic background, i.e. further changes in the tumor genome (Cranston and Ponder, 2003). Thus, additional initiating and driver mechanisms involved in MTC tumorigenesis remain to be uncovered. In order to identify further changes in the tumor genome, we performed here array-CGH with DNA from primary tumors and metastases and some first functional analyses with MTC-derived cell lines.

Up to date, the cytogenetics of MTC has been studied sparsely, because the cells are difficult to grow in culture (Herrmann, 2003). At present the Mitelman database has 327 karyotypes of cases with thyroid cancer (http://cgap.nci.nih.gov/Chromosomes/Mitelman) (Status: Oct 06, 2010). However, none of these cases relate to MTC. The few published cases have not identified recurrent structural rearrangements yet (Wurster-Hill *et al.*, 1986, Scappaticci *et al.*, 1992). MTC has also not been extensively analyzed by CGH. Older studies employing chromosome CGH described alterations involving chromosomes 1p, 3q, 3p, 4, 9q13-22, 11c-q12, 13q, 19, and 22q (Hemmer *et al.*, 1999, Frisk *et al.*, 2001, Marsh *et al.*, 2003). A more recent study used array-CGH and found frequent allelic loss in 7q36.1, 12p13.31, 13q12.11, and 19p13.3-11 (Ye *et al.*, 2008). In summary, the previously published CGH-data (

Table 9) did not reveal recurrently gained and lost regions in the MTC genomes.

In our study losses of 1p, 4q, and 22q were the most common changes. There was no gain or loss unique to hereditary or sporadic tumors. However, loss of chromosome 22 occurred more frequently in the sporadic cases and suggests that loss of genes located on this chromosome may contribute to occurrence and/or progression of sporadic MTCs.

However, compared to other tumor entities (Pinkel and Albertson, 2005), our data suggest that copy number changes in MTC are relatively rare. This is further supported by the large number of balanced tumors without any chromosomal changes (12/52, 23%), which occurred more frequently in the hereditary cases (5/11, 45%) than in sporadic tumors (7/41, 17%). In contrast, analyses of metastases demonstrated an increase in imbalances, especially of gains, which were only rarely observed in primary tumors. Comparisons between primary tumors and metastases showed that metastases indeed harbor a larger number of chromosomal imbalances.

We used several cell lines to investigate the significance of tumors with balanced array-CGH profiles. Due to technical difficulties and poor growth *in vitro*, only few cultures of human MTCs have been reported to date. In 1981 Leong et al. established the first continuous cell line from a human MTC, the TT cell line (Berger *et al.*, 1984, Leong *et al.*, 1981). For many years TT was the only available human MTC cell line. Subsequently the MTC-SK cell line was established (Pfragner *et al.*, 1990) and later the MZ-CRC-1 cell line (Cooley *et al.*, 1995, Morisi *et al.*, 2007).

For genomic analyses we used here five continuous MTC cell lines. These cell lines confirmed that at least a subset of MTCs does not acquire chromosomal instability or gross chromosomal rearrangements which can be identified with molecular cytogenetic means or with high-resolution array-CGH. By our SCID mouse experiments we unequivocally demonstrated that these balanced tumor cell lines are tumorigenic. As these balanced cell lines did also not carry known pathogenic *RET*-mutations they may represent excellent models to elucidate novel pathways involved in MTC tumorigenesis.

However, our analyses did not exclude the presence of certain balanced structural rearrangements, such as small inversions or translocations below the resolution of M-

FISH, which is estimated to be in the range of approximately 3 Mb (Azofeifa *et al.*, 2000). Such rearrangements could result in fusion transforming genes. In this respect thyroid cancer is of special interest, because the existence of fusion transforming genes has been shown in both papillary and follicular thyroid cancer, but not for MTC yet. In papillary thyroid cancer somatic rearrangement, both intrachromosomal and interchromosomal, of *RET* and *NTRK1*, on chromosomes 10 and 1, respectively, generate several forms of fusion transforming genes (Bongarzone *et al.*, 1989). In addition, *RET/PTC1* is a chimeric transforming sequence generated by a paracentromeric inversion of chromosome 10q, inv(10)(q11.2q21.2) (Grieco *et al.*, 1990, Pierotti *et al.*, 1992). In follicular thyroid carcinomas a t(2;3)(q13;p25) chromosomal translocation resulting in a fusion product between *PAX8* and the peroxisome proliferator-activated receptor gamma (*PPARγ*) genes was reported (Kroll *et al.*, 2000). In analogy it is possible that other fusion-regions may be identified in MTC.

The presence of such a putative fusion transcript was apparently not assessed with the approaches we used in our study. Alternatively, we cannot exclude the presence of one or several mutations, which may have been sufficient to transform the cells. As a consequence, further approaches will be necessary. Next-generation sequencing technologies are now being exploited not only to analyze static genomes, but also dynamic transcriptomes in an approach termed RNA-seq (Wang *et al.*, 2009). These approaches provide fascinating information about transcriptional and post-transcriptional gene regulation, and they also give unique insight into the richness of transcript structures and processing on a global scale and at unprecedented resolution. RNA-seq should be capable of identifying putative fusion transcripts. Alternatively, next generation sequencing strategies, such as whole exome sequencing, could unravel the mutation status and thus pinpoint involved genes (Meyerson *et al.*, 2010). Accordingly, these cell lines should be assessable for further analyses with the new advancing technologies.

1.6. CONCLUSION

The role of *RET* and *RET* pathway in MTC pathogenesis is well documented (Drosten and Putzer, 2006, Messina and Robinson, 2007). However, tumor phenotype and progression is influenced by the genetic background, i.e. further changes in the tumor genome (Cranston and Ponder, 2003). Thus, additional initiating and driver mechanisms involved in MTC tumorigenesis remain to be uncovered.

As MTC is resistant to chemotherapy and radiation therapy both in patients and in preclinical models, an improvement in the clinical outcome is likely to be achieved only by identification of the molecular events that underlie its pathogenesis. Such molecular events could evolve to promising candidates for therapeutic targets as well as for diagnostic molecular markers in patients with MTC.

Array-CGH revealed that the vast majority of primary MTCs did not acquire multiple gains and losses. There was no gain or loss unique to hereditary or sporadic tumors. Analyses of metastases demonstrated an increase in imbalances, especially of gains, which were only rarely observed in primary tumors. Comparisons between primary tumors and metastases showed that metastasis indeed harbor a larger number of chromosomal imbalances. However, an interesting finding was that a large percentage of tumors had balanced array-CGH profiles.

Our data suggest that MTCs – in contrast to most other tumor entities – do not acquire a multitude of genomic imbalances. SCID mouse experiments performed with chromosomally normal cell lines and without RET mutations suggest that presently unknown submicroscopic genomic changes are sufficient in MTC tumorigenesis.

1.7. ACKNOWLEDGEMENTS

The authors thank Maria Langer-Winter for editing the manuscript. They are grateful to Reinhard Ullmann (Max Planck Institute for Molecular Genetics, Berlin, Germany) for providing us with software tools for array- CGH analysis. The patients were treated and material was kindly provided by B. Niederle, C. Scheuba (Section of Endocrine Surgery, Division of General Surgery, Department of Surgery, Medical University Vienna; n = 49), R. Roka and N. Neuhold (Department of Surgery and Department of Pathology, Kaiserin Elisabeth Spital, Vienna; n = 3), D. Depisch (Department of Surgery, General Hospital, Wr. Neustadt; n = 3), W. Buchinger (Division of Nuclear Medicine, Hospital Barmherzige Brüder, Graz; n = 3), G. Wolf (Division of General Surgery, Department of Surgery, Medical University Graz; n = 2), W. Pimpl (Department of Surgery, Hospital Bad Aussee; n = 1) and H.-J. Böhmig (Department of Surgery, Hospital Elisabethinen, Linz; n = 1). This work was funded by Oesterreichische Nationalbank, project number: 12569 (to R.P. and M.R.S.). Karin Flicker was supported by the PhD-Program Molecular Medicine of the Medical University of Graz.

1.8. CONTRIBUTIONS OF THE AUTHORS

Karin Flicker performed the experiments, data analysis and contributed in writing the manuscript. Peter Ulz performed sequencing and analysis of the RET sequencing data. Harald Höger performed the mouse experiments. Oskar Haas and Petra Zeitlhofer performed RET sequencing and provided data on the germline *RET* mutation status. Annemarie Behmel contributed in writing the manuscript. Bruno Niederle and Christian Scheuba provided tumor samples. Bruno Niederle provided the clinical data. Wolfgang Buchinger provided tumor samples. Roswitha Pfragner was responsible for the study design, provided the cell lines and tumor tissue, performed cell culture, and contributed in writing the paper. Michael R. Speicher was responsible for the study design, performed data analysis, and wrote the manuscript.

Part II

ARRAY COMPARATIVE GENOMIC HYBRIDIZATION IN UTERINE SARCOMAS

Section I:

Array Comparative Genomic Hybridization of Endometrial Stromal Sarcomas

Section II:

Genetic Identification of Diagnostically Challenging Uterine Smooth Muscle Tumors

2. ARRAY COMPARATIVE GENOMIC HYBRIDIZATION OF ENDOMETRIAL STROMAL SARCOMAS

2.1. ABSTRACT

Endometrial stromal sarcomas are rare neoplasms of the uterus. According to their nomenclature they can be subdivided into three groups: (1) endometrial stromal nodules (ESN), a benign neoplasm; (2) low grade endometrial stromal sarcomas (ESS) and (3) an aggressive invasive tumor termed undifferentiated endometrial sarcoma (UES). The aim of this study was to apply array-CGH to compare genomic alterations among the three tumor groups, thereby gaining new information on specific regions with copy number variations (CNVs) which might contribute to the development of the different histological grades.

ESN displayed losses on 7p, 18p and 19 and gains on 1q, 6p, 8q, 11p and had the lowest number of copy number variations detected. For ESS multiple gains and losses were detected. In more than 80% of ESS aberrations were identified, only two samples did not harbor any gains or losses. The most frequent deletions were found on chromosome 7p, 11p, 16q, 19q and 22, frequent gains were observed on chromosomes 1q, 6p, 11q, 12q and 17q. The highest number of gains and losses was detected in UES, a unique loss was identified on chromosome 13.

In general, endometrial stromal sarcomas present as a heterogeneous genotype. The number of aberrations directly correlates with their histological grading and aggressiveness. An accumulation of gains and losses was seen from ESN to ESS and UES.

2.2. INTRODUCTION

Endometrial stromal sarcomas are among the rarest neoplasms of the female genital tract. They comprise less than 5% of all primary malignant neoplasms with endometrial stromal tumors accounting for less than 10% thereof (Aaro *et al.*, 1966, Koss *et al.*, 1965). These tumors are subdivided into benign and malignant and can be divided into three groups: a) endometrial stromal nodules (ESN); b) low-grade endometrial stromal sarcoma (ESS); and c) undifferentiated endometrial sarcoma (UES) (Norris and Taylor, 1966).

2.2.1. Endometrial stromal nodules (ESN)

Endometrial stromal nodules (ESN) are benign tumors with a uniform growth pattern resembling the stromal cells of normal proliferative-phase endometrium. The tumors usually occur in women from 40 to 55 years (Dionigi *et al.*, 2002). They are low-grade, well differentiated neoplasms composed of cells resembling those of the proliferative endometrial stroma and a rich network of thin-walled arteriolar type vessels. The most important feature to distinguish ESN from ESS and UES is the status of margin (Moinfar *et al.*, 2007, Kim *et al.*, 2005).

2.2.2. Endometrial stromal sarcomas (ESS)

Endometrial stromal sarcomas (ESS) are rare tumors accounting for 0.5% of malignant uterine tumors (Aaro *et al.*, 1966, Koss *et al.*, 1965). ESS are characterized by an invasive growth pattern (Moinfar *et al.*, 2007). Usually woman at a median age range between 45 and 57 years are affected (Ashraf-Ganjoei *et al.*, 2006), the majority of cases occurs in women <50 years old (Chang *et al.*, 1990, Evans, 1982). Although ESS have propensity for local recurrence, distant metastasis is uncommon (Berchuck *et al.*, 1990, Lenhard *et al.*, 2006). Survival data are relatively inconclusive until today, a wide range was reported in literature (Ashraf-Ganjoei *et al.*, 2006, Lenhard *et al.*, 2006, Bodner *et al.*, 2001). Women suffering from ESS may have an extrauterine disease at time of presentation (Ashraf-Ganjoei *et al.*, 2006).

2.2.3. Undifferentiated endometrial stromal sarcomas (UES)

Undifferentiated endometrial sarcomas (UES) are considered high-grade that lack a specific differentiation and which do not have histological resemblance to ESS (Moinfar *et al.*, 2007). UES is an aggressive tumor which mostly occurs in postmenopausal women with a poor prognosis even when surgically treated at an early stage (Evans, 1982) (Kurihara *et al.*, 2008).

The histological distinction between UES and ESS has important implications regarding prognosis. The growth of UES is infiltrative and destructive and in contrast to ESS in patients having the more aggressive UES extrauterine metastasis is likely at time of diagnosis and life expectancy is drastically reduced (Berchuck *et al.*, 1990, Lenhard *et al.*, 2006).

2.2.4. Diagnosis and Treatment

Abnormal vaginal bleeding is usually the primary symptom at presentation at the clinics. These fast growing tumors are associated with pelvic and abdominal pain as well as pelvic or abdominal mass. In young woman uterine sarcomas are rarely seen (Lenhard *et al.*, 2006, Weitmann *et al.*, 2001).

Metastasis is usually found in lung, peritoneal cavity with omentum and upper abdomen. In bone and brain metastases are rarely seen (Chu *et al.*, 2003, Reich and Regauer, 2007). Local recurrence may occur up to 20-30 years after initial treatment (Hrzenjak *et al.*, 2005).

Diagnosis is based on fractional curettage, hysteroscopy or endometrial biopsy and even by change during hysterectomy (Reich and Regauer, 2007). Treatment options for ESS are surgery, radiotherapy, chemotherapy, hormonal therapy and treatment with tyrosine kinase inhibitors (Moinfar *et al.*, 2007, Bodner *et al.*, 2001).

2.2.5. Genetic alterations and chromosomal abnormalities

Due to the rarity of endometrial stromal tumors little is known about their epidemiology, pathogenesis, molecular biology, and about their genetic mechanisms involved. Molecular analysis showed the presence of the fusion gene JAZF1-JJAZ1 as a non-random translocation t(7;17) mostly in tumors with classical histology (Koontz *et al.*, 2001). A few cytogenetic studies have been conducted so far, which revealed a highly complex, heterogeneous pattern of chromosomal aberrations, with chromosomal gains and losses identified in more than 80% of the samples (Dal Cin *et al.*, 1992, Dal Cin *et al.*, 1991, Halbwedl *et al.*, 2005, Hrynchak *et al.*, 1994, Iliszko *et al.*, 1998, Laxman *et al.*, 1993). Identification of specific genetic changes could be useful in terms of diagnostic markers and could be relevant for treatment options.

2.2.6. Aim of the study

The aim of this study was to characterize ESN, ESS and UES on a high resolution level by array-CGH to get more information about aberrations involved in endometrial stromal tumors. Characterization of gains and losses could lead to the identification of oncogenes or tumor suppressor genes which could be responsible for the development of these tumors. Whether a transition occurs from ESN to ESS and UES or from ESS to UES is still unknown.

2.3. MATERIALS AND METHODS

2.3.1. Tumor samples and DNA Isolation

The tumor samples were formalin fixed, paraffin embedded tissue archival samples. For DNA extraction, 10 µm sections were cut and tumor tissue was needle-microdissected. DNA extraction was performed with a FFPE DNA isolation kit (#56404, Qiagen, Hilden, Germany) according to the manufacturer's instructions. The quality of the extracted DNA was evaluated using a multiplex PCR approach (van Beers *et al.*, 2006). Samples with three or four bands on a 1.5 % agarose gel were used for further array-CGH analysis. Needle-microdissection was done by Bettina Strohmeier and Bernadette Liegl, DNA isolation and quality evaluation was done by Karin Flicker.

2.3.2. Array-CGH

The platform used for hybridizations were conventional 4x44k oligonucleotide arrays (hg18) from Agilent. Samples were labeled with the Bioprime Array-CGH Genomic Labeling System (#18095-12, Invitrogen, Carlsberg, CA) according to the manufacturer's instructions. Briefly, 500 ng test DNA and female reference DNA (Promega, #G152A) were differentially labeled with dCTP-Cy5 or dCTP-Cy3 (#PA53021 and #PA55021, GE Healthcare, Piscataway, NJ). Samples were hybridized rotating for 48h at 65 °C. Slides were scanned using a microarray scanner (#G2505B; Agilent Technologies, Santa Clara, CA).

2.3.3. Data analysis

Array-CGH data were analyzed using the Agilent Genomic Workbench 5.0 software (statistical algorithm: ADM-2; sensitivity threshold: 7.0, aberration filter: 10 with an average log ratio: 0.27).

A more detailed analysis concerning the involvement of genes in a certain region was done online with the 'UCSC genome browser' (http://genome.ucsc.edu/cgi-bin/hgGateway?org=Human&db=hg18&hgsid=126007020), the query oriented data management system 'BioMart' (http://www.biomart.org/) and the online tool 'Cancer Genes' (http://cbio.mskcc.org/CancerGenes/Select.action).

2.4. RESULTS

In total 30 tumors, consisting of 4 ESN cases, 22 ESS cases and 4 UES cases, were analyzed by array-CGH.

2.4.1. Copy number changes in ESN

The benign ESN tumors did not harbor a high number of gains and losses as identified by array-CGH. Losses could be identified on chromosomes 7p, 18p and 19 and gains on chromosomes 1q, 6p, 8q, and 11q. In all fours samples aberrations could be identified but they did not share a lot of gains or losses. A region with a size of 3.2 MB on chromosome 7p was lost in 75% of the cases (3 of 4 cases).

Figure 19.Genomic aberrations in ESN by array-CGH.

The ideogram summarizes gains and losses of four ESN. The bars on each side of the zero line indicate to what percentage a region was gained or lost in our samples. Green bars

present lost regions, red bars present gained regions. Deletions were observed on chromosomes 7p, 18p and 19, gains occurred on chromosomes 1q, 6p, 8q, and 11q.

2.4.2. Copy number changes in ESS

Endometrial stromal sarcomas present as a very heterogeneous group. More than 90% of ESS show aberrations (20/22, 91%). In two out of 22 cases no gains and losses were identified. On almost every chromosome gains or losses could be detected. The single tumors do not share a lot of aberrations. The most frequent aberrations occurring in more than 15% of the samples were deletions on chromosome 7p (4/22, 18%), 11p (4/22, 18%), 16q (4/22, 18%), 19q (4/22, 18%) and 22 (5/22, 23%), frequent gains were observed on chromosomes 1q (5/22, 23%), 6p (6/22, 27%), 11q (5/22, 23%), 12q (5/22, 23%) and 17q (5/22, 23%).

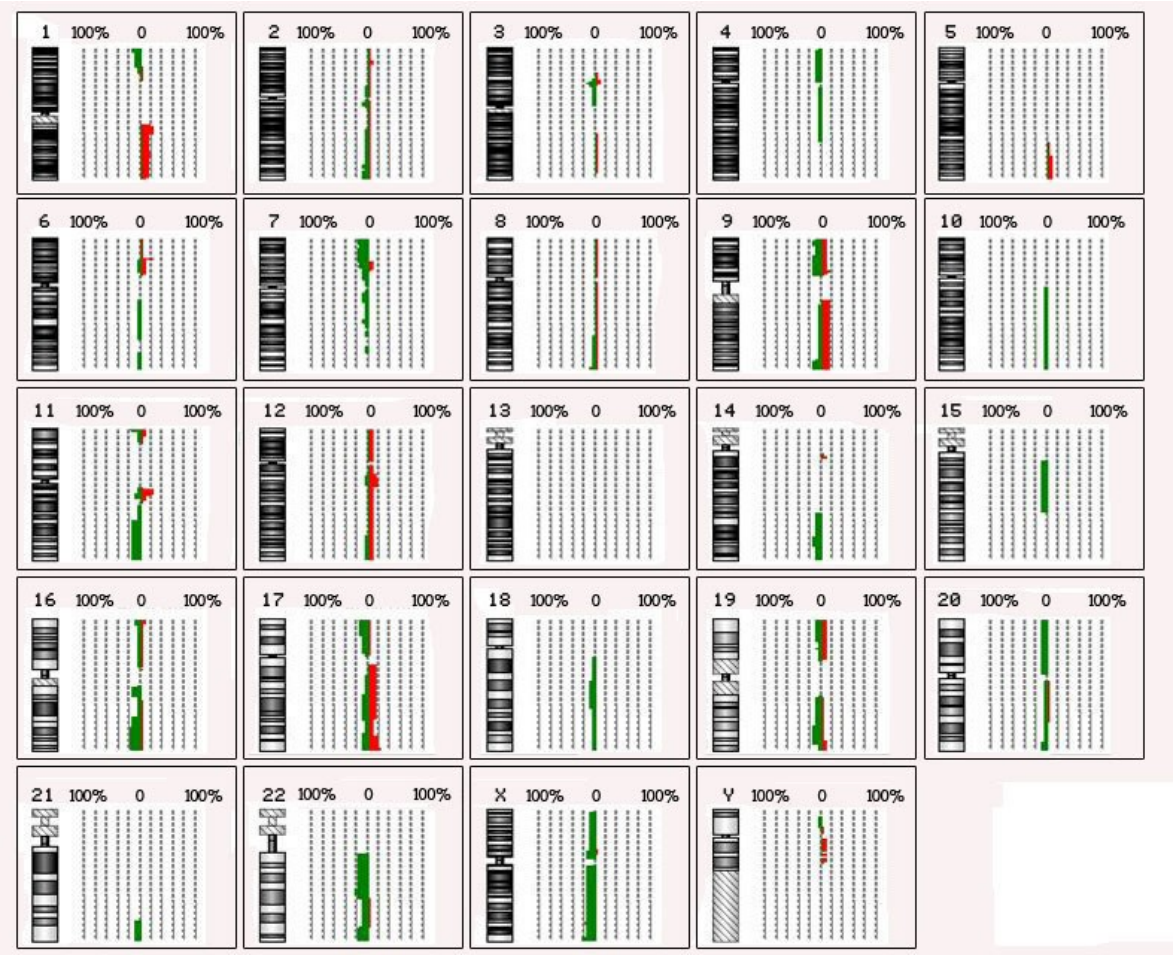

Figure 20. Genomic aberrations in ESS by array-CGH.

The ideogram summarizes gains and losses of 22 ESS. The bars on each side of the zero line indicate to what percentage a region was gained or lost in our samples. Green bars

represent lost regions, red bars represent gained regions. Two out of 22 ESS were balanced. Gains and losses were detected on almost every chromosome. Most frequent changes were defined as changes occurring in more than 15% of the samples. Any changes detected on chromosome Y are quality dependent.

2.4.3. Copy number changes in UES

UES show a high number of chromosomal aberrations. On every chromosome aberrations could be detected. Aberrations that occurred in two or more samples were gains on chromosomes 1p, 17p, 18q and 20q, and losses on chromosomes 1q, 2q, 3p, 4q, 7p, 8p, 9p, 10q, 11q, 12p, 13q, 14q, 16q, 18q and 22q. The gain on chromosome 1q and the loss on chromosome 13 could be detected in all 4 UES samples (4/4, 100%). Other frequently observed changes were deletions on chromosome 1q (3/4, 75%), 2q (3/4, 75%) and a gain on 17p (3/4, 75%).

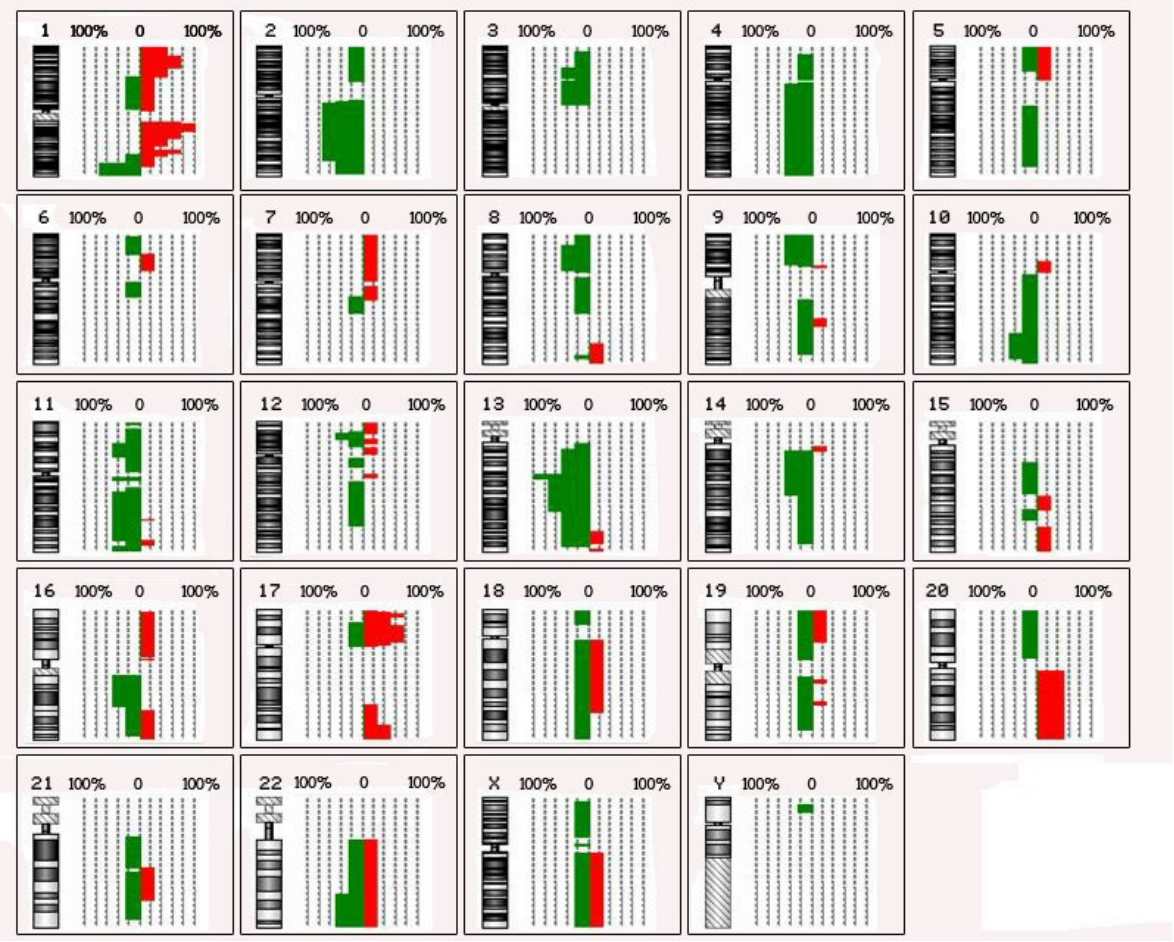

Figure 21. Genomic aberrations in UES by array-CGH.

The ideogram summarizes gains and losses of four UES. The bars on each side of the zero line indicate to what percentage a region was gained or lost in our samples. Green bars represent lost regions, red bars represent gained regions. All four UES have CNVs. Gains and losses were detected on almost every chromosome. Deletions occurred more often than gains. The gain on 1q and the loss on chromosome 13 are shared by all 4 samples. Any changes detected on chromosome Y are quality dependent.

Overall this data suggest an increase in copy number changes from the benign phenotype ESN to ESS and to the most aggressive phenotype UES.

2.5. DISCUSSION

Endometrial stromal sarcomas are among the rarest neoplasms of the female genital tract. They comprise less than 5% of all primary malignant neoplasms with endometrial stromal tumors accounting for less than 10% thereof (Aaro *et al.*, 1966, Koss *et al.*, 1965). Due to the rarity of endometrial stromal tumors little is known about their epidemiology, pathogenesis, molecular biology, and about their genetic mechanisms involved. Array-CGH is a powerful tool to scan for copy number changes in a tumor genome with a high resolution. Therefore the aim of this study was to apply array-CGH to identify tumor-specific copy number changes and to detect the genes therein, which could be used as specific markers.

Several CGH studies revealed a highly complex and heterogeneous pattern of chromosomal aberrations (Halbwedl *et al.*, 2005, Micci *et al.*, 2004, Micci *et al.*, 2006, Sandberg, 2007). Also in this study a great heterogeneity was observed between samples and between the different tumors, especially in tumors classified as ESS a great heterogeneity could be observed.

The array-CGH data obtained in this study indicate a direct correlation between the number of aberrations and the histological grading of the tumors. The benign phenotype ESN harbors the lowest number of copy number variations. In ESN cases losses were detected on 7p, 18p and 19 and gains on 1q, 6p, 8q, and 11p (Figure 20). In addition to the high heterogeneity of ESS cases a high number of copy number changes was detected among their tumor genome (Figure 20). Only a few recurring gains and losses occurring in more than 15% of the samples were detected in ESS. In two of 22 cases no gains or losses were found. UES, which is a very aggressive tumor with a poor prognosis (Koontz *et al.*, 2001), harbored the highest number of gains and losses, on all chromosomes aberrations could be detected (Figure 21). A unique loss on chromosome 13 was detected in UES cases (4/4, 100%). Chromosome 13 was not involved in copy number changes in ESN and ESS. This loss on chromosome 13 may have an important role in the development of UES and could potentially represent a driver copy number change in development of this tumor entity.

2.5.1. Specific and shared copy number changes among ESN, ESS and UES

2.5.1.1. Loss of chromosomal region 7p

Involvement of chromosomal region 7p has been described in several studies, very often in connection with the fusion gene JAZF1/JJAZ1 (Hrzenjak *et al.*, 2005, Koontz *et al.*, 2001, Sandberg, 2007). Molecular analysis showed the presence of the fusion gene JAZF1-JJAZ1 as a non-random translocation t(7;17) mostly in tumors with classical histology (Koontz *et al.*, 2001). The fusion gene JAZF1/JJAZ1 has been described in ESS and ESN tumors but not for UES cases so far. Therefore presence of the fusion gene is thought as an early event in the development and progression of ESN and ESS (Moinfar *et al.*, 2007, Hrzenjak *et al.*, 2005, Koontz *et al.*, 2001).

In this study a loss on chromosome 7p was one of the most frequent events observed among ESS tumors (4/22 cases, 18%) and ESN tumors (3/4, 75%). A loss of 7p was also observed among UES cases (2/4, 50%), one UES case showed a gain on 7p suggesting that this loss is more specific for ESN and ESS tumors. The lost region on 7p15 has a size of ~3.2 MB (chr7:24875887-28103809). The region locates 25 cancer relevant genes, among them the tumor suppressor gene HOXA5. Also the JAZF1 gene is located in this region. The loss of chromosomal region 7p may be an early event in the development of these tumors. If there is a progression from ESN to UES needs to be assessed in future studies.

2.5.1.2. Involvement of chromosome 1q

Chromosome 1 is hypothesized to play a role in the development of uterine stromal tumors. Several structural abnormalities such as trisomy or tetrasomy and isochromosome formation were described for chromosome 1q in sarcomas (Micci *et al.*, 2004, Milatovich *et al.*, 1990, Suzuki *et al.*, 1997), often resulting in a gain of chromosome 1q material (Micci *et al.*, 2004).

In this study in all three tumor entities a gain on chromosome 1q was detected. The gained region on chromosome 1 has a size of ~12.4 MB (chr1:148,523,800-160,947,845 bp) and locates a high number of genes. A total of 326 cancer relevant genes could be identified.

The presence of an oncogene that acts as driver mechanism in the development of uterine endometrial tumors can be hypothesized.

2.5.1.3. Loss of chromosome 13

An aberration solely identified in UES cases was a loss on chromosome 13. The lost region has a size of ~3.7 MB (chr13:47270425-50987005) and locates 26 cancer relevant genes. Among them there are the 4 tumor suppressor genes *FAM10A4, KCNRG, TRIM13,* and the well known tumor suppressor *RB1*. The loss of chromosome 13 was a unique event for UES as chromosome 13 was not involved in chromosomal aberrations in ESN or ESS. Therefore it can be hypothesized that this loss may present a driver mechanism for the development of UES. A loss of chromosome 13 was not described so far for UES.

2.5.1.4. Further chromosomal aberrations

Several overlapping regions could be identified among the different tumor entities (summarized in

Table 13). No commonly shared regions could be identified on chromosome 5. Chromosome 13 was only altered in UES but no gains and losses occurred in ESN and ESS. A loss on chromosome 18p was only found between ESN and UES but was not present in ESS cases.

In Table 14 an overview of all gains and losses as identified by array-CGH is presented.

Table 13. Overview of shared regions between ESN, ESS and UES. The table summarizes the shared genetic alteration between ESN, ESS and UES as identified by array-CGH.

Chromosome	Tumor Entity	Shared Genetic Alteration
1	ESN, ESS, UES	+1q
2	ESS, UES	-2q, +2q
3	ESS, UES	-3p
4	ESS, UES	-4
6	ESN, ESS, UES	+6p
7	ESN, ESS, UES ESS, UES	-7p -7q
8	ESN, ESS, UES ESS, UES	+8q -8q
9	ESS, UES	-9, +9
10	ESS, UES	-10q
11	ESN, ESS, UES ESS, UES	+11p -11q
12	ESS, UES	+12
13	UES	-13
14	ESS, UES	-14
15	ESS, UES	-15
16	ESS, UES	-16q
17	ESS, UES	-17p
18	ESN, UES ESS, UES	-18p -18q
19	ESN, ESS, UES ESS, UES	-19 +19
20	ESS, UES	-20p
21	ESS, UES	-21q
22	ESS, UES	-22, +22
X	ESS, UES	-X

Table 14. Summary of gains and losses per tumor entity. The table provides an overview of all gains and losses as identified by array-CGH.

Chromosome	Tumor Entity	Genetic Alteration	Chromosome	Tumor Entity	Genetic Alteration
1	ESN ESS UES	+1q +1q, -1p, +1p, +1p, +1q, -1p, -1q	**13**	UES	-13
2	ESS UES	-2, +2 -2, +2q	**14**	ESS UES	-14, +14 -14, +14
3	ESS UES	-3p, +3 -3	**15**	ESS UES	-15 -15, +15
4	ESS UES	-4 -4	**16**	ESS UES	-16, +16 -16p, +16p, 16q
5	ESS UES	+5q -5p, -5q, +5p	**17**	ESS UES	-17q, -17p, +17p, +17q -17q, -17p, +17p, +17q
6	ESN ESS UES	+6p -6p, -6q, +6p -6p, -6q, +6p	**18**	ESN ESS UES	-18p -18q -18p, -18q, +18q
7	ESN ESS UES	-7p -7p -7p, -7q, +7p, +7q	**19**	ESN ESS UES	-19 -19q, -19p, +19p, +19q -19q, -19p, +19p, +19q
8	ESN ESS UES	+8p -8q, +8q -8p, -8q, +8q	**20**	ESS UES	-20p, -20q, +20q -20p, +20q
9	ESS UES	-9, +9 -9p, -9q, +9p, +9q	**21**	ESS UES	-21 -21, +21
10	ESS UES	-10q, +10q -10q, +10p	**22**	ESS UES	-22 -22, +22
11	ESN ESS UES	+11p -11q, -11p, +11p, +11q -11q, -11p, +11p, +11q	**X**	ESS UES	-X -X, +X
12	ESS UES	-12q, +12 -12p, -12q, +12q			

2.6. CONCLUSION

The aim of this study was to detect copy number changes in ESN, ESS and UES by a high-resolution array-CGH. In summary the results indicate the presence of different gains and losses in ESN, ESS and UES. A great heterogeneity was observed between the single tumors, especially of tumors classified as ESS. In more than 90% of the samples gains and losses were detected by array-CGH. The number of aberrations detected in this study directly correlates with their histological grading and their clinical behavior. An accumulation of aberrations from ESN to ESS and UES was observed. Two cases of ESS did not harbor any gains or losses. A unique loss on chromosome 13 was identified in all UES cases (4/4, 100%). It may be hypothesized that this loss could have a key role in the development of UES and that it may therefore present as a driver mechanisms in development of this tumor entity.

To understand the pathogenesis of these tumors behind the observed copy number changes several investigations need to be done in future. Array-CGH studies may be useful in identifying chromosomal changes with prognostic significance but further studies are necessary to understand the molecular mechanism of endometrial carcinogenesis. The identification of potential target genes and pathway analysis on the genes with altered copy number changes will be important to provide clues to the various biological processes underlying the tumorigenesis behind these tumors.

2.7. CONTRIBUTIONS

Karin Flicker planed and conducted the experiments and performed data analysis. Bernadette Liegl, Bettina Strohmeier and Elvira Stacher provided the samples and were responsible for needle microdissection. Michael R. Speicher planed the experiments and supported data analysis. Farid Moinfar provided the samples and planed the experiments.

2.8. ACKNOWLEDGEMENTS

I thank Bernadette Liegl and Farid Moinfar from the Institute of Pathology, Medical University of Graz for providing the tumor samples.

3. GENETIC IDENTIFICATION OF DIAGNOSTICALLY CHALLENGING UTERINE SMOOTH MUSCLE TUMORS

3.1. ABSTRACT

Uterine smooth muscle neoplasms are a heterogeneous, partly diagnostically challenging group of tumors with benign, malignant and intermediate tumor subgroups. It is generally believed that uterine leiomyosarcomas (uLMS) arise de novo, rather than from a precursor lesion. However, recently it has been hypothesized that uLMS may arise from preexisting leiomyoma (LM) like areas, especially with cellular or atypical morphology. The aim of this study was to focus on the genetic aspects of diagnostically challenging smooth muscle tumors with special interest of cellular and atypical uLMs and uLMS.

In total 16 uLMs (of usual type, hormonally treated, infracted), 11 atypical/cellular uLMs and 15 uLMS were evaluated morphologically, immunohistochemically and were subsequently analysed by array-CGH. As expected, copy number changes were rarely seen in uLMs. The only recurrent aberration was loss of chromosome 19 material, which was observed in 7 out of 16 (44%) cases. In contrast, in atypical/cellular uLMs the number of copy number changes increased significantly involving almost all chromosomes. The most frequent changes (≥ 35%) included gains on chromosomes 1q, 11q, 16p and 17q and a loss of material on chromosome 13q. In uLMSs there was a further increase of copy number changes. Here frequent alterations included losses on 1p, 3p, 6p, 10q, 13q, 14q and 16q, and gains of 1q, 11q and 17p. By comparing three morphologic different uterine smooth muscle tumors we observed a continuous increase of copy number changes from uLM to cellular/atypical uLM and uLMS. Between the group of cellular/atypical uLM and uLMS several overlapping copy number changes were identified. This suggests that similar or identical pathways may be involved in the evolution of these tumors.

3.2. INTRODUCTION

Uterine smooth muscle neoplasms are a heterogeneous, diagnostically challenging group. They encompass a variety of benign and malignant neoplasms with intermediate subgroups (Takeda *et al.*, 2011, Solomon *et al.*, 2005). Among uterine smooth muscle tumors, leiomyoma is the most common benign neoplasm in women of reproductive age (Moinfar *et al.*, 2007, Sandberg, 2005a). The uterine smooth muscle neoplasms are morphologically diverse and over the years quite a number of different tumor types have been described.

3.2.1. Uterine leiomyoma

Leiomyomas (also known as uterine fibroids or fibromas) are the most common neoplasm of the female genital tract, accounting for approximately 30% of all hysterectomies performed in the United States annually (Sandberg, 2005a, Cramer and Patel, 1990). Leiomyomas are benign tumors of the uterus that arise from smooth muscle cells of the myometrum (Packenham *et al.*, 1997, Mashal *et al.*, 1994) and they mainly occur in reproductive-aged women with a frequency of 77% (Cramer and Patel, 1990). Leiomyomas may lead to infertility, spontaneous abortions, premature labor, or dystocia (Greenberg and Kazamel, 1995). There is strong evidence that these tumors are hormonally responsive and dependent. Woman which are affected mostly have multiple tumors with an average number 6.5 tumors (Cramer and Patel, 1990). Usually a hysterectomy is the treatment endpoint, however, one treatment option for women who did not complete childbearing may be a myomectomy, a more conservative surgical procedure (Ligon and Morton, 2001).

3.2.2. Atypical leiomyoma

Atypical leiomyoma are considered a subgroup of LM and clinically benign. Bizarre leiomyomas have a wider range of morphologic changes and mitotic activity (Downes and Hart, 1997). Although most leiomyomas usually do not present a diagnostic problem, subtypes of leiomyoma mimic malignancy in one or more aspects and so are of great interest (Toledo and Oliva, 2008). Bizarre leiomyoma, also referred to as atypical, pleomorphic, or symplastic leiomyoma, is one of a group of rare leiomyoma variants that require precise histopathological evaluation so that they are not misinterpreted as

leiomyosarcomas (Downes and Hart, 1997, Downes and Hart, 1997, Sung *et al.*, 2009). Especially when diagnosed in a younger woman, this tumor leads to challenging treatment issues involving fertility preservation (Takeda *et al.*, 2011).

3.2.3. Uterine leiomyosarcoma

Uterine leiomyosarcomas (LMS) are malignant neoplasms that arise from smooth muscle tissue. In contrast to the common benign smooth muscle tumors uterine LMS are rare, comprising approximately 1 % of all uterine malignancies (Packenham *et al.*, 1997). Nevertheless, LMS is the most common uterine sarcoma (Cramer and Patel, 1990, Gattas *et al.*, 1999, Kazmierczak *et al.*, 1998, Klotzbucher *et al.*, 1999, Schoenmakers *et al.*, 1995, Mittal *et al.*, 2009).

Leiomyosarcomas most commonly occur in the fifth and sixth decade of live presenting with symptoms like dysfunctional uterine bleeding and pelvic pain (Brooks *et al.*, 2004, Mayerhofer *et al.*, 1999). Uterine leiomyosarcoma is an aggressive tumor with the tendency to recur locally and metastasize mainly to lung and liver. The 5-year survival rate varies between 45% and 60% depending on the different studies presented over the years. However, stage of disease is a significant prognostic factor related to the outcome (Brooks *et al.*, 2004, Mayerhofer *et al.*, 1999, Dinh *et al.*, 2004, Giuntoli *et al.*, 2003, Hsieh *et al.*, 2003).

The diagnostic criteria to assess malignancy in uterine smooth muscle neoplasms are based on a landmark study by Bell et al in 1994 (Bell *et al.*, 1994). Leiomyomas and LMS are distinguished by a number of macro- and microscopic features. The crucial features include nuclear atypia (notably at low power, 10x objective), mitotic activity per 10 hpf and the presence or absence of coagulative necrosis (Bell *et al.*, 1994). The diagnosis of malignancy is made, if a combination of these criteria is fulfilled.

3.2.4. Molecular genetics and cytogenetics

On molecular basis leiomyomas are thought to represent separate clonal neoplasms arising independently within the uterus (Mashal *et al.*, 1994). Approximately a half of leiomyomas show karyotypically detectable chromosomal abnormalities, including copy number

changes in addition to structural changes that include translocations, deletions and inversions (Pandis *et al.*, 1991, Rein *et al.*, 1991). Molecular data on uterine spindle cell leiomyosarcomas and leiomyosarcomas occurring in soft tissues demonstrate that these tumors are cytogenetically characterized by complex numerical and structural changes that may vary from one cell to the next within a tumor, highlighting the degree of genomic instability (Fletcher *et al.*, 1990, Sreekantaiah *et al.*, 1993).

Different types of abnormalities have been identified, these are simple karyotypes showing deletion of 7q and 3q, t(12;14), and rearrangements involving 6p21, 3q and 10q and trisomy 12 (Ligon and Morton, 2001, Vanharanta *et al.*, 2007, Vanharanta *et al.*, 2005). A number of gains and losses were detected in LMS but consistent structural chromosomal alterations have not been noted. The most frequent losses by CGH include 10q, 11q, 13q and 2p, the most common gains were found on Xp, 1q, 5p, 8q, and 17p (Moinfar *et al.*, 2007, Packenham *et al.*, 1997, Christacos *et al.*, 2006). In addition frequent loss of heterozygosity particularly for chromosomes 10 and 13 has been described (Hu *et al.*, 2001, Quade *et al.*, 1999).

The wide range of chromosomal aberrations indicates that multiple different pathogenetic mechanisms may be involved in tumor formation. Overall, specific genetic patterns do not correlate with morphology. However, deletion of 1p seems to be associated with leiomyomas with cellular and atypical morphology (Christacos *et al.*, 2006). The large number of chromosomal aberrations detected in LMS suggests that an increased genetic instability plays a role in the formation of these tumors (Packenham *et al.*, 1997).

3.2.5. Pathogenesis of smooth muscle neoplasms

Little is known about the pathogenesis of uterine smooth muscle neoplasms. It is not known so far if uterine leiomyosarcomas arise de novo or from precursor lesions (Mittal *et al.*, 2009). Most published histologic, immunohistochemical, cytogenetic, molecular, comparative genomic hybridization and gene expression studies indicated a difference between leiomyoma and leiomyosarcoma (Sandberg, 2005a, Sandberg, 2005b). A recent study on the origin of uterine LMS hypothesized that LMS could arise from pre-existing leiomyoma-like areas, especially with cellular or atypical morphology (Mittal *et al.*, 2009).

3.2.6. Aim of the study

Genetic alterations such as DNA copy number amplification and losses are known to be involved in the activation of proto-oncogenes and in the inactivation of tumor suppressor genes, respectively. It is known that an accumulation of genetic changes leads to disturbances in the cell cycle of cells and therefore to tumor progression. The aim of this study was to focus on genetic aberrations of diagnostic challenging smooth muscle tumors by array-CGH. The goal was to compare gains and losses of LM, atypical LM and LMS to detect similarities and differences among the three different tumor types.

3.3. MATERIALS AND METHODS

3.3.1. Tumor Samples and Immunophenotyping

Cellular, atypical and hormonally treated leiomyomas and leiomyosarcomas (and leiomyosarcoma metastases) as well as leiomyomas of usual type and normal myometrium as a control group were retrieved from the pathology files from the departments of pathology of Medical University of Graz Austria, Yale University USA, and "Hospices Civilis de Lyon" France. Four micron hematoxylin and eosin stained sections generated from formalin-fixed paraffin embedded tissue were reviewed to confirm the diagnoses prior to inclusion in the study. All cases were re-examined at the pathology Graz to evaluate the following histologic features: type of margin (circumscribed or infiltrative), cell types (epithelioid, spindled, multinucleated), cytologic atypia (mild, moderate, severe), necrosis (absent, present, ischemic or coagulative) and mitotic rate (expressed as the number of mitotic figures per 10 high power fields [HPFs] in the most mitotic area, using a 40X objective and a 10X ocular, field size 0.25 mm^2). The Envision Plus detection system (Dako, Carpinteria, CA) was used for all antibodies. Tumor samples were provided by Farid Moinfar and Bernadette Liegl from the Pathology Graz. Immunophenotyping was performed by Bernadette Liegl.

3.3.2. DNA Isolation

For DNA extraction 10 µm sections were cut, tumor areas of interest were marked and needle-microdissected. DNA extraction was performed with a FFPE DNA isolation kit (Qiagen, #56404) according to the protocol 'Isolation of genomic DNA from FFPE tissue sections'. The quality of the DNA was evaluated using a multiplex PCR approach (van Beers *et al.*, 2006). Samples with three or four bands on a 1.5 % agarose gel were used for further array-CGH analysis. Needle microdissection was done by Bernadette Liegl, DNA isolation and quality evaluation was done by Karin Flicker.

3.3.3. Array-CGH

The platforms used for hybridizations were 4x44 k oligonucleotide arrays (hg18) and 8x60k oligonucleotide arrays (hg18) from Agilent. Samples were labeled with the Bioprime Array-CGH Genomic Labeling System (#18095-12, Invitrogen, Carlsberg, CA) according to the manufacturer's instructions. Briefly, 500 ng test DNA and female reference DNA (Promega, #G152A) were differentially labeled with dCTP-Cy5 or dCTP-Cy3 (#PA53021 and #PA55021, GE Healthcare, Piscataway, NJ). Samples were hybridized rotating for 48h at 65 °C. Slides were scanned using a microarray scanner (#G2505B; Agilent Technologies, Santa Clara, CA). Data were analyzed using the Agilent Genomic Workbench 5.0 software (statistical algorithm: ADM-2; sensitivity threshold: 8.0; aberration filter: 10; log ratio: 0.3).

3.4. RESULTS

The smooth muscle tumors were characterized by their clinical features, their macroscopic and microscopic features and by array-CGH.

3.4.1. Clinical Features of the Patients

The age at presentation ranged from 32 to 61 years (median age 43.5 years) in patients with usual leiomyoma, hormonally treated/infracted and cellular LM. The age range in patients with at-LM was from 32 to 67 years (median age 45 years) and from 46 to 80 years (median age 57.5 years) in patients with LMS.

The tumor size ranged from 0.5 cm to 14.3 cm (median size of 3.4 cm in LM) in LM and from 2.5 cm to 20 cm in at-LM (median size of 5.5 cm in LM). The size in LMS ranged from 5 cm to 10.5 cm (median size of 9 cm in LM).

The clinical history presentation of LM patients was fibroid mass, (probably) Lupron therapy, benign ovarian mass, bleeding, pelvic mass, and uterine mass. In at-LM patients fibroid mass, uterine mass, rapidly growing, pelvic mass and bleeding, LMS patients clinical history presentation was uterine mass, postmenopausal and an enlarged uterus.

Details of the clinical features of the LM, at-LM and LMS diagnosed patients in this study are summarized in the following tables (Table 15 - Table 17).

Table 15. Clinical features of patients with Leiomyoma (LM). The table summarizes the case number, age, size [cm], clinical history, procedure, diagnosis, mitoses per 10 hpf, necrosis and other diagnostic factors (if applicable).
Hyst … hysterectomy; Myomect … myomectomy

Case	Age	Size [cm]	Clinical History	Procedure	Diagnosis	Mitoses [x/10 hpf]	Necrosis	Other
S10-340 7L	37	14.3	post Lupron Therapy	Myomect	Leiomyoma with Necrosis	0-1	Present ischemic	
S10-340 2) 1L		0.8	post Lupron Therapy		Leiomyom with no Necrosis	0-1	Absent	
S10-3311	41	3.8	Probable Lupron Therapy	Myomect	Leiomyoma	1-2	Present Multifocal	
S08-8539	61	2.2	Benign ovarian mass	Hyst	Leiomyoma with focal atypia	0-1	Absent	
S10-8561	40	10	Parasitic fibroid, supropubic mass Lupron treatment	Myomect	Infarcted Leiomyoma	0-1	Infarct	Desmin
S10-8206-2 -1	42	0.5	Menorrhagia	Hyst	LM with focal atypia, bilateral ovarian teratoma	0-1	Absent	
S05-9067	51	unk	Bleeding	Hyst	Cellular LM	0-1	Absent	
S05-17839	52	unk	Enlarging pelvic mass	Hyst	LM with edema and prominent vasculature	0-1	Absent	
102554/2006	45	12	Fibroid	Hyst	LM	0-1	Absent	
129259/2008 (T1)	41	0.8	Fibroid	Hyst	LM	0	Absent	
129259/2008 (T2)	41	0.6	Fibroid	Hyst	LM	0	Absent	
122152/2008 (T)	39	8	Fibroid	Hyst	LM	0	Absent	
122152/2008 (T1)	39	6	Fibroid	Hyst	LM	0	Absent	
110387/2008 (T1)	41	0.7	Fibroid	Hyst	LM	0	Absent	
110387/2008 (T2)	41	1	Fibroid	Hyst	LM	0	Absent	
9674/2007 (T1)	32	3	Uterine mass	Hyst	LM	0	Absent	
S07-13445-9	32	12.5	Post Lupron Therapy	Myomect	LM	1	Present	
S10-3311-7A	41	3.8	Probable Lupron Therapy	Myomect	LM	2	Present	

Table 16. Clinical features of patients with Atypical Leiomyoma (at-LM). The table summarizes the case number, age, size [cm], clinical history, procedure, diagnosis, mitoses per 10 hpf, necrosis and other diagnostic factors (if applicable).
Hyst … hysterectomy; Myomect … myomectomy

Case	Age	Size [cm]	Clinical History	Procedure	Diagnosis	Mitoses [x/10 hpf]	Necrosis	Other
S09-7031	49	10	Rapidly growing	Hyst	at-LM	2 at 400X	Present ischemic	p16+ ER-PR+ Ki 67 15%
S08-12580	36	20	Pelvic mass	Hyst	at-LM	1-2	Absent	
S10-8654	30	8.5	Fibroid	Myomect	at-LM	0-1	Absent	Desmin
120920/2008 T2	40	unk	Fibroid	Hyst	at-LM	2	Absent	
56320/2007	45	2.5	Fibroid	Hyst	at-LM	4	Absent	
80344/2006 (T1)	67	3	Bleeding	Hyst	at-LM	1	Absent	
58543/2004	50	7	Fibroid	Hyst	at-LM	2	Absent	
135631/2002	74	7	Fibroid	Hyst	at-LM	1	Absent	
87445/2002 (T1)	73	2.5	Fibroid	Hyst	at-LM	2	Absent	
34714/1997	36	5.5	Fibroid	Hyst	at-LM	2	Absent	
7043/0(07-36-302	50	5	Fibroid	Hyst	at-LM	5	Absent	
1076/08 D	38	unk	Fibroid	Hyst	at-LM	3	Absent	
9674/2007 (T2)	32	4	Uterine mass	Hyst	at-LM	4	Absent	

Table 17. Clinical features of patients with Leiomyosarcoma (LMS). The table summarizes the case number, age, size [cm], clinical history, procedure, diagnosis, mitoses per 10 hpf, necrosis and other diagnostic factors (if applicable). Hyst … hysterectomy; Myomect … myomectomy

Case	Age	Size [cm]	Clinical History	Procedure	Diagnosis	Mitoses [x/10 hpf]	Necrosis	Other
One patient 3 samples S98-878 S02-9238 S05-229	51	unk	Enlarged uterus	Hyst	LMS LMS Metastasis LMS Metastasis omentum	up to 43	Present	Many studies available P53+ in 80 % Ki 67 40 %
S06-3466	80	8	Enlarged uterus	Hyst	LMS with osteoclastic giant cells	18	Present, cystic grossly	
S07-45677	59	8	Postmenopausal	Hyst	LMS with epitheloid features and clear cell changes	>30	Present	
S08-41602	57	10.5	Uterine mass	Hyst	LMS and incidentalendometrioid carcinoma	2	Present	
79271/2007	46	5	Uterine mass	Hyst	LMS (G3)	32	Absent	SMA+ Desmin + h-Caldesmon+
9591/05	51	9	Uterine mass	Hyst	LMS (G3)	12	Present	SMA+ Desmin + h-Caldesmon+
889 Bei KN (T1) 889 Bei KN (T2)	61	10	Uterine mass	Hyst	LMS			
2907/10 14 Neu 2907/10 3 Neu 2907/10 4 Neu 2907/10 9 Neu	58	14	Uterine mass	Hyst	LMS	17	Present	

3.4.2. Macroscopic features

All leiomyomas including the usual type, hormonally treated, infracted, cellular and all atypical leiomyomas were well circumscribed tumors with a firm, rubbery consistency. From the atypical leiomyomas some cases showed a more yellowish cutting surface and a softer consistency. All leiomyosarcomas were less well circumscribed. They were characterized by a softer consistency and on cutting surface the color varied from gray to cream. In the majority of leiomyosarcomas necrosis appearing as yellow or green areas and red to brown areas of haemorrhage were present.

3.4.3. Microscopic features

3.4.3.1. Leiomyomas

All leiomyomas showed classic morphologic features. The tumors were composed of intersecting fascicles of spindle cells. The spindle cells showed bland elongated nuclei with blunt ends and eosinophilic cytoplasm. Nuclear atypia, necrosis and mitotic activity were not seen. One of the leiomyomas was characterized by the presence of prominent vascular structures and an oedematous matrix. The hormonally treated leiomyomas as well as the infracted leiomyoma showed identical morphology to the leiomyomas of usual type; however, areas of ischemic necrosis were sometimes present. Ischemic necrosis was defined as an area of necrosis surrounded by a zone of granulation tissue and hyalinized tissue typical for ischemia. The cellular leiomyoma showed classic morphologic features, however, the cellularity was significantly higher than in the leiomyomas of usual type described above.

3.4.3.1. Atypical leiomyomas

The atypical leiomyomas were characterized by the presence of cells with enlarged and pleomorphic nuclei. Focal multinucleated tumor cells were seen. The atypical cells were unifocal, multifocal or diffuse in distribution. The pleomorphic cells were appreciable in low power examination (10x objectives). The nuclei were enlarged with coarse chromatin and sometimes nuclear pseudoinclusions were present. Abundant eosinophilic cytoplasm

was seen. The mitotic activity ranged from 0 to 4 per 10/hpf. Coagulative necrosis was absent.

3.4.3.1. Leiomyosarcoma

The vast majority of the analysed leiomyosarcomas were composed purely of spindle cells. The spindle cells were arranged in interlacing fascicles and the nuclei showed moderate to severe nuclear atypia. The nuclei were hyperchromatic and nucleoli were sometimes appreciable. The mitotic activity varied between 2 and 43 per 10/hpf.

3.4.4. Genetic characterization by array-CGH

Array-CGH was performed to identify genomic alterations in 20 cases LM, including cellular and hormonally treated cases, 13 cases at-LM and 14 cases LMS. By comparing the chromosomal aberrations between the tumor entities a continuous increase in gains and losses was observed from LM to at-LM and LMS. As expected, aberrations were rarely seen in LM but were high in at-LM and LMS. A high number of gains and losses detected in at-LM were also found in LMS, additional gains and losses could be identified in LMS.

3.4.4.1. Copy number changes in LM

In general a low number of gains and losses was identified in LM by array-CGH. In 16/20 LM cases gains and losses were identified, the remaining samples (4/20, 20%) did not harbor any copy number changes. No recurring aberrations were detected among the different LM changes, in general deletions were detected more often than gains. In LM most frequent changes (≥ 20% of cases) were losses on chromosomes 1q (4/20, 20%), 7q (5/20, 25%), 16p (4/20, 20%), 17 (5/20, 25%), 19 (7/20, 35%), and 22 (4/20, 20%), and gains on chromosomes 1q (4/20, 20%) and 16 (4/20, 20%) (Figure 22).

One high level amplification was detected on chromosomal region Xq22.3. This region was identified to be gained at a higher level also in samples of atypical LM and LMS.

Figure 22. Genomic aberrations of leiomyoma (LM), n=20.

The ideogram summarizes gains and losses of 20 cases of leiomyoma. The bars on each side of the chromosome indicate to what percentage a region was gained or lost in our samples. Green bars present lost regions, red bars present gained regions. Deletions were mostly observed on chromosome 19. In 16 out of 20 samples gains and losses were identified.

3.4.4.2. Copy number changes in atypical LM

In general atypical LM show a high number of genomic aberrations and a higher frequency of copy number changes compared to LM could be identified. In all 13 at-LM cases gains or losses were identified (Figure 23).

All 13 cases of at-LM showed a high number of gains and losses, aberrations were detected on every chromosome. Most frequent changes occurring in ≥ 20% of cases in at-LM were losses on chromosomes 1p (3/13, 23%), 1p (3/13, 23%), 4p (3/13, 23%), 4q (3/13, 23%), 6q (3/13, 23%), 7q (3/13, 23%), 12p (3/13, 23%), 12q (3/13, 23%), 13 (8/13, 62%), 16q (3/13, 23%), 17p (3/13, 23%), 19p (3/13, 23%), and 22 (3/13, 23%), and gains on chromosomes 1p (5/13, 38%), 1q (7/13, 54%), 3p (5/13, 38%), 6p (4/13, 31%), 7q (5/13, 38%), 8q (3/13, 23%), 9q (4/13, 31%), 11q (7/13, 54%), 12q (4/13, 31%), 14 (3/13, 23%), 16p (7/13, 54%), 16q (4/13, 31%), 17p (4/13, 31%), 17q (6/13, 46%), 19p (6/13, 46%), 19q (7/13, 54%), 20 (4/13, 31%), and 22 (5/13, 38%) (Figure 23).

Figure 23. Genomic aberrations of atypical leiomyoma (at-LM), n=13.

The ideogram summarizes gains and losses of 13 cases of atypical leiomyoma. The bars on each side of the chromosome indicate to what percentage a region was gained or lost in our samples. Green bars present lost regions, red bars present gained regions.

3.4.4.3. Chromosomal changes in LMS

LMS harbored the highest number of gains and losses and compared to at-LM and LM (Figure 24).

Figure 24. Genomic aberrations of leiomyosarcoma (LMS), n=14.

The ideogram summarizes gains and losses of 14 cases of leiomyosarcoma. The bars on each side of the chromosome indicate to what percentage a region was gained or lost in our samples. Green bars present lost regions, red bars present gained regions.

In all 14 LMS multiple gains and losses were identified, deletions occurred in general more often than gains. Copy number changes were splitted to aberration occurring in ≥ 50%, ≥ 30% and ≥ 20% of the cases.

Most frequent changes occurring in ≥ 50% of cases were losses on chromosomes 1p (8/14, 57%), 6p (6/14, 64%), 10q (9/14, 64%), 13 (12/14, 86%), 14 (7/14, 50%),and 16 (7/14, 50%), and gains on chromosomes 1q (7/14, 50%), 8q (7/14, 50%), and 17 p (8/14, 57%) (Figure 24).

Most frequent changes occurring in ≥ 30% of cases were losses on chromosomes 1q (6/14, 43%), 3p (6/14, 43%), 4p (5/14, 36%), 7p (5/14, 36%), 7q (6/14, 43%), 8q (5/14, 36%), 9p (5/14, 36%), 11 (4/14, 29%), 16 (7/14, 50%), 17 (6/14, 42%), 19q (5/14, 36%), 20q and 21 (7/14, 43%), and 22 (7/14, 43%), and gains on chromosomes 7q (5/14, 36%), 9q (5/14, 36%), 11q (6/14, 43%), 16p (5/14, 36%), 17q (6/14, 43%) and 19p (6/14, 43%) (Figure 24).

Most frequent changes occurring in ≥ 20% of cases were losses on chromosomes 2q (4/14, 29%), 3q (4/14, 29%), 4q (4/14, 29%), 8p (4/14, 29%), 9p (5/14, 36%), 9q (3/13, 22%), 10p (4/14, 29%), 11 (4/14, 29%), 18p (4/14, 29%), 19p (4/14, 29%), 20q (4/14, 29%), and gains on chromosomes 3p (3/14, 21%), 4q (3/14, 21%), 11p (4/14, 29%), 12 p (3/14, 22%), 12 q (4/14, 29%), 14q (3/14, 22%), 15 (3/14, 22%), and 19q (4/14, 29%), 20 (4/14, 29%), and 22 (4/14, 29%) (Figure 24).

In general the array-CGH data underline a high similarity between at-LM and LMS. In general at-LM demonstrate a similar pattern of gains and losses compared to LMS, with additional CNCs in LMS. Based on the overlapping genetic features seen in atLM and LMS we hypothesize that similar or identical pathways may be involved in the evolution of these tumors.

3.5. DISCUSSION

The pathogenesis of mesenchymal tumors and their malignant counterparts is still poorly understood. To date it is still under debate if benign mesenchymal tumors have the potential for malignant transformation. From a cytogenetic point of view uterine smooth muscle tumors are a heterogeneous group and common driver mechanisms for the development of uterine LM, at-LM and LMS remain to be discovered.

In this study array-CGH was used to identify genomic gains and losses in a group of benign and malignant smooth muscle tumors of the uterus including 20 cases LM (usual type, cellular, and hormonally treated), 13 cases at-LM and 14 cases LMS to identify genomic regions which may harbor genes critical for the development of these tumors and leading to a better understanding of the pathogenesis of these tumors.

This study demonstrates that more than 90% of investigated smooth muscle tumors, benign and malignant, show gains and losses by array-CGH. Different CGH studies of LM and LMS have been performed in the past which showed already the involvement different gains and losses in these tumors (Moinfar *et al.*, 2007, Laxman *et al.*, 1993, Sandberg, 2005a, Mittal *et al.*, 2009, Sreekantaiah *et al.*, 1993, Sandberg, 2005b).

Here an increase in CNCs was observed from benign to malignant tumors. As expected, LM showed a low number of CNCs, a few cases of LM did not show any gains or losses (4/20 cases, 20%). In contrast, all cases of at-LM and LMS showed a high number of CNCs involving all chromosomes. Some of these gains and losses were shared between at-LM and LMS (Figure 25). LMS harbor additional gains and losses compared to at-LM which may occur from increasing genomic instability during tumor progression. Cytogenetic data on LMS indicate that these tumors typically have highly complex karyotypes with numerical and structural abnormalities (Packenham et al. 1997, Sreekantaiah C et al. 1993, Christacos N. et al. 2006; Sandberg AA, 2004).

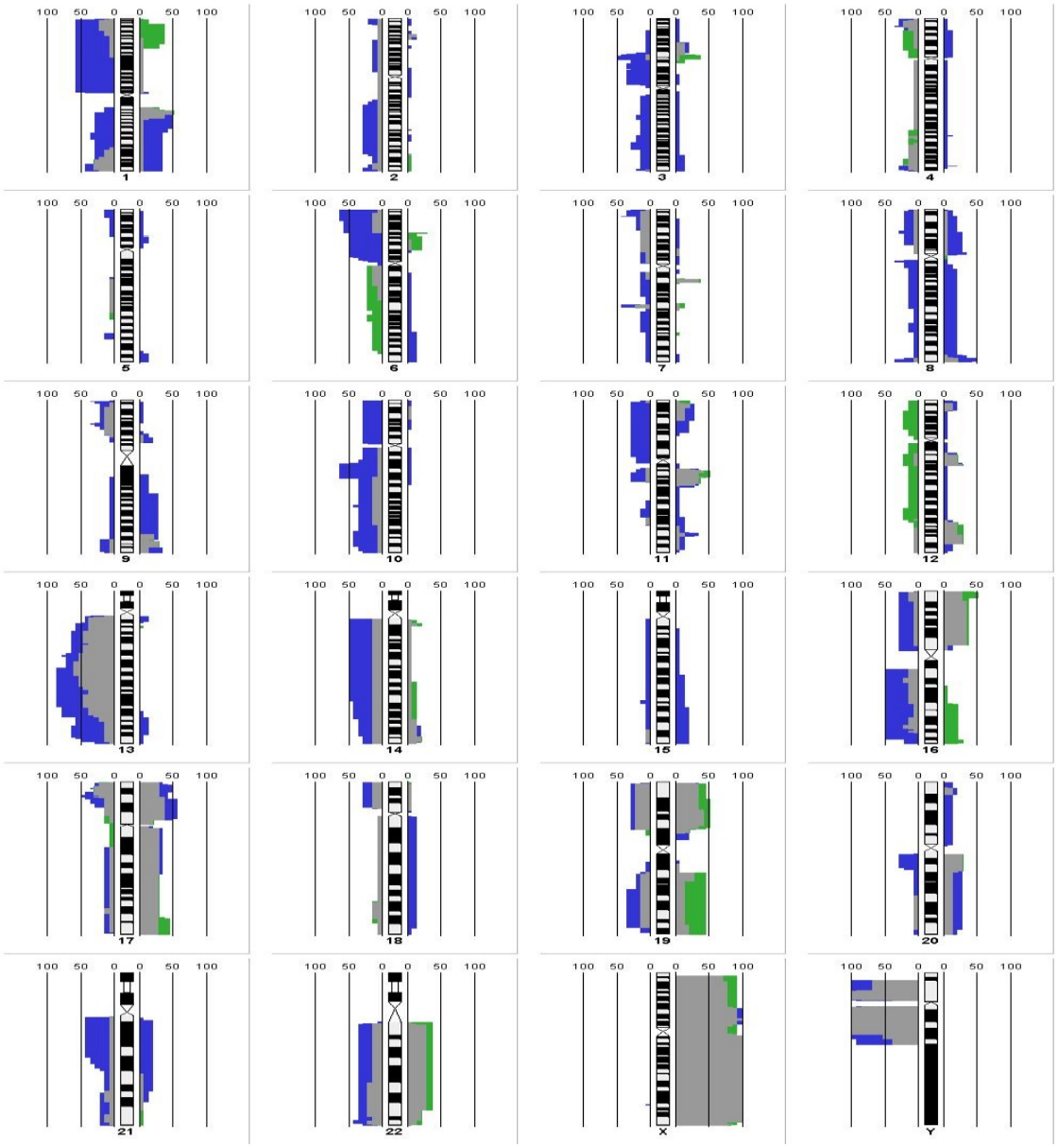

Figure 25. Comparism of copy number changes between at-LM and LMS.

This figure shows an overlay of the copy number changes between at-LM and LMS. Green regions represent at-LM, blue regions LMS and overlapping copy number changes are displayed in grey. Changes to the left represent losses, changes to the right represent gains.

As can be seen from the figures a number of CNCs are shared between at-LM and LMS. Shared gains and losses between at-LM and LMS were losses on chromosome 1q, 4p, and 13, 16q, 17p, 19p, and 22, and gains on chromosome 1q, 7q, 12q, 16p, 17, 19p, 20q, and 22. The most important differences between at-LM and LMS are losses on chromosomes 1, 3, 6, 10, 14, and 16, and 21 which were primarily found in LMS. This suggests that genes of importance in the development and progression of LMS may be located at these

sites. In this study the size of lost and gained regions is relatively big and a number of cancer related genes are located in this regions. Further studies will be necessary to identify potential target genes.

The fact that at-LM resemble the array-CGH profile of LMS is very interesting as at-LM are benign from a histologic point of view. Literature shows that changes seen in soft tissue leiomyosarcomas and uterine leiomyosarcomas are suggesting similar genetic pathways of these smooth muscle neoplasms (Mittal *et al.*, 2009, Mittal *et al.*, 2009) and that uterine LMS could arise from pre-existing leiomyoma-like areas that often have symplastic or cellular morphology (Mittal *et al.*, 2009). The array-CGH data obtained in this study strengthen this observation.

3.5.1. Chromosomal changes identified in uterine smooth muscle tumors

3.5.1.1. Involvement of chromosome 13

A chromosome that was frequently deleted in cases of at-LM and LMS was chromosome 13q. In our samples deletions on chromosome 13q14.2 occurred in 86% of LMS cases and in 62% of at-LM. Interestingly, this region harbors the tumor suppressor *RB1*. The involvement of *RB1* in different malignancies as well as a role of *RB1* in LMS is a frequent reported finding (Classon and Harlow 2003) and an involvement of region 13q13-q14 was published by other groups (Sreekantaiah et al 1993(Wang *et al.*, 2003) and was related to a more aggressive phenotype with a shorter survival time (Wang *et al.*, 2003). Interestingly in our study in 62% of at-LM this region was deleted.

3.5.1.2. Involvement of chromosome 7

Chromosomal region 7q11.23 was gained in 3 of 20 LM cases (15%), 5 of 14 LMS cases (36%), and in 5 of 13 at-LM cases (38%). The size of the gain is ~3.2 MB (chr7:72891088-75969802, hg19) and locates 41 cancer related genes among them the oncogene *HSPB1*. Del(7)(q22q23) is described to occur in a frequency of ~17% in karyotypically abnormal fibroids (Ozisik 1993a, Sargent 1994, Ishwad 1995, Ishwad 1997, Vanharanta et al, 2007).

3.5.1.3. Involvement of chromosome 10

Loss of DNA copy number of 10q is associated with aggressive behavior of leiomyosarcomas (Hu *et al.*, 2001). Large tumors and tumors associated with metastases showed commonly 10q deletions. In 35% of LMS samples analyzed by array-CGH a deletion of the whole chromosome arm 10q, in 64% of cases a deletion in chromosomal region 10q, in 15% of at-LM cases and in one case of LM a loss of 10q could be identified. In our cases the shortest region of overlap in 10q21.3 has a size of ~1.4 MB (chr10:68100738-69467832, hg19) and locates the two genes CTNNA3 and LRRTM3.

3.5.1.4. Involvement of chromosome 1

Losses and structural rearrangements of chromosome 1, particularly as ring chromosome, were described to occur with other chromosomal abnormalities (Sandberg AA, 2005; Mark J et al, 1990; Mark J et al, 1988, Havel G et al., 1989; Christacos N.C. 2006). Deletions of parts or whole arms of chromosome 1 were found frequently in our samples. LMS show a loss of 1p in 57% of the samples. In atypical LM and in LM losses of terminal parts of both ends of chromosome 1 were found. A gain on chromosome 1, especially region 1q21.3-q23.1 was found in 4/20, 20% LM cases, in 7/13, 54% at-LM cases and in 7/14, 50% LMS cases. The shortest region of overlap is in chromosomal region 1q21.3-q23.1 with a size of ~3.1 MB (chr1:153635083-156764762; hg19) and locates 101 cancer related genes, among them the five oncogenes *SLC39A1, RAB13, RAB25, EFNA1, and CKS1B*.

3.5.1.5. Involvement of chromosome 3

A 4.8 MB loss on chromosome 3p21.31-21.1 was detected in 43% of LMS cases, however, chromosome 3 was not lost in LM or at-LM cases. Changes including chromosome 3 were described in literature to occur at low frequency (Hodge JC and Morton CC, 2007). As chromosome 3 is only lost in LMS cases in our study this loss could be specific for LMS. The lost region on chromosome 3p has a size of (chr3:48483519-53288687; hg19) and locates 114 cancer related genes, among them the tumor suppressor genes *BAP1, CYB561D2, HYAL1*.

3.6. CONCLUSION

Changes seen in soft tissue leiomyosarcomas and uterine leiomyosarcomas are suggesting that the pathogeneses of these smooth muscle neoplasms may follow similar genetic pathways (Mittal *et al.*, 2009). In this study a low number of gains and losses was detected in LM, in contrast, at-LM and LMS harbored a high number of gains and losses. The relatively similar genomic alterations in at-LM and LMS suggest that these tumors may develop from similar genetic pathways and that a transition may occur from at-LM to LMS. Additionally, the cytogenetic heterogeneity of LM, at-LM and LMS suggests an involvement of multiple pathways with multiple hits needed for tumor development and progression. Until now it is not clear which genetic aspects lead to the development of LM, at-LM and LMS and key events for their development remain to be discovered.

3.7. ACKNOWLEDGEMENTS

Thank you to Bernadette Liegl and Farid Moinfar from the Institute of Pathology, Medical University of Graz for providing and organizing the tumor samples not only from the Medical University of Graz but also from Yale University USA, and "Hospices Civilis de Lyon".

3.8. CONTRIBUTIONS

Karin Flicker planed and performed the experiments and data analysis. Bernadette Liegl provided the tumor samples, the clinical information and performed needle-microdissection. Farid Moinfar provided tumor samples and planed the experiments.

4. APPENDIX - PART I: HIGH-RESOLUTION ANALYSIS OF ALTERATIONS IN MTC GENOMES

4.1. SUPPLEMENTARY TABLE 1: SUMMARY OF CHROMOSOMAL GAINS AND LOSSES FOR EACH TUMOR

All base pair positions are according to hg18.

4.1.1. Hereditary MTC cases (n=11)

The following tumors were balanced (and are therefore not listed): H1, H4, H5, H8, H10

H2					
Chr	**Cytoband**	**Start [bp]**	**Stop [bp]**	**Aberration Size [bp]**	**Copy Number Change**
chr8	q22.3 - q24.3	103.731.731	146.250.965	42.519.235	Gain

H3					
Chr	**Cytoband**	**Start**	**Stop**	**Aberration Size [bp]**	**Copy Number Change**
chr1	p36.33 - p12	842.526	120.387.087	119.544.562	Loss
chr1	p36.33 - p33	981.092	46.796.400	45.815.309	Loss
chr1	q21.1 - q44	143.638.935	246.329.477	102.690.543	Loss
chr2	q35	217.256.548	217.261.895	5.348	Loss
chr4	p16.3 - p11	133.213	48.758.199	48.624.987	Loss
chr4	q11 - q35.2	52.383.658	190.706.472	138.322.815	Loss
chr5	p15.33 - p12	204.537	45.376.547	45.172.011	Loss
chr5	q11.2 - q35.3	52.182.965	180.559.134	128.376.170	Loss
chr7	q22.1	98.814.496	102.140.976	3.326.481	Loss
chr15	q11.2 - q26.3	18.741.516	100.283.019	81.541.504	Loss

H6					
Chr	**Cytoband**	**Start [bp]**	**Stop [bp]**	**Aberration Size [bp]**	**Copy Number Change**
chr1	p36.33 - p33	777.154	46.796.400	46.019.247	Gain
chr1	q21.1 - q22	144.151.404	154.612.279	10.460.876	Gain
chr3	p21.31 - p21.1	46.848.262	53.190.771	6.342.510	Gain
chr3	q11.2 - q13.31	95.329.130	115.564.979	20.235.850	Loss
chr3	q29	197.118.167	198.405.985	1.287.819	Gain
chr5	q35.2 - q35.3	175.243.241	179.964.488	4.721.248	Gain

chr6	p21.33 - p21.1	30.632.368	44.334.676	13.702.309	Gain
chr7	p22.3 - p22.1	887.188	6.837.609	5.950.422	Gain
chr7	q11.21 - q11.23	64.944.535	75.807.738	10.863.204	Gain
chr7	q21.3 - q22.1	97.690.443	102.343.323	4.652.881	Gain
chr7	q31.1 - q31.33	107.625.491	124.218.243	16.592.753	Loss
chr8	q22.3 - q24.12	104.962.729	120.187.777	15.225.049	Loss
chr9	q33.3 - q34.3	125.833.183	140.128.884	14.295.702	Gain
chr10	q24.1 - q24.33	98.382.543	105.421.426	7.038.884	Gain
chr11	p11.2	45.854.645	48.065.426	2.210.782	Gain
chr11	q12.2 - q13.4	60.641.647	73.619.849	12.978.203	Gain
chr12	p13.31	6.102.129	8.102.746	2.000.618	Gain
chr12	q13.11 - q14.1	47.008.908	56.492.179	9.483.272	Gain
chr12	q24.11 - q24.31	107.703.537	122.808.604	15.105.068	Gain
chr14	q24.2 - q24.3	72.432.103	75.067.922	2.635.820	Gain
chr15	q15.1 - q21.1	38.488.281	42.795.205	4.306.925	Gain
chr16	p13.3 - p11.2	361.931	31.620.665	31.258.735	Gain
chr16	q21 - q24.3	64.010.749	88.601.765	24.591.017	Gain
chr17	p13.3 - p13.1	585.856	9.510.961	8.925.106	Gain
chr17	q11.2 - q25.3	24.007.613	78.300.608	54.292.996	Gain
chr17	q21.33 - q22	47.062.751	51.923.074	4.860.324	Loss
chr19	p13.3 - p13.11	323.961	19.699.685	19.375.725	Gain
chr19	q13.11 - q13.43	37.590.737	61.512.241	23.921.505	Gain
chr20	q11.21 - q13.2	29.351.938	50.222.569	20.870.632	Gain
chr22	q11.21 - q13.31	16.435.103	45.486.984	29.051.882	Gain

H7					
Chr	**Cytoband**	**Start [bp]**	**Stop [bp]**	**Aberration Size [bp]**	**Copy Number Change**
chr1	p36.33 - p12	751.596	120.449.334	119.697.739	Loss
chr1	p36.33 - p33	777.154	46.796.400	46.019.247	Loss
chr1	p32.2 - p12	56.858.721	119.725.036	62.866.316	Loss
chr1	q21.1 - q22	143.638.935	154.718.285	11.079.351	Loss
chr3	p21.31 - p21.1	46.694.060	53.867.826	7.173.767	Loss
chr4	q12 - q35.2	56.151.753	189.695.132	133.543.380	Loss
chr7	q11.21 - q11.23	64.944.535	75.807.738	10.863.204	Loss
chr7	q21.3 - q22.1	97.637.020	102.343.323	4.706.304	Loss
chr8	q24.3	143.623.121	146.092.035	2.468.915	Loss
chr9	q33.3 - q34.3	129.159.725	140.128.884	10.969.160	Loss
chr11	p15.5	283.443	2.138.447	1.855.005	Loss
chr11	q12.2 - q13.3	60.377.924	69.840.706	9.462.783	Loss
chr12	q13.11 - q14.1	47.008.908	56.503.038	9.494.131	Loss
chr12	q24.11 - q24.33	107.709.648	131.856.662	24.147.015	Loss
chr16	p13.3 - p11.2	36.566	31.601.429	31.564.864	Loss
chr17	p13.3 - p13.1	585.856	9.349.373	8.763.518	Loss

chr17	q12 - q25.3	31.135.214	77.992.343	46.857.130	Loss
chr19	p13.3 - p13.11	231.880	19.699.685	19.467.806	Loss
chr19	q13.11 - q13.42	37.554.515	60.930.783	23.376.269	Loss
chr22	q11.21 - q13.33	16.435.103	49.525.271	33.090.169	Loss

H9					
Chr	**Cytoband**	**Start [bp]**	**Stop [bp]**	**Aberration Size [bp]**	**Copy Number Change**
chr7	q11.21 - q11.23	65.025.291	75.807.738	10.782.448	Loss
chr7	q22.1	98.093.249	102.311.168	4.217.920	Loss
chr8	q24.3	143.623.121	146.037.529	2.414.409	Loss
chr17	p13.3 - p13.1	505.704	9.349.373	8.843.670	Loss
chr19	p13.3 - p13.11	231.880	19.699.685	19.467.806	Loss
chr19	q13.11 - q13.42	38.668.269	60.848.954	22.180.686	Loss

H11					
Chr	**Cytoband**	**Start [bp]**	**Stop [bp]**	**Aberration Size [bp]**	**Copy Number Change**
chr15	q11.1 - q11.2	18.362.355	19.988.504	1.626.150	Gain
chr17	q25.1	69.343.797	70.183.632	839.836	Gain

4.1.2. Sporadic MTC cases with a *RET* mutation (n=15)

The following cases were balanced (and are therefore not listed): S4, S8, S14

S1					
Chr	**Cytoband**	**Start [bp]**	**Stop [bp]**	**Aberration Size [bp]**	**Copy Number Change**
chr3	p25.3	8.994.311	10.306.422	1.312.112	Loss
chr3	p21.31 - p21.1	50.634.902	51.979.577	1.344.676	Loss
chr3	q21.3	128.515.674	130.802.608	2.286.935	Loss
chr3	q22.3 - q23	140.307.347	143.995.564	3.688.218	Loss
chr13	q12.13 - q12.3	24.640.862	29.321.920	4.681.059	Loss
chr13	q14.2 - q14.3	47.357.404	50.278.439	2.921.036	Loss
chr14	q32.2 - q32.33	96.980.172	106.330.010	9.349.839	Loss
chr21	q11.2 - q21.1	13.897.497	15.778.033	1.880.537	Loss
chr22	q11.21 - q13.33	16.749.638	49.525.271	32.775.634	Loss
chr22	q12.1 - q12.3	25.251.509	31.727.477	6.475.969	Loss

S2					
Chr	**Cytoband**	**Start [bp]**	**Stop [bp]**	**Aberration Size [bp]**	**Copy Number Change**
chr1	p36.33 - p11.2	554.068	120.885.991	120.331.924	Loss
chr1	p36.31 - p33	5.972.059	47.587.905	41.615.847	Loss
chr1	p32.2 - p12	56.892.264	119.675.140	62.782.877	Loss
chr1	q21.1 - q21.2	143.706.443	149.584.358	5.877.916	Loss
chr4	q11 - q35.2	52.383.658	190.887.401	138.503.744	Loss
chr7	q11.22 - q11.23	70.231.904	75.982.831	5.750.928	Loss

S3					
Chr	**Cytoband**	**Start [bp]**	**Stop [bp]**	**Aberration Size [bp]**	**Copy Number Change**
chr1	q21.1 - q44	143.638.935	247.179.432	103.540.498	Gain
chr1	q21.1 - q23.1	143.638.935	155.169.678	11.530.744	Gain
chr1	q24.2 - q41	166.538.602	221.182.063	54.643.462	Gain
chr2	p25.3 - q11.1	32.244	95.198.404	95.166.161	Gain
chr2	q11.1 - q37.3	95.403.666	242.690.178	147.286.513	Gain
chr3	p26.3 - p11.1	68.749	90.336.893	90.268.145	Gain
chr4	p16.3 - p11	61.352	48.758.199	48.696.848	Gain
chr4	q22.2 - q35.2	94.794.389	191.133.809	96.339.421	Gain
chr5	p15.33 - q11.1	204.537	49.726.129	49.521.593	Gain
chr5	q11.1 - q35.3	50.058.777	180.617.248	130.558.472	Gain
chr6	p25.3 - q11.1	352.031	62.760.249	62.408.219	Gain
chr6	q11.1 - q27	62.815.577	170.732.174	107.916.598	Gain
chr7	p22.2 - p22.1	4.340.344	6.837.609	2.497.266	Loss
chr7	q22.1	98.895.133	102.140.976	3.245.844	Loss
chr8	p23.3 - q11.1	211.411	47.800.700	47.589.290	Gain
chr8	q11.1 - q24.3	47.987.761	144.766.759	96.778.999	Gain
chr11	q11	54.866.423	55.573.029	706.607	Gain
chr11	q11 - q25	55.635.935	134.373.758	78.737.824	Gain
chr15	q11.1 - q26.3	18.362.355	100.283.019	81.920.665	Gain
chr16	q11.2 - q24.3	45.121.858	88.638.909	43.517.052	Gain
chr16	q11.2 - q12.1	45.312.314	46.954.007	1.641.694	Gain
chr17	p13.3 - q11.1	210.770	22.857.162	22.646.393	Gain
chr17	q11.1 - q25.3	22.952.317	78.586.437	55.634.121	Gain
chr18	p11.32 - q11.1	4.116	17.030.723	17.026.608	Gain
chr18	q11.1 - q23	17.030.723	76.018.550	58.987.828	Gain
chr19	p13.11 - p12	19.686.840	24.132.722	4.445.883	Gain
chr21	q11.2 - q22.3	13.562.063	46.892.494	33.330.432	Gain
chr22	q11.1 - q13.33	15.908.242	49.525.271	33.617.030	Loss

S5					
Chr	**Cytoband**	**Start [bp]**	**Stop [bp]**	**Aberration Size [bp]**	**Copy Number Change**
chr1	p36.33 - p11.2	749.422	120.885.991	120.136.570	Loss
chr4	q11 - q35.2	52.383.658	190.887.401	138.503.744	Loss

S6					
Chr	**Cytoband**	**Start [bp]**	**Stop [bp]**	**Aberration Size [bp]**	**Copy Number Change**
chr1	p36.33 - p11.2	842.526	120.982.834	120.140.309	Loss
chr4	p16.3 - p11	211.249	48.758.199	48.546.951	Loss
chr4	q11 - q35.2	52.383.658	191.133.809	138.750.152	Loss
chr22	q11.1 - q13.2	15.908.242	41.237.931	25.329.690	Loss

S7					
Chr	**Cytoband**	**Start [bp]**	**Stop [bp]**	**Aberration Size [bp]**	**Copy Number Change**
chr1	p36.33 - p11.2	554.068	120.885.991	120.331.924	Loss
chr1	p31.3 - p13.3	67.984.280	109.620.005	41.635.726	Loss
chr2	p25.3	978.075	1.649.497	671.423	Gain
chr2	q11.2 - q37.3	96.172.570	242.690.178	146.517.609	Gain
chr7	p22.3 - p11.2	149.068	56.754.495	56.605.428	Gain
chr7	q11.21 - q36.3	62.153.388	158.602.640	96.449.253	Gain
chr7	q22.2 - q31.33	105.090.871	126.197.468	21.106.598	Gain
chr17	p13.3 - p11.2	350.991	21.054.334	20.703.344	Loss

S9					
Chr	**Cytoband**	**Start [bp]**	**Stop [bp]**	**Aberration Size [bp]**	**Copy Number Change**
chr22	q11.1 - q13.33	15.908.242	49.525.271	33.617.030	Loss

S10					
Chr	**Cytoband**	**Start [bp]**	**Stop [bp]**	**Aberration Size [bp]**	**Copy Number Change**
chr1	p36.33 - p12	749.422	120.449.334	119.699.913	Loss
chr6	p22.1 - p21.31	28.579.301	33.655.725	5.076.425	Loss
chr8	p23.3 - p11.23	445.082	38.704.081	38.259.000	Loss
chr9	p24.3 - p21.1	204.167	31.464.040	31.259.874	Loss
chr13	q12.11 - q34	18.975.349	114.077.263	95.101.915	Loss
chr16	q11.2 - q24.3	45.172.398	87.891.244	42.718.847	Gain
chr17	p13.3 - p13.1	585.856	8.184.122	7.598.267	Loss
chr19	p13.3 - p13.11	231.880	19.650.002	19.418.123	Loss
chr19	q13.11 - q13.42	38.668.269	60.853.886	22.185.618	Loss

S11					
Chr	**Cytoband**	**Start [bp]**	**Stop [bp]**	**Aberration Size [bp]**	**Copy Number Change**
chr1	p33 - p11.2	49.187.166	120.885.991	71.698.826	Loss
chr22	q11.1 - q13.33	15.908.242	49.525.271	33.617.030	Loss

S12					
Chr	**Cytoband**	**Start [bp]**	**Stop [bp]**	**Aberration Size [bp]**	**Copy Number Change**
chr2	p25.3 - q11.1	196.012	94.892.966	94.696.955	Loss
chr3	q11.2 - q29	97.749.583	198.794.989	101.045.407	Loss

S13					
Chr	**Cytoband**	**Start [bp]**	**Stop [bp]**	**Aberration Size [bp]**	**Copy Number Change**
chr3	p21.31 - p21.1	46.596.619	53.867.826	7.271.208	Loss
chr6	p22.1 - p21.31	28.579.301	33.655.725	5.076.425	Loss
chr7	q21.3 - q22.1	97.637.020	102.343.323	4.706.304	Loss
chr9	q33.3 - q34.3	129.159.725	140.128.884	10.969.160	Loss
chr11	q12.2 - q13.4	59.754.144	71.325.821	11.571.678	Loss
chr12	q13.11 - q14.1	47.008.908	56.503.038	9.494.131	Loss
chr12	q24.11 - q24.31	109.599.951	122.711.086	13.111.136	Loss
chr16	p13.3 - p11.2	36.566	31.601.429	31.564.864	Loss
chr17	p13.3 - p13.1	585.856	9.264.074	8.678.219	Loss
chr17	q12 - q25.3	33.805.434	77.992.343	44.186.910	Loss
chr19	p13.3 - p13.11	231.880	19.699.685	19.467.806	Loss
chr19	q13.11 - q13.42	38.668.269	60.853.886	22.185.618	Loss
chr22	q11.21 - q13.33	16.435.103	49.525.271	33.090.169	Loss

S15					
Chr	**Cytoband**	**Start [bp]**	**Stop [bp]**	**Aberration Size [bp]**	**Copy Number Change**
chr1	p32.3 - p12	52.043.557	120.146.842	68.103.286	Loss
chr3	p26.3 - p11.1	224.527	90.264.318	90.039.792	Loss
chr3	q11.2 - q29	95.157.223	199.288.361	104.131.139	Loss
chr15	q11.2 - q26.3	20.424.929	99.630.363	79.205.435	Loss

4.1.3. Sporadic MTC cases without a *RET* mutation (n=26)

The following tumors were balanced (and are therefore not listed): S19, S24, S25, S33

S16					
Chr	**Cytoband**	**Start [bp]**	**Stop [bp]**	**Aberration Size [bp]**	**Copy Number Change**
chr4	p16.3 - p11	62.247	48.758.199	48.695.953	Loss
chr4	q11 - q35.2	52.383.658	190.352.061	137.968.404	Loss
chr7	p22.3 - p11.2	149.068	56.531.775	56.382.708	Loss
chr7	q11.21 - q36.3	65.025.291	158.781.538	93.756.248	Loss
chr15	q11.2 - q26.3	19.108.924	99.630.363	80.521.440	Loss
chr18	q11.1 - q23	17.054.751	76.083.258	59.028.508	Loss
chr22	q11.1 - q13.33	15.908.242	49.525.271	33.617.030	Loss

S17					
Chr	**Cytoband**	**Start [bp]**	**Stop [bp]**	**Aberration Size [bp]**	**Copy Number Change**
chr1	p36.33 - p12	751.596	120.449.334	119.697.739	Loss
chr1	q21.1 - q44	143.638.935	247.179.432	103.540.498	Loss
chr22	q11.1 - q13.33	15.908.242	49.525.271	33.617.030	Loss

S18					
Chr	**Cytoband**	**Start [bp]**	**Stop [bp]**	**Aberration Size [bp]**	**Copy Number Change**
chr19	p13.3 - p12	323.961	24.093.968	23.770.008	Loss

S20					
Chr	**Cytoband**	**Start [bp]**	**Stop [bp]**	**Aberration Size [bp]**	**Copy Number Change**
chr1	p36.33 - p12	751.596	120.449.334	119.697.739	Loss

S21					
Chr	**Cytoband**	**Start [bp]**	**Stop [bp]**	**Aberration Size [bp]**	**Copy Number Change**
chr1	p36.33 - p11.2	842.526	120.982.834	120.140.309	Loss
chr1	q21.1 - q44	143.638.935	247.179.432	103.540.498	Loss

S22					
Chr	**Cytoband**	**Start [bp]**	**Stop [bp]**	**Aberration Size [bp]**	**Copy Number Change**
chr16	p13.3 - p11.1	46.071	34.847.526	34.801.456	Gain
chr16	q11.2 - q24.3	45.172.398	88.622.123	43.449.726	Gain

S23					
Chr	**Cytoband**	**Start [bp]**	**Stop [bp]**	**Aberration Size [bp]**	**Copy Number Change**
chr1	p36.33 - p11.2	751.596	120.885.991	120.134.396	Loss
chr1	p36.31 - p33	5.917.949	46.683.368	40.765.420	Loss
chr1	p36.21	13.903.740	14.806.781	903.042	Loss
chr1	p36.11 - p35.3	26.668.410	29.400.550	2.732.141	Loss
chr1	p35.1 - p34.3	33.538.135	35.095.223	1.557.089	Loss
chr1	p33	47.757.028	50.439.726	2.682.699	Loss
chr1	p32.3 - p12	55.676.662	120.449.334	64.772.673	Loss
chr1	p13.3 - p13.2	108.680.558	115.055.260	6.374.703	Loss
chr1	q21.1 - q44	143.699.872	247.118.628	103.418.757	Loss
chr1	q21.1 - q23.1	144.124.545	155.113.898	10.989.354	Loss
chr1	q21.3	150.223.179	151.576.690	1.353.512	Loss
chr1	q22	153.372.347	154.511.627	1.139.281	Loss
chr1	q23.3 - q25.2	160.947.445	176.215.486	15.268.042	Loss
chr1	q25.3 - q32.1	183.544.689	197.882.610	14.337.922	Loss
chr1	q32.1	199.633.226	204.169.103	4.535.878	Loss
chr1	q32.3 - q41	211.481.873	221.182.063	9.700.191	Loss
chr2	p25.1	9.135.487	11.391.743	2.256.257	Loss
chr2	p23.3 - p23.2	24.006.550	27.854.195	3.847.646	Loss
chr2	p22.3	31.996.375	32.781.716	785.342	Loss
chr2	p22.2 - p22.1	38.399.431	39.266.674	867.244	Loss
chr2	p13.1 - p11.2	75.177.571	84.799.148	9.621.578	Gain
chr2	p11.2	85.054.135	85.779.538	725.404	Loss
chr2	q11.2	96.143.659	96.947.123	803.465	Loss
chr2	q14.3 - q21.1	127.522.246	131.621.693	4.099.448	Loss
chr2	q33.1	201.430.495	201.858.277	427.783	Loss
chr2	q33.1 - q33.2	202.787.522	204.103.009	1.315.488	Loss
chr2	q33.3 - q35	208.984.326	215.714.254	6.729.929	Gain
chr2	q35	218.517.593	220.182.836	1.665.244	Loss
chr3	p25.3	9.265.382	10.306.422	1.041.041	Loss
chr3	p21.31 - p21.1	46.729.265	53.674.949	6.945.685	Loss
chr3	p14.3 - p14.2	56.627.015	58.573.817	1.946.803	Loss
chr3	p13 - p11.1	73.714.189	90.264.318	16.550.130	Gain
chr3	q21.3	129.776.828	131.172.730	1.395.903	Loss
chr3	q27.1 - q27.2	184.234.305	187.138.313	2.904.009	Loss
chr3	q29	195.797.116	199.251.329	3.454.214	Loss
chr4	p16.3 - p16.1	145.900	8.359.881	8.213.982	Loss
chr4	p14	38.984.514	40.503.948	1.519.435	Loss
chr4	p13 - p12	42.182.124	47.291.581	5.109.458	Gain
chr4	q12	57.238.714	57.631.818	393.105	Loss
chr4	q21.22 - q21.23	83.493.304	84.746.131	1.252.828	Loss
chr5	p15.1 - p13.3	17.766.284	31.244.817	13.478.534	Gain

chr5	q11.1 - q11.2	50.094.582	52.607.429	2.512.848	Gain
chr5	q13.2	68.439.732	68.900.170	460.439	Loss
chr5	q23.2	125.801.797	126.215.336	413.540	Loss
chr5	q31.2	137.547.051	137.830.534	283.484	Loss
chr5	q33.1	149.738.758	150.627.135	888.378	Loss
chr5	q35.1 - q35.3	170.670.272	180.617.248	9.946.977	Loss
chr6	p22.3	17.520.696	18.332.393	811.698	Loss
chr6	p21.33 - p21.1	30.234.715	44.495.477	14.260.763	Loss
chr6	p21.33 - p21.32	31.586.601	32.013.239	426.639	Loss
chr6	q13	73.990.578	74.420.942	430.365	Loss
chr6	q15 - q16.2	90.922.413	99.392.781	8.470.369	Gain
chr6	q25.1	149.867.990	151.881.179	2.013.190	Loss
chr7	p22.3 - p22.1	289.341	6.837.609	6.548.269	Loss
chr7	p21.3 - p15.3	8.183.128	20.656.357	12.473.230	Gain
chr7	p13	43.648.776	45.070.231	1.421.456	Loss
chr7	p12.3 - p11.2	48.109.127	55.150.628	7.041.502	Gain
chr7	p11.2	55.605.323	56.150.069	544.747	Loss
chr7	q11.21 - q11.23	64.907.043	76.078.892	11.171.850	Loss
chr7	q11.22	66.308.980	71.271.388	4.962.409	Loss
chr7	q21.11 - q21.3	77.668.192	96.624.761	18.956.570	Gain
chr7	q21.3 - q22.1	97.458.242	101.901.301	4.443.060	Loss
chr7	q33	135.263.760	137.194.927	1.931.168	Gain
chr8	p12 - p11.23	37.673.288	38.667.907	994.620	Loss
chr8	q24.3	141.111.376	146.144.978	5.033.603	Loss
chr9	p22.1	18.940.659	19.501.724	561.066	Loss
chr9	p13.3 - p13.2	32.972.595	36.647.430	3.674.836	Loss
chr9	q31.3 - q32	113.347.242	116.433.944	3.086.703	Loss
chr9	q33.3 - q34.3	125.833.183	140.128.884	14.295.702	Loss
chr9	q33.3 - q34.13	129.209.062	133.327.473	4.118.412	Loss
chr10	p14 - p13	11.829.240	15.249.336	3.420.097	Loss
chr10	q21.3	69.834.320	70.841.079	1.006.760	Loss
chr10	q23.2	88.267.131	88.855.043	587.913	Loss
chr10	q24.32 - q24.33	103.740.122	105.196.986	1.456.865	Loss
chr11	p15.5 - p15.4	186.766	4.084.022	3.897.257	Loss
chr11	p15.4	8.227.796	10.285.626	2.057.831	Loss
chr11	p15.1	18.223.212	18.677.765	454.554	Loss
chr11	p15.1 - p13	20.896.118	31.732.174	10.836.057	Gain
chr11	p11.2	46.194.612	48.038.503	1.843.892	Loss
chr11	q12.1	56.884.263	57.331.065	446.803	Loss
chr11	q12.2 - q14.1	60.453.624	77.881.951	17.428.328	Loss
chr11	q12.3 - q13.2	61.946.842	67.109.444	5.162.603	Loss
chr11	q23.3	116.128.327	119.102.149	2.973.823	Loss
chr12	p13.33	302.961	1.007.702	704.742	Loss
chr12	p13.33	2.776.593	3.015.806	239.214	Loss

chr12	p13.31	6.058.256	9.031.994	2.973.739	Loss
chr12	p13.2	10.453.331	11.072.969	619.639	Gain
chr12	p13.2 - p13.1	11.965.659	12.986.021	1.020.363	Loss
chr12	p11.21	31.326.650	32.930.828	1.604.179	Loss
chr12	q13.11 - q14.1	47.174.625	56.517.093	9.342.469	Loss
chr12	q21.1 - q21.33	70.593.567	90.696.355	20.102.789	Gain
chr12	q24.11 - q24.33	107.512.288	132.231.480	24.719.193	Loss
chr12	q24.23 - q24.31	118.772.150	122.743.353	3.971.204	Loss
chr13	q12.11	18.652.920	21.011.618	2.358.699	Loss
chr13	q21.1 - q32.1	52.523.623	94.062.800	41.539.178	Gain
chr13	q22.1	72.396.103	72.630.492	234.390	Loss
chr13	q33.1 - q33.3	100.837.894	108.602.909	7.765.016	Gain
chr14	q11.2 - q12	19.827.045	23.877.483	4.050.439	Loss
chr14	q12	24.238.052	30.040.054	5.802.003	Gain
chr14	q13.1 - q13.2	33.942.549	34.942.054	999.506	Loss
chr14	q21.1 - q22.1	39.307.829	48.874.670	9.566.842	Gain
chr14	q22.1	49.093.370	49.926.811	833.442	Loss
chr14	q24.2 - q24.3	72.469.986	77.459.141	4.989.156	Loss
chr14	q31.1 - q31.3	81.320.805	87.763.756	6.442.952	Gain
chr14	q32.31 - q32.33	101.467.325	105.067.740	3.600.416	Loss
chr15	q11.2	20.335.687	21.208.577	872.891	Loss
chr15	q15.1	38.552.112	39.684.507	1.132.396	Loss
chr15	q22.31	62.292.133	64.629.036	2.336.904	Loss
chr15	q24.1 - q24.2	72.539.942	73.754.558	1.214.617	Loss
chr15	q26.1	88.093.920	89.430.956	1.337.037	Loss
chr16	p13.3 - p11.2	125.498	31.449.816	31.324.319	Loss
chr16	p12.3 - p11.2	16.806.918	28.051.335	11.244.418	Loss
chr16	p11.2	28.242.379	31.298.591	3.056.213	Loss
chr16	q13 - q21	54.980.477	57.306.344	2.325.868	Loss
chr16	q21	57.784.982	64.078.253	6.293.272	Gain
chr16	q21 - q24.3	64.983.947	88.651.933	23.667.987	Loss
chr16	q22.1	66.074.897	69.159.883	3.084.987	Loss
chr17	p13.3 - p11.2	84.087	21.054.334	20.970.248	Loss
chr17	p13.3 - p13.1	222.982	8.203.652	7.980.671	Loss
chr17	q11.2 - q25.3	23.548.474	78.623.371	55.074.898	Loss
chr17	q21.2 - q21.31	37.122.892	40.660.335	3.537.444	Loss
chr17	q25.1 - q25.3	70.436.180	78.300.608	7.864.429	Loss
chr18	q21.31 - q21.32	53.357.558	54.863.176	1.505.619	Loss
chr18	q21.33 - q22.2	59.461.828	65.596.569	6.134.742	Gain
chr19	p13.3 - p13.11	258.517	19.687.240	19.428.724	Loss
chr19	q13.11 - q13.43	37.540.308	63.761.216	26.220.909	Loss
chr19	q13.32 - q13.33	50.008.855	55.986.476	5.977.622	Loss
chr20	p13 - p12.3	2.179.111	5.733.948	3.554.838	Loss
chr20	q11.21 - q13.2	29.436.337	50.255.147	20.818.811	Loss

chr20	q11.21 - q11.23	29.501.335	35.316.253	5.814.919	Loss
chr20	q13.33	59.942.509	62.266.665	2.324.157	Loss
chr21	q21.1 - q21.2	18.540.495	23.986.496	5.446.002	Gain
chr21	q22.11 - q22.3	31.446.665	46.811.728	15.365.064	Loss
chr22	q11.1 - q13.33	15.908.242	49.525.271	33.617.030	Loss
chr22	q11.23 - q12.1	24.161.484	27.217.336	3.055.853	Loss
chr22	q12.3	31.173.092	33.907.894	2.734.803	Loss
chr22	q13.1 - q13.2	36.298.038	41.845.253	5.547.216	Loss

S26

Chr	Cytoband	Start [bp]	Stop [bp]	Aberration Size [bp]	Copy Number Change
chr12	q12	40.839.968	41.262.211	422.244	Gain

S27

Chr	Cytoband	Start [bp]	Stop [bp]	Aberration Size [bp]	Copy Number Change
chr2	q35	217.256.548	219.003.046	1.746.499	Loss
chr13	q12.11 - q34	18.601.503	114.077.263	95.475.761	Loss
chr22	q11.1 - q13.33	15.908.242	49.525.271	33.617.030	Loss

S28

Chr	Cytoband	Start [bp]	Stop [bp]	Aberration Size [bp]	Copy Number Change
chr3	p21.31	47.058.961	50.172.130	3.113.170	Loss
chr5	p15.33 - p11	204.537	45.865.553	45.661.017	Gain
chr5	q11.1 - q14.3	50.058.777	89.289.163	39.230.387	Gain
chr7	q21.3 - q22.1	96.807.009	101.900.581	5.093.573	Loss
chr19	p13.3 - p13.11	774.354	19.699.685	18.925.332	Loss
chr21	q11.2 - q22.3	14.334.342	46.847.350	32.513.009	Loss

S29

Chr	Cytoband	Start [bp]	Stop [bp]	Aberration Size [bp]	Copy Number Change
chr1	p36.33 - p11.2	749.422	120.885.991	120.136.570	Loss
chr2	q35	217.256.548	219.375.201	2.118.654	Loss
chr18	p11.32 - q11.1	170.029	16.976.246	16.806.218	Loss
chr18	q11.1 - q23	17.054.751	76.083.258	59.028.508	Loss
chr22	q11.1 - q13.33	15.908.242	49.525.271	33.617.030	Loss

S30					
Chr	**Cytoband**	**Start [bp]**	**Stop [bp]**	**Aberration Size [bp]**	**Copy Number Change**
chr2	q35	217.011.163	219.447.339	2.436.177	Loss
chr21	q11.2 - q22.3	13.897.497	46.881.029	32.983.533	Loss

S31					
Chr	**Cytoband**	**Start [bp]**	**Stop [bp]**	**Aberration Size [bp]**	**Copy Number Change**
chr2	q35	216.985.822	219.447.339	2.461.518	Loss
chr7	q11.21 - q11.23	65.217.921	75.982.831	10.764.911	Loss
chr7	q21.3 - q22.1	96.744.531	101.900.781	5.156.251	Loss
chr19	p13.3 - p13.11	258.517	19.650.002	19.391.486	Loss
chr22	q11.1 - q13.33	15.908.242	49.525.271	33.617.030	Loss

S32					
Chr	**Cytoband**	**Start [bp]**	**Stop [bp]**	**Aberration Size [bp]**	**Copy Number Change**
chr3	p26.3 - p11.1	1.084.690	90.264.318	89.179.629	Loss
chr3	q11.2 - q29	95.088.005	199.288.361	104.200.357	Loss

S34					
Chr	**Cytoband**	**Start [bp]**	**Stop [bp]**	**Aberration Size [bp]**	**Copy Number Change**
chr6	p22.1 - p21.31	28.579.301	33.655.725	5.076.425	Loss
chr8	q24.3	142.501.060	146.144.978	3.643.919	Loss
chr9	q34.13 - q34.3	134.776.562	140.128.884	5.352.323	Loss
chr11	p15.5 - p15.4	186.766	2.906.439	2.719.674	Loss
chr16	p13.3	36.566	3.105.259	3.068.694	Loss
chr21	q22.13 - q22.3	37.514.915	46.881.029	9.366.115	Loss
chr22	q11.21 - q12.1	16.749.638	26.608.203	9.858.566	Loss

S35					
Chr	**Cytoband**	**Start [bp]**	**Stop [bp]**	**Aberration Size [bp]**	**Copy Number Change**
chr1	p36.33 - p11.2	751.596	120.885.991	120.134.396	Loss
chr1	p36.33 - p33	1.238.823	46.892.258	45.653.436	Loss
chr1	p32.2 - p12	56.892.264	120.449.334	63.557.071	Loss
chr1	q21.1 - q44	143.699.872	247.179.432	103.479.561	Loss
chr1	q21.1 - q21.3	144.124.545	150.054.940	5.930.396	Loss
chr1	q21.3 - q23.1	151.858.829	155.198.265	3.339.437	Loss
chr1	q31.1 - q32.1	184.914.697	197.748.854	12.834.158	Loss
chr1	q32.1	199.633.226	204.063.972	4.430.747	Loss
chr2	p23.3 - p23.2	24.006.550	27.854.195	3.847.646	Loss

chr2	p11.2	85.220.080	86.416.734	1.196.655	Loss
chr2	q35	216.985.822	220.182.836	3.197.015	Loss
chr3	p25.3	9.078.424	10.608.497	1.530.074	Loss
chr3	p21.31 - p21.1	46.037.702	53.674.949	7.637.248	Loss
chr3	q27.1 - q27.2	184.234.305	186.031.441	1.797.137	Loss
chr3	q29	195.797.116	199.251.329	3.454.214	Loss
chr4	p16.3 - p11	62.247	48.758.199	48.695.953	Loss
chr4	p16.3 - p16.1	145.900	8.483.887	8.337.988	Loss
chr4	q11 - q35.2	52.383.658	190.887.401	138.503.744	Loss
chr5	q35.1 - q35.3	170.670.272	180.617.248	9.946.977	Loss
chr6	p21.33 - p21.1	30.234.715	44.495.477	14.260.763	Loss
chr7	p22.3 - p22.1	289.341	6.837.609	6.548.269	Loss
chr7	p13	43.873.013	45.070.231	1.197.219	Loss
chr7	q11.23	71.858.792	76.078.892	4.220.101	Loss
chr7	q21.3 - q22.1	97.718.447	101.901.301	4.182.855	Loss
chr8	q24.3	141.111.376	146.144.978	5.033.603	Loss
chr9	p13.3	32.977.863	36.207.456	3.229.594	Loss
chr9	q33.3 - q34.3	129.209.062	140.128.884	10.919.823	Loss
chr11	p15.5	186.766	2.372.342	2.185.577	Loss
chr11	p11.2	46.194.612	47.797.805	1.603.194	Loss
chr11	q12.2 - q14.1	60.414.578	77.881.951	17.467.374	Loss
chr11	q23.3	115.831.877	119.627.461	3.795.585	Loss
chr12	p13.31	6.058.256	8.173.377	2.115.122	Loss
chr12	q13.11 - q14.1	45.896.474	56.621.280	10.724.807	Loss
chr12	q23.3 - q24.33	107.455.164	132.231.480	24.776.317	Loss
chr14	q32.2 - q32.33	99.601.773	105.080.540	5.478.768	Loss
chr16	p13.3 - p11.2	36.566	31.449.816	31.413.251	Loss
chr16	p11.2	28.242.379	31.412.274	3.169.896	Loss
chr16	q21 - q24.3	64.964.976	88.651.933	23.686.958	Loss
chr16	q22.1 - q22.2	65.787.480	69.754.119	3.966.640	Loss
chr17	p13.3 - p13.1	48.339	8.299.092	8.250.754	Loss
chr17	p11.2	15.990.223	21.096.429	5.106.207	Loss
chr17	q11.1 - q25.3	22.952.317	78.623.371	55.671.055	Loss
chr17	q21.2 - q21.31	37.122.892	40.660.335	3.537.444	Loss
chr17	q25.1 - q25.3	70.436.180	78.289.253	7.853.074	Loss
chr19	p13.3 - p13.11	231.880	19.687.240	19.455.361	Loss
chr19	q13.11 - q13.43	37.779.853	63.784.527	26.004.675	Loss
chr19	q13.31 - q13.33	49.953.481	55.730.849	5.777.369	Loss
chr22	q11.1 - q13.33	15.950.607	49.525.271	33.574.665	Loss

S36

Chr	Cytoband	Start [bp]	Stop [bp]	Aberration Size [bp]	Copy Number Change
chr7	q11.21 - q11.23	64.944.535	75.807.738	10.863.204	Loss

chr7	q21.3 - q22.1	97.718.447	103.035.469	5.317.023	Loss
chr17	p13.3 - p13.1	585.856	9.264.074	8.678.219	Loss
chr19	p13.3 - p13.11	231.880	19.699.685	19.467.806	Loss
chr19	q13.11 - q13.42	38.668.269	61.012.235	22.343.967	Loss

S37

Chr	Cytoband	Start [bp]	Stop [bp]	Aberration Size [bp]	Copy Number Change
chr1	p36.33 - p12	842.526	120.387.087	119.544.562	Loss
chr5	p15.33 - p15.2	204.537	10.339.748	10.135.212	Loss
chr6	p25.3 - q11.1	352.031	62.760.249	62.408.219	Gain
chr6	q11.1 - q27	62.815.577	170.732.174	107.916.598	Gain
chr7	q22.1	98.814.496	102.236.054	3.421.559	Loss
chr9	q33.3 - q34.3	127.692.606	139.972.873	12.280.268	Loss
chr19	p13.3 - p13.11	689.976	19.650.002	18.960.027	Loss
chr19	q12 - q13.42	33.277.715	60.859.808	27.582.094	Loss
chr21	q11.2 - q22.3	14.092.032	46.881.029	32.788.998	Loss
chr22	q11.21 - q13.33	16.673.751	49.525.271	32.851.521	Loss

S38

Chr	Cytoband	Start [bp]	Stop [bp]	Aberration Size [bp]	Copy Number Change
chr6	p21.33 - p21.32	30.764.855	32.369.849	1.604.995	Loss
chr6	p21.1 - q11.1	44.465.851	62.669.387	18.203.537	Gain
chr7	q11.21 - q11.23	64.944.535	75.807.738	10.863.204	Loss
chr7	q21.3 - q22.1	97.718.447	102.236.054	4.517.608	Loss
chr9	q33.3 - q34.3	129.159.725	140.128.884	10.969.160	Loss
chr10	p15.3 - p11.21	173.528	38.690.953	38.517.426	Loss
chr10	q11.21 - q26.3	42.289.571	135.254.661	92.965.091	Loss
chr13	q12.11 - q34	18.601.503	112.120.581	93.519.079	Loss
chr19	p13.3 - p13.11	231.880	19.650.002	19.418.123	Loss
chr19	q13.12 - q13.42	40.328.113	60.853.886	20.525.774	Loss
chr22	q11.1 - q13.33	15.908.242	49.525.271	33.617.030	Loss

S39

Chr	Cytoband	Start [bp]	Stop [bp]	Aberration Size [bp]	Copy Number Change
chr1	p36.33 - p11.2	749.422	120.885.991	120.136.570	Loss
chr1	p31.3 - p13.3	65.808.792	108.562.965	42.754.174	Loss
chr1	q21.1 - q44	143.638.935	247.118.628	103.479.694	Loss
chr1	q21.1 - q22	144.124.545	154.583.545	10.459.001	Loss
chr2	q35	217.256.548	219.251.685	1.995.138	Loss
chr7	q22.1	98.286.065	102.236.054	3.949.990	Loss

S40					
Chr	**Cytoband**	**Start [bp]**	**Stop [bp]**	**Aberration Size [bp]**	**Copy Number Change**
chr1	p36.33 - p33	749.422	51.040.067	50.290.646	Gain
chr5	p15.33 - q11.1	148.043	50.059.177	49.911.135	Gain
chr5	q11.1 - q35.3	50.094.582	180.617.248	130.522.667	Gain
chr6	p25.3 - q11.1	238.241	62.669.387	62.431.147	Gain
chr6	q11.1 - q27	62.815.577	170.734.368	107.918.792	Gain
chr7	p22.3 - p11.1	289.912	57.613.887	57.323.976	Gain
chr7	q11.21 - q36.3	62.153.388	158.602.640	96.449.253	Gain
chr8	p23.3 - p11.21	181.330	43.175.454	42.994.125	Gain
chr8	q11.1 - q24.3	47.655.022	146.250.965	98.595.944	Gain
chr9	p24.3 - p13.1	322.256	39.147.095	38.824.840	Gain
chr9	q12 - q34.3	68.362.627	140.128.884	71.766.258	Gain
chr10	p15.3 - p11.21	268.652	35.243.462	34.974.811	Gain
chr11	p15.5 - q11	186.766	55.420.138	55.233.373	Gain
chr11	q11 - q13.4	55.509.438	70.964.624	15.455.187	Gain
chr11	q12.2 - q13.2	59.754.144	67.577.131	7.822.988	Gain
chr11	q13.2 - q13.3	68.460.891	70.182.908	1.722.018	Gain
chr12	p13.33 - p11.1	49.767	34.278.666	34.228.900	Gain
chr12	q12 - q24.33	37.052.171	132.278.200	95.226.030	Gain
chr12	q15	67.472.809	68.638.699	1.165.891	Gain
chr13	q12.12 - q34	24.361.117	114.077.263	89.716.147	Loss
chr14	q11.2 - q32.33	19.364.851	106.330.010	86.965.160	Gain
chr15	q11.2 - q26.3	19.108.924	100.168.859	81.059.936	Gain
chr16	p13.3 - p11.1	36.566	34.847.526	34.810.961	Gain
chr16	q11.2 - q24.3	45.172.398	88.622.123	43.449.726	Gain
chr16	q23.1 - q24.3	77.250.938	88.610.945	11.360.008	Gain
chr18	p11.32 - q11.1	170.029	16.976.246	16.806.218	Gain
chr18	q11.1 - q23	17.054.751	76.083.258	59.028.508	Gain
chr19	p13.3 - p12	231.880	24.132.722	23.900.843	Gain
chr19	q12 - q13.43	32.964.137	63.784.527	30.820.391	Gain
chr20	p13 - p11.21	18.380	25.611.816	25.593.437	Gain
chr20	p13 - p12.3	3.155.913	6.494.855	3.338.943	Gain
chr20	p11.23 - p11.21	19.247.588	25.611.816	6.364.229	Gain
chr20	q11.1 - q13.33	28.081.398	62.363.774	34.282.377	Gain
chr20	q13.32 - q13.33	56.319.675	61.535.654	5.215.980	Gain
chr21	q11.2 - q22.3	13.339.194	46.892.494	33.553.301	Gain
chr22	q11.1 - q13.33	15.979.229	48.785.654	32.806.426	Gain
chr22	q12.1 - q12.3	24.906.393	30.560.081	5.653.689	Gain

S41					
Chr	**Cytoband**	**Start [bp]**	**Stop [bp]**	**Aberration Size [bp]**	**Copy Number Change**
chr1	p36.33 - p12	749.422	120.449.334	119.699.913	Loss
chr17	p13.3 - p11.2	84.087	21.386.460	21.302.374	Loss
chr20	p13 - p11.21	73.854	25.680.695	25.606.842	Loss
chr22	q11.23 - q13.33	23.318.202	49.525.271	26.207.070	Loss

4.1.4. Metastases (n=10)

The following metastasis was balanced (and is therefore not listed): M5

M1					
Chr	**Cytoband**	**Start [bp]**	**Stop [bp]**	**Aberration Size [bp]**	**Copy Number Change**
chr16	p13.3 - p11.1	46.071	34.847.526	34.801.456	Gain

M2					
Chr	**Cytoband**	**Start**	**Stop**	**Aberration Size [bp]**	**Copy Number Change**
chr1	p34.2 - p11.2	41.624.498	120.982.834	79.358.337	Loss
chr3	p26.3 - p11.1	134.511	90.336.893	90.202.383	Loss
chr3	q11.2 - q29	95.063.226	199.324.877	104.261.652	Loss
chr6	p25.3 - q11.1	352.031	62.760.249	62.408.219	Gain
M2					
Chr	**Cytoband**	**Start**	**Stop**	**Aberration Size [bp]**	**Copy Number Change**
chr6	q11.1 - q27	62.815.577	170.732.174	107.916.598	Gain
chr7	p22.3 - p11.1	187.415	57.498.524	57.311.110	Gain
chr7	q11.21 - q36.3	62.153.388	158.602.640	96.449.253	Gain
chr7	q22.3 - q32.1	106.901.516	127.008.130	20.106.615	Gain
chr9	p24.3 - p13.1	261.057	39.147.095	38.886.039	Loss
chr9	q13 - q34.3	70.327.067	140.074.109	69.747.043	Loss
chr10	q11.21	42.209.050	43.742.403	1.533.354	Gain
chr11	q14.1	77.267.663	78.576.359	1.308.697	Gain
chr13	q11 - q34	18.361.437	114.077.263	95.715.827	Loss
chr14	q11.2 - q32.33	19.323.379	106.330.010	87.006.632	Gain
chr15	q11.2 - q26.3	18.835.460	100.201.137	81.365.678	Gain
chr16	p13.3 - p11.1	46.071	34.903.141	34.857.071	Gain
chr16	q11.2 - q24.3	45.121.858	88.638.909	43.517.052	Gain
chr18	p11.32 - q11.1	187.911	17.030.723	16.842.813	Loss
chr18	q11.1 - q23	17.030.723	76.083.258	59.052.536	Loss
chr22	q11.1 - q13.33	15.908.242	49.525.271	33.617.030	Loss

M3					
Chr	**Cytoband**	**Start [bp]**	**Stop [bp]**	**Aberration Size [bp]**	**Copy Number Change**
chr16	p13.3 - p11.2	161.772	34.242.295	34.080.524	Gain

M4					
Chr	**Cytoband**	**Start [bp]**	**Stop [bp]**	**Aberration Size [bp]**	**Copy Number Change**
chr7	q22.1	98.873.384	102.343.323	3.469.940	Loss
chr18	p11.32 - p11.21	4.116	13.185.588	13.181.473	Loss
chr22	q11.1 - q13.33	15.908.242	49.525.271	33.617.030	Loss

M-H5					
Chr	**Cytoband**	**Start [bp]**	**Stop [bp]**	**Aberration Size [bp]**	**Copy Number Change**
chr2	q35	217.256.548	218.517.993	1.261.446	Loss
chr6	p25.3 - q11.1	352.031	62.760.249	62.408.219	Gain
chr6	q11.1 - q27	62.815.577	170.732.174	107.916.598	Gain
chr13	q11 - q34	18.361.437	114.077.263	95.715.827	Loss
chr14	q11.2 - q32.33	19.323.379	106.160.375	86.836.997	Loss
chr15	q22.31	64.551.926	64.687.866	135.941	Gain

M-S3					
Chr	**Cytoband**	**Start [bp]**	**Stop [bp]**	**Aberration Size [bp]**	**Copy Number Change**
chr1	q21.1 - q44	143.638.935	247.179.432	103.540.498	Gain
chr3	p26.3 - p11.1	68.749	90.176.536	90.107.788	Gain
chr4	p16.3 - p11	61.352	48.758.199	48.696.848	Gain
chr4	q22.2 - q35.2	94.835.945	191.133.809	96.297.865	Gain
chr5	p15.33 - q11.1	260.781	49.726.129	49.465.349	Gain
chr5	q11.1 - q35.3	50.058.777	180.617.248	130.558.472	Gain
chr6	p25.3 - q11.1	352.031	62.760.249	62.408.219	Gain
chr6	q11.1 - q27	62.815.577	170.732.174	107.916.598	Gain
chr8	p23.3 - q11.1	369.218	47.800.700	47.431.483	Gain
chr8	q11.1 - q24.3	47.987.761	146.250.965	98.263.205	Gain
chr11	p11.12 - q11	51.289.059	55.509.838	4.220.780	Gain
chr11	q11 - q25	55.635.935	134.251.979	78.616.045	Gain
chr15	q11.1 - q26.3	18.362.355	100.283.019	81.920.665	Gain
chr16	p13.3 - p11.2	46.071	31.701.259	31.655.189	Gain
chr16	q11.2 - q24.3	45.121.858	88.638.909	43.517.052	Gain
chr16	q11.2 - q12.1	45.312.314	46.954.007	1.641.694	Gain
chr16	q21	57.078.335	65.103.578	8.025.244	Gain
chr17	p13.3 - q11.1	210.770	22.857.162	22.646.393	Gain

chr17	q11.1 - q25.3	22.878.858	78.586.437	55.707.580	Gain
chr18	p11.32 - q11.1	131.896	17.030.723	16.898.828	Gain
chr18	q11.1 - q23	17.030.723	76.018.550	58.987.828	Gain
chr19	p13.3 - p12	278.073	24.132.722	23.854.650	Gain
chr19	q12 - q13.43	32.964.137	63.672.982	30.708.846	Gain
chr21	q11.2 - q22.3	13.562.063	46.892.494	33.330.432	Gain
chr22	q11.1 - q13.33	15.908.242	49.525.271	33.617.030	Loss

M-S12					
Chr	**Cytoband**	**Start**	**Stop**	**Aberration Size [bp]**	**Copy Number Change**
chr2	p25.3 - p11.2	32.244	89.871.469	89.839.226	Loss
chr3	q11.2 - q29	97.384.082	198.794.989	101.410.908	Loss

M-S25					
Chr	**Cytoband**	**Start**	**Stop**	**Aberration Size [bp]**	**Copy Number Change**
chr1	p33 - p12	48.035.835	120.387.087	72.351.253	Loss
chr4	q13.3	70.741.351	75.325.642	4.584.292	Gain
chr5	p15.33 - p14.3	204.537	21.826.809	21.622.273	Loss
chr5	q11.1 - q32	50.058.777	146.891.603	96.832.827	Loss
chr11	q12.2	59.865.051	60.470.050	605.000	Loss
chr13	q11 - q34	18.361.437	114.077.263	95.715.827	Loss
chr17	q11.1 - q12	22.878.858	31.891.735	9.012.878	Loss
chr20	p13 - p12.3	69.321	5.087.382	5.018.062	Gain

M-S40					
Chr	**Cytoband**	**Start**	**Stop**	**Aberration Size [bp]**	**Copy Number Change**
chr1	p36.33 - p33	749.422	51.040.067	50.290.646	Gain
chr5	p15.33 - q11.1	148.043	50.059.177	49.911.135	Gain
chr5	q11.1 - q35.3	50.094.582	180.617.248	130.522.667	Gain
chr6	p25.3 - q11.1	204.328	62.669.387	62.465.060	Gain
chr6	q11.1 - q27	62.815.577	170.734.368	107.918.792	Gain
chr7	p22.3 - p11.1	149.068	57.613.887	57.464.820	Gain
chr7	q11.21 - q36.3	62.153.388	158.781.538	96.628.151	Gain
chr7	q22.1	98.286.065	102.236.054	3.949.990	Gain
chr8	p23.3 - p11.21	181.330	43.175.454	42.994.125	Gain
chr8	q11.1 - q24.3	47.655.022	146.250.965	98.595.944	Gain
chr9	p24.3 - p13.1	204.167	39.277.259	39.073.093	Gain
chr9	q12 - q34.3	68.362.627	140.128.884	71.766.258	Gain
chr10	p15.3 - p11.21	138.006	35.243.462	35.105.457	Gain
chr11	p15.5 - q11	186.766	55.460.512	55.273.747	Gain
chr11	q11 - q13.1	55.509.438	64.880.545	9.371.108	Gain

chr11	q13.2 - q13.4	68.460.891	70.964.624	2.503.734	Gain
chr12	p13.33 - p11.1	49.767	34.278.666	34.228.900	Gain
chr12	q12 - q24.33	37.052.171	132.278.200	95.226.030	Gain
chr12	q13.13 - q14.1	51.523.945	56.492.179	4.968.235	Gain
chr12	q15	67.472.809	68.638.699	1.165.891	Gain
chr13	q12.12 - q34	24.361.117	114.077.263	89.716.147	Loss
chr14	q11.2 - q32.33	19.364.851	106.330.010	86.965.160	Gain
chr15	q11.2 - q26.3	19.108.924	100.168.859	81.059.936	Gain
chr16	p13.3 - p11.1	36.566	34.847.526	34.810.961	Gain
chr16	q11.2 - q24.3	45.172.398	88.622.123	43.449.726	Gain
chr18	p11.32 - q11.1	170.029	16.976.246	16.806.218	Gain
chr18	q11.1 - q23	17.054.751	76.083.258	59.028.508	Gain
chr19	p13.3 - p12	231.880	24.132.722	23.900.843	Gain
chr19	q12 - q13.43	32.964.137	63.784.527	30.820.391	Gain
chr20	p13 - p11.21	18.380	25.381.671	25.363.292	Gain
chr20	p13 - p12.2	3.143.718	10.342.347	7.198.630	Gain
chr20	p11.23 - p11.21	19.247.588	25.381.671	6.134.084	Gain
chr20	q11.1 - q13.33	28.081.398	62.363.774	34.282.377	Gain
chr20	q11.21 - q11.23	29.715.947	36.007.307	6.291.361	Gain
chr20	q13.12 - q13.32	43.692.664	56.162.254	12.469.591	Gain
chr20	q13.32 - q13.33	56.231.363	62.175.281	5.943.919	Gain
chr21	q11.2 - q22.3	13.339.194	46.892.494	33.553.301	Gain
chr22	q11.1 - q13.33	15.908.242	49.356.486	33.448.245	Gain
chr22	q11.23 - q12.2	23.931.575	30.034.353	6.102.779	Gain

4.2. SUPPLEMENTARY TABLE 2: SUMMARY OF SHORTEST REGIONS OF OVERLAP (SROS)

Summary of overlapping regions for the hereditary cases (n=11), sporadic cases with a *RET* mutation (n=15), sporadic cases without a *RET* mutation (n=26), and for the metastases (n=10). Base pairs according to hg18.

4.2.1. Hereditary MTC cases (n=11)

Chr	Start [bp]	Stop [bp]	Aberration Size [bp]	Gain %	Del %	Cases
chr1	842.526	120.387.087	119.544.562		18	H3, H7
chr1	143.638.935	144.151.404	512.470		18	H3, H7
chr1	144.151.404	154.718.285	10.566.882		18	H3, H7
chr4	56.151.753	189.695.132	133.543.380		18	H3, H7
chr7	65.025.291	75.807.738	10.782.448		18	H7, H9
chr7	98.093.249	98.814.496	721.248		18	H7, H9
chr7	98.814.496	102.140.976	3.326.481		27	H3, H7, H9
chr7	102.140.976	102.311.168	170.193		18	H7, H9
chr8	143.623.121	146.037.529	2.414.409		18	H7, H9
chr17	585.856	9.349.373	8.763.518		18	H7, H9
chr17	47.062.751	51.923.074	4.860.324		18	H6, H7
chr17	69.343.797	70.183.632	839.836	18		H6, H11
chr19	231.880	323.961	92.082		18	H7, H9
chr19	323.961	19.699.685	19.375.725		18	H7, H9
chr19	38.668.269	60.848.954	22.180.686		18	H7, H9

4.2.2. Sporadic MTC with a *RET* Mutation (n=15)

Chr	Start [bp]	Stop [bp]	Aberration Size [bp]	Gain %	Del %	Cases
chr1	554.068	749.422	195.355		13	S2, S7
chr1	749.422	842.526	93.105		27	S2, S5, S7, S10
chr1	842.526	49.187.166	48.344.641		33	S2, S5, S6, S7, S10
chr1	49.187.166	52.043.557	2.856.392		40	S2, S5, S6, S7, S10, S11
chr1	52.043.557	120.146.842	68.103.286		47	S2, S5, S6, S7, S10, S11, S15
chr1	120.146.842	120.449.334	302.493		40	S2, S5, S6, S7, S10, S11
chr1	120.449.334	120.885.991	436.658		33	S2, S5, S6, S7, S11
chr2	978.075	1.649.497	671.423	13		S3, S7
chr2	96.172.570	242.690.178	146.517.609	13		S3, S7
chr3	8.994.311	10.306.422	1.312.112		13	S1, S15
chr3	46.596.619	50.634.902	4.038.284		13	S13, S15
chr3	50.634.902	51.979.577	1.344.676		20	S1, S13, S15
chr3	51.979.577	53.867.826	1.888.250		13	S13, S15
chr3	97.749.583	128.515.674	30.766.092		13	S12, S15
chr3	128.515.674	130.802.608	2.286.935		20	S1, S12, S15
chr3	130.802.608	140.307.347	9.504.740		13	S12, S15
chr3	140.307.347	143.995.564	3.688.218		20	S1, S12, S15
chr3	143.995.564	198.794.989	54.799.426		13	S15, S12
chr4	52.383.658	94.794.389	42.410.732		20	S2, S5, S6
chr4	94.794.389	190.887.401	96.093.013		20	S2, S5, S6
chr6	28.579.301	33.655.725	5.076.425		13	S10, S13
chr7	98.895.133	102.140.976	3.245.844		13	S3, S13
chr13	24.640.862	29.321.920	4.681.059		13	S1, S10
chr13	47.357.404	50.278.439	2.921.036		13	S1, S10
chr16	45.172.398	87.891.244	42.718.847	13		S3, S10
chr17	585.856	8.184.122	7.598.267		20	S7, S10, S13
chr17	8.184.122	9.264.074	1.079.953		13	S7, S13
chr19	231.880	19.650.002	19.418.123		13	S10, S13
chr19	38.668.269	60.853.886	22.185.618		13	S10, S13
chr22	15.908.242	16.435.103	526.862		27	S3, S6, S9, S11
chr22	16.435.103	16.749.638	314.536		33	S3, S6, S9, S11, S13
chr22	16.749.638	41.237.931	24.488.294		40	S1, S3, S6, S9, S11, S13
chr22	41.237.931	49.525.271	8.287.341		33	S1, S3, S9, S11, S13

4.2.3. Sporadic MTC without a *RET* mutation (n=26)

Chr	Start [bp]	Stop [bp]	Aberration Size [bp]	Gain %	Del %	Cases
chr1	749.422	751.596	2.175		15	S16, S29, S39, S41,
chr1	751.596	842.526	90.931		31	S16, S17, S20, S23, S29, S35, S39, S41,
chr1	842.526	120.387.087	119.544.562		38	S16, S17, S20, S21, S23, S29, S35, S37, S39, S41
chr1	120.387.087	120.449.334	62.248		35	S16, S17, S20, S21, S23, S29, S35, S39, S41
chr1	120.449.334	120.885.991	436.658		23	S16, S21, S23, S29, S35, S39
chr1	143.638.935	143.699.872	60.938		12	S17, S21, S39
chr1	143.699.872	247.118.628	103.418.757		19	S17, S21, S23, S35, S39
chr1	247.118.628	247.179.432	60.805		12	S17, S21, S35
chr2	24.006.550	27.854.195	3.847.646		8	S23, S35
chr2	85.220.080	85.779.538	559.459		8	S23, S35
chr2	216.985.822	217.011.163	25.342		8	S31, S35
chr2	217.011.163	217.256.548	245.386		12	S30, S31, S35
chr2	217.256.548	218.517.593	1.261.046		23	S27, S29, S30, S31, S35, S39
chr2	218.517.593	219.003.046	485.454		27	S23, S27, S29, S30, S31, S35, S39
chr2	219.003.046	219.251.685	248.640		23	S23, S29, S30, S31, S35, S39
chr2	219.251.685	219.375.201	123.517		19	S23, S29, S30, S31, S35
chr2	219.375.201	219.447.339	72.139		15	S23, S30, S31, S35
chr2	219.447.339	220.182.836	735.498		8	S23, S35
chr3	9.078.424	9.265.382	186.959		8	S32, S35
chr3	9.265.382	10.306.422	1.041.041		12	S23, S32, S35
chr3	10.306.422	10.608.497	302.076		8	S32, S35
chr3	46.037.702	46.729.265	691.564		8	S32, S35
chr3	46.729.265	47.058.961	329.697		12	S23, S32, S35
chr3	47.058.961	50.172.130	3.113.170		15	S23, S28, S32, S35
chr3	50.172.130	53.674.949	3.502.820		12	S23, S32, S35
chr3	56.627.015	58.573.817	1.946.803		8	S23, S32
chr3	129.776.828	131.172.730	1.395.903		8	S23, S32
chr3	184.234.305	186.031.441	1.797.137		12	S23, S32, S35
chr3	186.031.441	187.138.313	1.106.873		8	S23, S32
chr3	195.797.116	199.251.329	3.454.214		12	S23, S32, S35
chr4	62.247	145.900	83.654		8	S16, S35
chr4	145.900	8.359.881	8.213.982		12	S16, S23, S35
chr4	8.359.881	38.984.514	30.624.634		8	S16, S35
chr4	38.984.514	40.503.948	1.519.435		12	S16, S23, S35

Chr	Start [bp]	Stop [bp]	Aberration Size [bp]	Gain %	Del %	Cases
chr4	40.503.948	42.182.124	1.678.177		8	S16, S35
chr4	42.182.124	48.758.199	6.576.076		8	S16, S35
chr4	52.383.658	57.238.714	4.855.057		8	S16, S35
chr4	57.238.714	57.631.818	393.105		12	S16, S23, S35
chr4	57.631.818	83.493.304	25.861.487		8	S16, S35
chr4	83.493.304	84.746.131	1.252.828		12	S16, S23, S35
chr4	84.746.131	190.352.061	105.605.931		8	S16, S35
chr5	204.537	10.339.748	10.135.212	8		S28, S40
chr5	10.339.748	17.766.284	7.426.537	8		S28, S40
chr5	17.766.284	31.244.817	13.478.534	12		S23, S28, S40
chr5	31.244.817	45.865.553	14.620.737	8		S28, S40
chr5	50.058.777	50.059.177	401	8		S28, S40
chr5	50.094.582	52.607.429	2.512.848	12		S23, S28, S40
chr5	52.607.429	68.900.170	16.292.742	8		S28, S40
chr5	68.900.170	89.289.163	20.388.994	8		S28, S40
chr5	170.670.272	180.617.248	9.946.977		8	S23, S35
chr6	352.031	18.332.393	17.980.363	8		S37, S40
chr6	18.332.393	30.234.715	11.902.323	8		S37, S40
chr6	30.234.715	30.764.855	530.141	8		S37, S40
chr6	30.234.715	30.764.855	530.141		12	S23, S34, S35
chr6	30.764.855	32.369.849	1.604.995	8		S37, S40
chr6	30.764.855	32.369.849	1.604.995		15	S23, S34, S35, S38
chr6	32.369.849	33.655.725	877	8		S37, S40
chr6	32.369.849	33.655.725	1.285.877		12	S23, S34, S35
chr6	33.655.725	44.465.851	10.810.127	8		S37, S40
chr6	33.655.725	44.465.851	10.810.127		8	S23, S35
chr6	44.465.851	44.495.477	29.627	12		S37, S38, S40
chr6	44.465.851	44.495.477	29.627		8	S23, S35
chr6	44.495.477	62.669.387	18.173.911	12		S37, S38, S40
chr6	62.815.577	74.420.942	11.605.366	8		S37, S40
chr6	74.420.942	90.922.413	16.501.472	8		S37, S40
chr6	90.922.413	99.392.781	8.470.369	12		S23, S37, S40
chr6	99.392.781	151.881.179	52.488.399	8		S37, S40
chr6	151.881.179	170.732.174	18.850.996	8		S37, S40
chr7	289.341	289.912	572		12	S16, S23, S35
chr7	289.912	6.837.609	6.547.698		12	S16, S23, S35
chr7	8.183.128	20.656.357	12.473.230	8		S23, S40
chr7	43.648.776	43.873.013	224.238		8	S16, S23
chr7	43.873.013	45.070.231	1.197.219		12	S16, S23, S35
chr7	48.109.127	55.150.628	7.041.502	8		S23, S40
chr7	55.605.323	56.150.069	544.747		8	S16, S23
chr7	64.944.535	65.025.291	80.757		12	S23, S36, S38

Chr	Start [bp]	Stop [bp]	Aberration Size [bp]	Gain %	Del %	Cases
chr7	65.025.291	65.217.921	192.631		15	S16, S23, S36, S38
chr7	65.217.921	71.858.792	6.640.872		19	S16, S23, S31, S36, S38
chr7	71.858.792	75.807.738	3.948.947		23	S16, S23, S31, S35, S36, S38
chr7	75.807.738	75.982.831	175.094		15	S16, S23, S31, S35
chr7	75.982.831	76.078.892	96.062		12	S16, S23, S35
chr7	77.668.192	96.624.761	18.956.570	8		S23, S40
chr7	96.744.531	96.807.009	62.479		8	S16, S31
chr7	96.807.009	97.458.242	651.234		12	S16, S28, S31
chr7	97.458.242	97.718.447	260.206		15	S16, S23, S28, S31
chr7	97.718.447	98.286.065	567.619		27	S16, S23, S28, S31, S35, S36, S38
chr7	98.286.065	98.814.496	528.432		31	S16, S23, S28, S31, S35, S36, S38, S39
chr7	98.814.496	101.900.581	3.086.086		35	S16, S23, S28, S31, S35, S36, S37, S38, S39
chr7	101.900.581	101.900.781	201		31	S16, S23, S31, S35, S36, S37, S38, S39
chr7	101.900.781	101.901.301	521		27	S16, S23, S35, S36, S37, S38, S39
chr7	101.901.301	102.236.054	334.754		19	S16, S36, S37, S38, S39
chr7	102.236.054	103.035.469	799.416		8	S16, S36
chr7	135.263.760	137.194.927	1.931.168	8		S23, S40
chr8	141.111.376	142.501.060	1.389.685		8	S23, S35
chr8	142.501.060	146.144.978	3.643.919		12	S23, S34, S35
chr9	32.977.863	36.207.456	3.229.594		8	S23, S35
chr9	127.692.606	129.159.725	1.467.120		8	S23, S37
chr9	129.159.725	129.209.062	49.338		12	S23, S37, S38
chr9	129.209.062	134.776.562	5.567.501		15	S23, S35, S37, S38
chr9	134.776.562	139.972.873	5.196.312		19	S23, S34, S35, S37, S38
chr9	139.972.873	140.128.884	156.012		15	S23, S34, S35, S38
chr10	11.829.240	15.249.336	3.420.097		8	S23, S38
chr10	69.834.320	70.841.079	1.006.760		8	S23, S38
chr10	88.267.131	88.855.043	587.913		8	S23, S38
chr10	103.740.122	105.196.986	1.456.865		8	S23, S38
chr11	186.766	2.372.342	2.185.577		12	S23, S34, S35
chr11	2.372.342	2.906.439	534.098		8	S23, S34
chr11	20.896.118	31.732.174	10.836.057	8		S23, S40
chr11	46.194.612	47.797.805	1.603.194		8	S23, S35
chr11	60.453.624	77.881.951	17.428.328		8	S23, S35
chr11	116.128.327	119.102.149	2.973.823		8	S23, S35
chr12	6.058.256	8.173.377	2.115.122		8	S23, S35
chr12	10.453.331	11.072.969	619.639	8		S23, S40
chr12	40.839.968	41.262.211	422.244	8		S26, S40

Chr	Start [bp]	Stop [bp]	Aberration Size [bp]	Gain %	Del %	Cases
chr12	47.174.625	56.517.093	9.342.469		8	S23, S35
chr12	70.593.567	90.696.355	20.102.789	8		S23, S40
chr12	107.512.288	132.231.480	24.719.193		8	S23, S35
chr13	18.652.920	21.011.618	2.358.699		8	S23, S27
chr13	24.361.117	52.523.623	28.162.507		8	S27, S40
chr13	52.523.623	72.396.102	19.872.480	8		S23, S38
chr13	52.523.623	72.396.102	19.872.480		8	S27, S40
chr13	72.396.102	72.396.103	2		8	S27, S40
chr13	72.396.103	72.630.492	234.390		12	S23, S27, S40
chr13	72.630.492	72.630.493	2		8	S27, S40
chr13	72.630.493	94.062.800	21.432.308	8		S23, S38
chr13	72.630.493	94.062.800	21.432.308		8	S27, S40
chr13	94.062.800	100.837.894	6.775.095		8	S27, S40
chr13	100.837.894	108.602.909	7.765.016	8		S23, S38
chr13	100.837.894	108.602.909	7.765.016		8	S27, S40
chr13	108.602.909	114.077.263	5.474.355		8	S27, S40
chr14	24.238.052	30.040.054	5.802.003	8		S23, S40
chr14	39.307.829	48.874.670	9.566.842	8		S23, S40
chr14	81.320.805	87.763.756	6.442.952	8		S23, S40
chr14	101.467.325	105.067.740	3.600.416		8	S23, S35
chr15	20.335.687	21.208.577	872.891		8	S16, S23
chr15	38.552.112	39.684.507	1.132.396		8	S16, S23
chr15	62.292.133	64.629.036	2.336.904		8	S16, S23
chr15	72.539.942	73.754.558	1.214.617		8	S16, S23
chr15	88.093.920	89.430.956	1.337.037		8	S16, S23
chr16	36.566	46.071	9.506		8	S34, S35
chr16	46.071	125.498	79.428	8		S22, S40
chr16	46.071	125.498	79.428		8	S34, S35
chr16	125.498	3.105.259	2.979.762	8		S22, S40
chr16	125.498	3.105.259	2.979.762		12	S23, S34, S35
chr16	3.105.259	31.449.816	28.344.558	8		S22, S40
chr16	3.105.259	31.449.816	28.344.558		8	S23, S35
chr16	31.449.816	34.847.526	3.397.711	8		S22, S40
chr16	45.172.398	57.306.344	12.133.947	8		S22, S40
chr16	57.306.344	57.784.982	478.639	8		S22, S40
chr16	57.784.982	64.078.253	6.293.272	12		S22, S23, S40
chr16	64.078.253	64.983.947	905.695	8		S22, S40
chr16	64.983.947	88.622.123	23.638.177	8		S22, S40
chr16	64.983.947	88.651.933	23.667.987		8	S23, S35
chr17	84.087	585.856	501.770		12	S23, S35, S41
chr17	585.856	8.299.092	7.713.237		15	S23, S35, S36, S41
chr17	8.299.092	9.264.074	964.983		12	S23, S36, S41

Chr	Start [bp]	Stop [bp]	Aberration Size [bp]	Gain %	Del %	Cases
chr17	9.264.074	15.990.223	6.726.150		8	S23, S41
chr17	15.990.223	21.054.334	5.064.112		12	S23, S35, S41
chr17	21.054.334	21.096.429	42.096		8	S35, S41
chr17	23.548.474	78.623.371	55.074.898		8	S23, S35
chr18	17.054.751	53.357.558	36.302.808		8	S16, S29
chr18	53.357.558	54.863.176	1.505.619		12	S16, S23, S29
chr18	54.863.176	59.461.828	4.598.653		8	S16, S29
chr18	59.461.828	65.596.569	6.134.742	8		S23, S40
chr18	59.461.828	65.596.569	6.134.742		8	S16, S29
chr18	65.596.569	76.083.258	10.486.690		8	S16, S29
chr19	231.880	258.517	26.638		12	S35, S36, S38
chr19	258.517	323.961	65.445		19	S23, S31, S35, S36, S38
chr19	323.961	689.976	366.016		23	S18, S23, S31, S35, S36, S38
chr19	689.976	774.354	84.379		27	S18, S23, S31, S35, S36, S37, S38
chr19	774.354	19.650.002	18.875.649		31	S18, S23, S28, S31, S35, S36, S37, S38
chr19	19.650.002	19.687.240	37.239		19	S18, S23, S28, S35, S36
chr19	19.687.240	19.699.685	12.446		12	S18, S28, S36
chr19	37.540.308	37.779.853	239.546		8	S23, S37
chr19	37.779.853	38.668.269	888.417		12	S23, S35, S37
chr19	38.668.269	40.328.113	1.659.845		15	S23, S35, S36, S37
chr19	40.328.113	60.853.886	20.525.774		19	S23, S35, S36, S37, S38
chr19	60.853.886	60.859.808	5.923		15	S23, S35, S36, S37
chr19	60.859.808	61.012.235	152.428		12	S23, S35, S36
chr19	61.012.235	63.761.216	2.748.982		8	S23, S35
chr20	2.179.111	5.733.948	3.554.838		8	S23, S41
chr21	14.092.032	14.334.342	242.311		8	S30, S37
chr21	14.334.342	18.540.495	4.206.154		12	S28, S30, S37
chr21	18.540.495	23.986.496	5.446.002	8		S23, S40
chr21	18.540.495	23.986.496	5.446.002		12	S28, S30, S37
chr21	23.986.496	31.446.665	7.460.170		12	S28, S30, S37
chr21	31.446.665	37.514.915	6.068.251		15	S23, S28, S30, S37
chr21	37.514.915	46.811.728	9.296.814		19	S23, S28, S30, S34, S37
chr21	46.811.728	46.847.350	35.623		15	S28, S30, S34, S37
chr21	46.847.350	46.881.029	33.680		12	S30, S34, S37
chr22	15.908.242	15.950.607	42.366		27	S16, S17, S23, S27, S29, S31, S38
chr22	15.950.607	15.979.229	28.623		31	S16, S17, S23, S27, S29, S31, S35, S38
chr22	15.979.229	16.673.751	694.523		31	S16, S17, S23, S27, S29, S31, S35, S38
chr22	16.673.751	16.749.638	75.888		35	S16, S17, S23, S27,

Chr	Start [bp]	Stop [bp]	Aberration Size [bp]	Gain %	Del %	Cases
						S29, S31, S35, S37, S38
chr22	16.749.638	23.318.202	6.568.565		38	S16, S17, S23, S27, S29, S31, S34, S35, S37, S38
chr22	23.318.202	26.608.203	3.290.002		42	S16, S17, S23, S27, S29, S31, S34, S35, S37, S38, S41
chr22	26.608.203	49.525.271	22.917.069		38	S16, S17, S23, S27, S29, S31, S35, S37, S38

4.2.4. Metastases (n=10)

Chr	Start [bp]	Stop [bp]	Aberration Size [bp]	Amp %	Del %	Cases
chr1	48.035.835	120.387.087	72.351.253		20	M2, M-S25
chr3	97.384.082	198.794.989	101.410.908		20	M2, M-S12
chr5	260.781	21.826.809	21.566.029	20		M-S3, M-S40
chr5	21.826.809	49.726.129	27.899.321	20		M-S3, M-S40
chr5	50.058.777	50.059.177	401	20		M-S3, M-S40
chr5	50.094.582	146.891.603	96.797.022	20		M-S3, M-S40
chr5	146.891.603	180.617.248	33.725.646	20		M-S3, M-S40
chr6	352.031	582.627	230.597	40		M2, M-S3, M-S40, M-H5
chr6	582.627	57.575.279	56.992.653	50		M2, M-S3, M-S40, M3, M-H5
chr6	57.575.279	62.669.387	5.094.109	40		M2, M-S3, M-S40, M-H5
chr6	62.669.387	62.760.249	90.863	30		M2, M-S3, M-H5
chr6	62.815.577	170.732.174	107.916.598	50		M2, M-S3, M-S40, M3, M-H5
chr6	170.732.174	170.734.368	2.195	20		M-S40, M3
chr7	187.415	289.912	102.498	20		M2, M-S40
chr7	289.912	50.485.236	50.195.325	30		M2, M3, M-S40
chr7	50.485.236	57.498.524	7.013.289	20		M2, M-S40
chr7	62.153.388	102.343.323	40.189.936	30		M2, M3, M-S40
chr7	102.343.323	156.826.258	54.482.936	30		M2, M3, M-S40,
chr7	156.826.258	158.602.640	1.776.383	20		M2, M-S40
chr8	369.218	43.175.454	42.806.237	20		M-S3, M-S40
chr8	47.655.022	47.800.700	145.679	20		M-S3, M-S40
chr8	47.987.761	146.250.965	98.263.205	20		M-S3, M-S40
chr9	129.209.062	133.174.607	3.965.546		20	M2, M4
chr11	51.289.059	55.460.512	4.171.454	20		M-S3, M-S40
chr11	55.509.438	55.509.838	401	20		M-S3, M-S40
chr11	55.635.935	60.470.050	4.834.116	20		M-S3, M-S40
chr11	60.470.050	64.880.545	4.410.496	20		M-S3, M-S40

Chr	Start [bp]	Stop [bp]	Aberration Size [bp]	Amp %	Del %	Cases
chr11	68.460.891	70.964.624	2.503.734	20		M-S3, M-S40
chr11	77.267.663	78.576.359	1.308.697	20		M2, M-S3
chr13	18.361.437	24.361.117	5.999.681		30	M-S25, M-H5, M2
chr13	24.361.117	114.077.263	89.716.147		40	M2, M-S25, M-H5, M-S40
chr14	19.364.851	106.160.375	86.795.525	20		M2, M-S40
chr14	106.160.375	106.330.010	169.636	20		M2, M-S40
chr15	18.835.460	19.108.924	273.465	20		M2, M-S3
chr15	19.108.924	64.551.926	45.443.003	30		M2, M-S3, M-S40
chr15	64.551.926	64.687.866	135.941	40		M2, M-S3, M-S40, M-H5
chr15	64.687.866	100.168.859	35.480.994	30		M2, M-S3, M-S40
chr15	100.168.859	100.201.137	32.279	20		M2, M-S3
chr16	46.071	161.772	115.702	40		M2, M-S3, M1, M-S40
chr16	161.772	31.701.259	31.539.488	50		M2, M-S3, M1, M-S40, M3
chr16	31.701.259	34.242.295	2.541.037	40		M2, M1, M-S40, M3
chr16	34.242.295	34.847.526	605.232	30		M2, M1, M-S40
chr16	45.121.858	45.172.398	50.541	20		M2, M-S3
chr16	45.172.398	88.622.123	43.449.726	50		M2, M-S3, M1, M-S40, M3
chr16	88.622.123	88.638.909	16.787	30		M2, M-S3, M3
chr18	170.029	187.911	17.883	20		M-S3, M-S40
chr18	187.911	13.185.588	12.997.678	20		M-S3, M-S40
chr18	187.911	13.185.588	12.997.678		20	M4, M2
chr18	13.185.588	16.976.246	3.790.659	20		M-S3, M-S40
chr18	17.054.751	76.018.550	58.963.800	20		M-S3, M-S40
chr19	278.073	737.350	459.278	30		M2, M-S3, M-S40
chr19	737.350	3.886.380	3.149.031	30		M2, M-S3, M-S40
chr19	737.350	3.886.380	3.149.031		20	M4, M-S12
chr19	3.886.380	19.699.685	15.813.306	30		M2, M-S3, M-S40
chr19	19.699.685	24.132.722	4.433.038	30		M2, M-S3, M-S40
chr19	32.964.137	34.864.830	1.900.694	30		M2, M-S3, M-S40
chr19	34.864.830	59.294.958	24.430.129	40		M2, M-S3, M-S12, M-S40
chr19	59.294.958	63.672.982	4.378.025	40		M2, M-S3, M-S12, M-S40
chr19	63.672.982	63.784.527	111.546	20		M2, M-S40
chr20	69.321	5.087.382	5.018.062	20		M-S25, M-S40
chr21	13.339.194	13.562.063	222.870	20		M3, M-S40
chr21	13.562.063	46.881.029	33.318.967	30		M-S3, M-S40, M3
chr21	46.881.029	46.892.494	11.466	30		M-S3, M-S40, M3
chr22	15.908.242	16.379.153	470.912		30	M2, M4, M-S3
chr22	16.379.153	49.525.271	33.146.119		40	M2, M4, M-H5, M-S3

5. CURRICULUM VITAE

PERSONAL DATA

First Name:	**Karin**
Second Name:	**Flicker**
Academic Degree:	$DI_{(FH)}$
Date/Place of Birth:	02 September 1982 / Graz
Nationality:	Austria
Address:	Otto-Loewi-Gasse 8/18, 8042 Graz
Mobilephone:	+43 664 40 59 133
E-mail:	karinflicker@gmx.at

EDUCATION

10/2007 – 12/2010	**PhD Program in Molecular Medicine** Medical University Graz Institute of Human Genetics, Prof. Speicher
10/2002 – 06/2006	**Study of Medical and Pharmaceutical Biotechnology** FH Krems, Austria Academic Degree: $DI_{(FH)}$
09/1997 – 07/2002	**HLW in Weiz** Main focus: foreign languages and business
09/1992 – 07/1997	**Secondary School in Passail**

WORKING EXPERIENCE

05/2011 – ongoing	**QPS Austria GmbH** Division: Clinical Department Clinical research associate Duties: Project Management, Monitoring, Regulatory Affairs
10/2007 – 12/2010	**Institute of Human Genetics, Medical University Graz** PhD student in the group of Prof. Michael Speicher Dissertation: Characterization of genomic changes in different tumor types
05/2007 – 10/2007	**Fresenius Kabi Graz** Division: Compliance Management Duties: Documentation of stability tests of pharmaceuticals
07/2005 – 12/2005	**Institute of Regenerative Medicine, Galway, Ireland** **National University of Galway, Ireland** Diploma Thesis: Lentiviral vector delivery of PDX-1 to adult mesenchymal stem cells

CONTINUING EDUCATION

05/2012 – 06/2012	University Course 'Clinical Trial Specialist' Medical University of Graz
05/2011 – 06/2011	Training as Clinical Monitor HCC Consulting, Vienna
2005 – 2006	Training as Safety Officer Safco Consulting GmbH, Vienna

ADDITIONAL SKILLS

LANGUAGES

German: native language
English: excellent in reading, writing and conversational skills
Certificate: CEIBT (Certificate in English for International Business and Trade)
French: basic knowledge

COMPUTER SKILLS

very good knowledge of MS Office (Excel, Word, Power Point, Access)

- Certificate: ECDL – European Computer Driving Licence

OTHER SKILLS

driving liscence 'B' (car)

PUBLICATIONS

Rankl J, **Flicker K,** Valentin A, Horn M, Uranüs S, Groselj-Strele A, Emberger W, Sill H. Hypersensitivity to alkylation treatment of primary fibroblasts from patients with therapy-related myeloid neoplasms. Leuk Res. 2012 Jul;36(7):e137-9. Epub 2012 Apr 4. No abstract available.

Flicker K, Ulz P, Höger H, Zeitlhofer P, Haas OA, Behmel A, Buchinger W, Scheuba C, Niederle B, Pfragner R, Speicher MR. High-resolution analysis of alterations in medullary thyroid carcinoma genomes. Int J Cancer. 2012 Jul 15;131(2):E66-73. doi: 10.1002/ijc.26494. Epub 2011 Nov 28.

Reinisch A, Hofmann NA, Obenauf AC, Kashofer K, Rohde E, Schallmoser K, **Flicker K,** Lanzer G, Linkesch W, Speicher MR, Strunk D. Humanized large-scale expanded endothelial colony-forming cells function in vitro and in vivo. Blood. 2009 Jun 25;113(26):6716-25

6. REFERENCES

Aaro, LA, Symmonds, RE & Dockerty, MB (1966). Sarcoma of the uterus. A clinical and pathologic study of 177 cases. *Obstet Gynecol* **94**: 101-9.

American Thyroid Association Guidelines Task Force, Kloos, RT, Eng, C, Evans, DB, Francis, GL, Gagel, RF*, et al.* (2009). Medullary thyroid cancer: management guidelines of the American Thyroid Association. *Thyroid* **19**: 565-612, 10.1089/thy.2008.0403.

Ashraf-Ganjoei, T, Behtash, N, Shariat, M & Mosavi, A (2006). Low grade endometrial stromal sarcoma of uterine corpus, a clinico-pathological and survey study in 14 cases. *World J Surg Oncol* **4**: 50, 10.1186/1477-7819-4-50.

Azofeifa, J, Fauth, C, Kraus, J, Maierhofer, C, Langer, S, Bolzer, A*, et al.* (2000). An optimized probe set for the detection of small interchromosomal aberrations by use of 24-color FISH. *Am J Hum Genet* **66**: 1684-8.

Baumgartner-Parzer, SM, Lang, R, Wagner, L, Heinze, G, Niederle, B, Kaserer, K*, et al.* (2005). Polymorphisms in exon 13 and intron 14 of the RET protooncogene: genetic modifiers of medullary thyroid carcinoma? *J Clin Endocrinol Metab* **90**: 6232-6.

Bell, SW, Kempson, RL & Hendrickson, MR (1994). Problematic uterine smooth muscle neoplasms. A clinicopathologic study of 213 cases. *Am J Surg Pathol* **18**: 535-58.

Berchuck, A, Rubin, SC, Hoskins, WJ, Saigo, PE, Pierce, VK & Lewis, JL,Jr. (1990). Treatment of endometrial stromal tumors. *Gynecol Oncol* **36**: 60-5.

Berger, CL, de Bustros, A, Roos, BA, Leong, SS, Mendelsohn, G, Gesell, MS*, et al.* (1984). Human medullary thyroid carcinoma in culture provides a model relating growth dynamics, endocrine cell differentiation, and tumor progression. *J Clin Endocrinol Metab* **59**: 338-43.

Bodner, K, Bodner-Adler, B, Obermair, A, Windbichler, G, Petru, E, Mayerhofer, S*, et al.* (2001). Prognostic parameters in endometrial stromal sarcoma: a clinicopathologic study in 31 patients. *Gynecol Oncol* **81**: 160-5, 10.1006/gyno.2001.6152.

Bongarzone, I, Pierotti, MA, Monzini, N, Mondellini, P, Manenti, G, Donghi, R*, et al.* (1989). High frequency of activation of tyrosine kinase oncogenes in human papillary thyroid carcinoma. *Oncogene* **4**: 1457-62.

Brooks, SE, Zhan, M, Cote, T & Baquet, CR (2004). Surveillance, epidemiology, and end results analysis of 2677 cases of uterine sarcoma 1989-1999. *Gynecol Oncol* **93**: 204-8, 10.1016/j.ygyno.2003.12.029.

Cebrian, A, Lesueur, F, Martin, S, Leyland, J, Ahmed, S, Luccarini, C*, et al.* (2005). Polymorphisms in the initiators of RET (rearranged during transfection) signaling pathway and susceptibility to sporadic medullary thyroid carcinoma. *J Clin Endocrinol Metab* **90**: 6268-74.

Cerrato, A, De Falco, V & Santoro, M (2009). Molecular genetics of medullary thyroid carcinoma: the quest for novel therapeutic targets. *J Mol Endocrinol* **43**: 143-55, 10.1677/JME-09-0024.

Chang, KL, Crabtree, GS, Lim-Tan, SK, Kempson, RL & Hendrickson, MR (1990). Primary uterine endometrial stromal neoplasms. A clinicopathologic study of 117 cases. *Am J Surg Pathol* **14**: 415-38.

Christacos, NC, Quade, BJ, Dal Cin, P & Morton, CC (2006). Uterine leiomyomata with deletions of Ip represent a distinct cytogenetic subgroup associated with unusual histologic features. *Genes Chromosomes Cancer* **45**: 304-12, 10.1002/gcc.20291.

Chu, MC, Mor, G, Lim, C, Zheng, W, Parkash, V & Schwartz, PE (2003). Low-grade endometrial stromal sarcoma: hormonal aspects. *Gynecol Oncol* **90**: 170-6.

Cooley, LD, Elder, FF, Knuth, A & Gagel, RF (1995). Cytogenetic characterization of three human and three rat medullary thyroid carcinoma cell lines. *Cancer Genet Cytogenet* **80**: 138-49.

Cramer, SF, Patel, A (1990). The frequency of uterine leiomyomas. *Am J Clin Pathol* **94**: 435-8.

Cranston, AN, Ponder, BA (2003). Modulation of medullary thyroid carcinoma penetrance suggests the presence of modifier genes in a RET transgenic mouse model. *Cancer Res* **63**: 4777-80.

Dal Cin, P, Aly, MS, De Wever, I, Moerman, P & Van Den Berghe, H (1992). Endometrial stromal sarcoma t(7;17)(p15-21;q12-21) is a nonrandom chromosome change. *Cancer Genet Cytogenet* **63**: 43-6.

Dal Cin, P, Van Den Berghe, H & Brosens, I (1991). Involvement of 6p in an endometrial polyp. *Cancer Genet Cytogenet* **51**: 279-80.

Dinh, TA, Oliva, EA, Fuller, AF,Jr, Lee, H & Goodman, A (2004). The treatment of uterine leiomyosarcoma. Results from a 10-year experience (1990-1999) at the Massachusetts General Hospital. *Gynecol Oncol* **92**: 648-52, 10.1016/j.ygyno.2003.10.044.

Dionigi, A, Oliva, E, Clement, PB & Young, RH (2002). Endometrial stromal nodules and endometrial stromal tumors with limited infiltration: a clinicopathologic study of 50 cases. *Am J Surg Pathol* **26**: 567-81.

Downes, KA, Hart, WR (1997). Bizarre leiomyomas of the uterus: a comprehensive pathologic study of 24 cases with long-term follow-up. *Am J Surg Pathol* **21**: 1261-70.

Drosten, M, Putzer, BM (2006). Mechanisms of Disease: cancer targeting and the impact of oncogenic RET for medullary thyroid carcinoma therapy. *Nat Clin Pract Oncol* **3**: 564-74, 10.1038/ncponc0610.

Dvorakova, S, Vaclavikova, E, Sykorova, V, Vcelak, J, Novak, Z, Duskova, J*, et al.* (2008). Somatic mutations in the RET proto-oncogene in sporadic medullary thyroid carcinomas. *Mol Cell Endocrinol* **284**: 21-7, 10.1016/j.mce.2007.12.016.

Eng, C, Clayton, D, Schuffenecker, I, Lenoir, G, Cote, G, Gagel, RF*, et al.* (1996). The relationship between specific RET proto-oncogene mutations and disease phenotype in multiple endocrine neoplasia type 2. International RET mutation consortium analysis. *JAMA* **276**: 1575-9.

Evans, HL (1982). Endometrial stromal sarcoma and poorly differentiated endometrial sarcoma. *Cancer* **50**: 2170-82.

Fletcher, JA, Morton, CC, Pavelka, K & Lage, JM (1990). Chromosome aberrations in uterine smooth muscle tumors: potential diagnostic relevance of cytogenetic instability. *Cancer Res* **50**: 4092-7.

Frisk, T, Zedenius, J, Lundberg, J, Wallin, G, Kytola, S & Larsson, C (2001). CGH alterations in medullary thyroid carcinomas in relation to the RET M918T mutation and clinical outcome. *Int J Oncol* **18**: 1219-25.

Gattas, GJ, Quade, BJ, Nowak, RA & Morton, CC (1999). HMGIC expression in human adult and fetal tissues and in uterine leiomyomata. *Genes Chromosomes Cancer* **25**: 316-22.

Geigl, JB, Uhrig, S & Speicher, MR (2006). Multiplex-fluorescence in situ hybridization for chromosome karyotyping. *Nat Protoc* **1**: 1172-84.

Giuntoli, RL,2nd, Metzinger, DS, DiMarco, CS, Cha, SS, Sloan, JA, Keeney, GL*, et al.* (2003). Retrospective review of 208 patients with leiomyosarcoma of the uterus: prognostic indicators, surgical management, and adjuvant therapy. *Gynecol Oncol* **89**: 460-9.

Greenberg, MD, Kazamel, TI (1995). Medical and socioeconomic impact of uterine fibroids. *Obstet Gynecol Clin North Am* **22**: 625-36.

Grieco, M, Santoro, M, Berlingieri, MT, Melillo, RM, Donghi, R, Bongarzone, I*, et al.* (1990). PTC is a novel rearranged form of the ret proto-oncogene and is frequently detected in vivo in human thyroid papillary carcinomas. *Cell* **60**: 557-63.

Halbwedl, I, Ullmann, R, Kremser, ML, Man, YG, Isadi-Moud, N, Lax, S*, et al.* (2005). Chromosomal alterations in low-grade endometrial stromal sarcoma and undifferentiated endometrial sarcoma as detected by comparative genomic hybridization. *Gynecol Oncol* **97**: 582-7.

Hemmer, S, Wasenius, VM, Knuutila, S, Franssila, K & Joensuu, H (1999). DNA copy number changes in thyroid carcinoma. *Am J Pathol* **154**: 1539-47.

Herrmann, M (2003). Standard and molecular cytogenetics of endocrine tumors. *Am J Clin Pathol* **119 Suppl**: S17-38.

Hofstra, RM, Landsvater, RM, Ceccherini, I, Stulp, RP, Stelwagen, T, Luo, Y*, et al.* (1994). A mutation in the RET proto-oncogene associated with multiple endocrine neoplasia type 2B and sporadic medullary thyroid carcinoma. *Nature* **367**: 375-6.

Hrynchak, M, Horsman, D, Salski, C, Berean, K & Benedet, JL (1994). Complex karyotypic alterations in an endometrial stromal sarcoma. *Cancer Genet Cytogenet* **77**: 45-9.

Hrzenjak, A, Moinfar, F, Tavassoli, FA, Strohmeier, B, Kremser, ML, Zatloukal, K*, et al.* (2005). JAZF1/JJAZ1 gene fusion in endometrial stromal sarcomas: molecular analysis by reverse transcriptase-polymerase chain reaction optimized for paraffin-embedded tissue. *J Mol Diagn* **7**: 388-95, 10.1016/S1525-1578(10)60568-5.

Hsieh, CH, Lin, H, Huang, CC, Huang, EY, Chang, SY & ChangChien, CC (2003). Leiomyosarcoma of the uterus: a clinicopathologic study of 21 cases. *Acta Obstet Gynecol Scand* **82**: 74-81.

Hu, J, Khanna, V, Jones, M & Surti, U (2001). Genomic alterations in uterine leiomyosarcomas: potential markers for clinical diagnosis and prognosis. *Genes Chromosomes Cancer* **31**: 117-24, 10.1002/gcc.1125.

Iliszko, M, Mandahl, N, Mrozek, K, Denis, A, Pandis, N, Pejovic, T*, et al.* (1998). Cytogenetics of uterine sarcomas: presentation of eight new cases and review of the literature. *Gynecol Oncol* **71**: 172-6.

Kazmierczak, B, Dal Cin, P, Wanschura, S, Bartnitzke, S, Van den Berghe, H & Bullerdiek, J (1998). Cloning and molecular characterization of part of a new gene fused to HMGIC in mesenchymal tumors. *Am J Pathol* **152**: 431-5.

Kim, KR, Jun, SY, Park, IA, Ro, JY & Nam, JH (2005). Endometrial stromal tumor with limited infiltration and probable extrauterine metastasis: report of a case. *Ann Diagn Pathol* **9**: 57-60.

Klotzbucher, M, Wasserfall, A & Fuhrmann, U (1999). Misexpression of wild-type and truncated isoforms of the high-mobility group I proteins HMGI-C and HMGI(Y) in uterine leiomyomas. *Am J Pathol* **155**: 1535-42, 10.1016/S0002-9440(10)65469-7.

Koontz, JI, Soreng, AL, Nucci, M, Kuo, FC, Pauwels, P, van Den Berghe, H*, et al.* (2001). Frequent fusion of the JAZF1 and JJAZ1 genes in endometrial stromal tumors. *Proc Natl Acad Sci U S A* **98**: 6348-53.

Koss, LG, Spiro, RH & Brunschwig, A (1965). Endometrial Stromal Sarcoma. *Surg Gynecol Obstet* **121**: 531-7.

Kroll, TG, Sarraf, P, Pecciarini, L, Chen, CJ, Mueller, E, Spiegelman, BM*, et al.* (2000). PAX8-PPARgamma1 fusion oncogene in human thyroid carcinoma [corrected]. *Science* **289**: 1357-60.

Kurihara, S, Oda, Y, Ohishi, Y, Iwasa, A, Takahira, T, Kaneki, E*, et al.* (2008). Endometrial stromal sarcomas and related high-grade sarcomas: immunohistochemical and molecular genetic study of 31 cases. *Am J Surg Pathol* **32**: 1228-38.

Laxman, R, Currie, JL, Kurman, RJ, Dudzinski, M & Griffin, CA (1993). Cytogenetic profile of uterine sarcomas. *Cancer* **71**: 1283-8.

Lenhard, SM, Untch, M, Himsl, I, Ditsch, N, Bittmann, I, Friese, K*, et al.* (2006). The high-grade endometrial sarcoma: a rare entity. *Arch Gynecol Obstet* **274**: 56-9, 10.1007/s00404-005-0100-4.

Leong, S., Horoszewicz, J.S., Shimaoka, K., Friedman, M., Kawinski, E., Song, M.J.*, et al.* (1981). A new cell line for study of human medullary thyroid carcinoma. In: Anonymous *Andreoli M, Monaco M, Robbins J (eds). Advances in Thyroid Neoplasia.* Rome: Field Educational Italia, pp 95-108.

Ligon, AH, Morton, CC (2001). Leiomyomata: heritability and cytogenetic studies. *Hum Reprod Update* **7**: 8-14.

Manie, S, Santoro, M, Fusco, A & Billaud, M (2001). The RET receptor: function in development and dysfunction in congenital malformation. *Trends Genet* **17**: 580-9.

Marsh, DJ, Theodosopoulos, G, Martin-Schulte, K, Richardson, AL, Philips, J, Roher, HD*, et al.* (2003). Genome-wide copy number imbalances identified in familial and sporadic medullary thyroid carcinoma. *J Clin Endocrinol Metab* **88**: 1866-72.

Mashal, RD, Fejzo, ML, Friedman, AJ, Mitchner, N, Nowak, RA, Rein, MS*, et al.* (1994). Analysis of androgen receptor DNA reveals the independent clonal origins of uterine leiomyomata and the secondary nature of cytogenetic aberrations in the development of leiomyomata. *Genes Chromosomes Cancer* **11**: 1-6.

Mayerhofer, K, Obermair, A, Windbichler, G, Petru, E, Kaider, A, Hefler, L*, et al.* (1999). Leiomyosarcoma of the uterus: a clinicopathologic multicenter study of 71 cases. *Gynecol Oncol* **74**: 196-201, 10.1006/gyno.1999.5436.

Messina, M, Robinson, BG (2007). Technology insight: gene therapy and its potential role in the treatment of medullary thyroid carcinoma. *Nat Clin Pract Endocrinol Metab* **3**: 290-301, 10.1038/ncpendmet0420.

Meyerson, M, Gabriel, S & Getz, G (2010). Advances in understanding cancer genomes through second-generation sequencing. *Nat Rev Genet* **11**: 685-96, 10.1038/nrg2841.

Micci, F, Panagopoulos, I, Bjerkehagen, B & Heim, S (2006). Consistent rearrangement of chromosomal band 6p21 with generation of fusion genes JAZF1/PHF1 and EPC1/PHF1 in endometrial stromal sarcoma. *Cancer Res* **66**: 107-12, 10.1158/0008-5472.CAN-05-2485.

Micci, F, Teixeira, MR, Haugom, L, Kristensen, G, Abeler, VM & Heim, S (2004). Genomic aberrations in carcinomas of the uterine corpus. *Genes Chromosomes Cancer* **40**: 229-46, 10.1002/gcc.20038.

Milatovich, A, Heerema, NA & Palmer, CG (1990). Cytogenetic studies of endometrial malignancies. *Cancer Genet Cytogenet* **46**: 41-53.

Mittal, KR, Chen, F, Wei, JJ, Rijhvani, K, Kurvathi, R, Streck, D*, et al.* (2009). Molecular and immunohistochemical evidence for the origin of uterine leiomyosarcomas from associated leiomyoma and symplastic leiomyoma-like areas. *Mod Pathol* **22**: 1303-11, 10.1038/modpathol.2009.96.

Moinfar, F, Azodi, M & Tavassoli, FA (2007). Uterine sarcomas. *Pathology* **39**: 55-71.

Morisi, R, Celano, M, Tosi, E, Schenone, S, Navarra, M, Ferretti, E*, et al.* (2007). Growth inhibition of medullary thyroid carcinoma cells by pyrazolo-pyrimidine derivates. *J Endocrinol Invest* **30**: RC31-4.

Mulligan, LM, Kwok, JB, Healey, CS, Elsdon, MJ, Eng, C, Gardner, E*, et al.* (1993). Germ-line mutations of the RET proto-oncogene in multiple endocrine neoplasia type 2A. *Nature* **363**: 458-60, 10.1038/363458a0.

Norris, HJ, Taylor, HB (1966). Mesenchymal tumors of the uterus. I. A clinical and pathological study of 53 endometrial stromal tumors. *Cancer* **19**: 755-66.

Packenham, JP, du Manoir, S, Schrock, E, Risinger, JI, Dixon, D, Denz, DN*, et al.* (1997). Analysis of genetic alterations in uterine leiomyomas and leiomyosarcomas by comparative genomic hybridization. *Mol Carcinog* **19**: 273-9.

Pandis, N, Heim, S, Bardi, G, Floderus, UM, Willen, H, Mandahl, N*, et al.* (1991). Chromosome analysis of 96 uterine leiomyomas. *Cancer Genet Cytogenet* **55**: 11-8.

Pfragner, R., Behmel, A., Ingolic, E. & Wirnsberger, H. (2004). Culture of human neuroendocrine tumor cells, R Pfragner & RI Freshney (eds.). In: Anonymous *Culture of Specialized Cells* Hoboken: J Wiley & Sons, pp 373-403.

Pfragner, R, Wirnsberger, G, Behmel, A, Wolf, G, Passath, A, Ingolic, E*, et al.* (1993). New continuous cell line from human medullary thyroid carcinoma: SINJ. Phenotypic analysis and *in vivo* carcinogenesis. *Int J Oncol* **2**: 831-6.

Pfragner, R, Hofler, H, Behmel, A, Ingolic, E & Walser, V (1990). Establishment and characterization of continuous cell line MTC-SK derived from a human medullary thyroid carcinoma. *Cancer Res* **50**: 4160-6.

Pfragner, R, Wirnsberger, GH, Ingolic, E & Niederle, B (2002). Medullary thyroid carcinomas in cell culture--models for future therapies. *Wien Klin Wochenschr* **114**: 279-83.

Pierotti, MA, Santoro, M, Jenkins, RB, Sozzi, G, Bongarzone, I, Grieco, M*, et al.* (1992). Characterization of an inversion on the long arm of chromosome 10 juxtaposing D10S170 and RET and creating the oncogenic sequence RET/PTC. *Proc Natl Acad Sci U S A* **89**: 1616-20.

Pinkel, D, Albertson, DG (2005). Array comparative genomic hybridization and its applications in cancer. *Nat Genet* **37 Suppl**: S11-7, 10.1038/ng1569.

Ponder, BA (1999). The phenotypes associated with ret mutations in the multiple endocrine neoplasia type 2 syndrome. *Cancer Res* **59**: 1736s,1741s; discussion 1742s.

Quade, BJ, Pinto, AP, Howard, DR, Peters, WA,3rd & Crum, CP (1999). Frequent loss of heterozygosity for chromosome 10 in uterine leiomyosarcoma in contrast to leiomyoma. *Am J Pathol* **154**: 945-50, 10.1016/S0002-9440(10)65342-4.

Reich, O, Regauer, S (2007). Hormonal therapy of endometrial stromal sarcoma. *Curr Opin Oncol* **19**: 347-52, 10.1097/CCO.0b013e3281a7ef3a.

Rein, MS, Friedman, AJ, Barbieri, RL, Pavelka, K, Fletcher, JA & Morton, CC (1991). Cytogenetic abnormalities in uterine leiomyomata. *Obstet Gynecol* **77**: 923-6.

Romei, C, Elisei, R, Pinchera, A, Ceccherini, I, Molinaro, E, Mancusi, F*, et al.* (1996). Somatic mutations of the ret protooncogene in sporadic medullary thyroid carcinoma are not restricted to exon 16 and are associated with tumor recurrence. *J Clin Endocrinol Metab* **81**: 1619-22.

Sandberg, AA (2007). The cytogenetics and molecular biology of endometrial stromal sarcoma. *Cytogenet Genome Res* **118**: 182-9, 10.1159/000108299.

Sandberg, AA (2005a). Updates on the cytogenetics and molecular genetics of bone and soft tissue tumors: leiomyoma. *Cancer Genet Cytogenet* **158**: 1-26, 10.1016/j.cancergencyto.2004.08.025.

Sandberg, AA (2005b). Updates on the cytogenetics and molecular genetics of bone and soft tissue tumors: leiomyosarcoma. *Cancer Genet Cytogenet* **161**: 1-19.

Santarpia, L, Ye, L & Gagel, RF (2009). Beyond RET: potential therapeutic approaches for advanced and metastatic medullary thyroid carcinoma. *J Intern Med* **266**: 99-113.

Santoro, M, Carlomagno, F, Romano, A, Bottaro, DP, Dathan, NA, Grieco, M*, et al.* (1995). Activation of RET as a dominant transforming gene by germline mutations of MEN2A and MEN2B. *Science* **267**: 381-3.

Scappaticci, S, Arrigoni, G, Capra, E, Maraschio, P & Fraccaro, M (1992). Cytogenetics of multiple endocrine neoplasia syndromes. I. Two different, unique clonal chromosome

changes in a medullary thyroid carcinoma and in a C-cell thyroid hyperplasia. *Cancer Genet Cytogenet* **59**: 51-3.

Schlumberger, M, Carlomagno, F, Baudin, E, Bidart, JM & Santoro, M (2008). New therapeutic approaches to treat medullary thyroid carcinoma. *Nat Clin Pract Endocrinol Metab* **4**: 22-32, 10.1038/ncpendmet0717.

Schoenmakers, EF, Wanschura, S, Mols, R, Bullerdiek, J, Van den Berghe, H & Van de Ven, WJ (1995). Recurrent rearrangements in the high mobility group protein gene, HMGI-C, in benign mesenchymal tumours. *Nat Genet* **10**: 436-44, 10.1038/ng0895-436.

Solomon, LA, Schimp, VL, Ali-Fehmi, R, Diamond, MP & Munkarah, AR (2005). Clinical update of smooth muscle tumors of the uterus. *J Minim Invasive Gynecol* **12**: 401-8, 10.1016/j.jmig.2005.05.022.

Sreekantaiah, C, Davis, JR & Sandberg, AA (1993). Chromosomal abnormalities in leiomyosarcomas. *Am J Pathol* **142**: 293-305.

Sung, CO, Ahn, G, Song, SY, Choi, YL & Bae, DS (2009). Atypical leiomyomas of the uterus with long-term follow-up after myomectomy with immunohistochemical analysis for p16INK4A, p53, Ki-67, estrogen receptors, and progesterone receptors. *Int J Gynecol Pathol* **28**: 529-34, 10.1097/PGP.0b013e3181a2b8d3.

Suzuki, A, Fukushige, S, Nagase, S, Ohuchi, N, Satomi, S & Horii, A (1997). Frequent gains on chromosome arms 1q and/or 8q in human endometrial cancer. *Hum Genet* **100**: 629-36.

Takeda, A, Imoto, S, Mori, M & Nakamura, H (2011). Successful pregnancy outcome after laparoscopic-assisted excision of a bizarre leiomyoma: a case report. *J Med Case Rep* **5**: 344, 10.1186/1752-1947-5-344.

Toledo, G, Oliva, E (2008). Smooth muscle tumors of the uterus: a practical approach. *Arch Pathol Lab Med* **132**: 595-605, 2.

van Beers, EH, Joosse, SA, Ligtenberg, MJ, Fles, R, Hogervorst, FB, Verhoef, S, *et al.* (2006). A multiplex PCR predictor for aCGH success of FFPE samples. *Br J Cancer* **94**: 333-7.

van Veelen, W, van Gasteren, CJ, Acton, DS, Franklin, DS, Berger, R, Lips, CJ*, et al.* (2008). Synergistic effect of oncogenic RET and loss of p18 on medullary thyroid carcinoma development. *Cancer Res* **68**: 1329-37, 10.1158/0008-5472.CAN-07-5754.

Vanharanta, S, Wortham, NC, Laiho, P, Sjoberg, J, Aittomaki, K, Arola, J*, et al.* (2005). 7q deletion mapping and expression profiling in uterine fibroids. *Oncogene* **24**: 6545-54.

Vanharanta, S, Wortham, NC, Langford, C, El-Bahrawy, M, van der Spuy, Z, Sjoberg, J*, et al.* (2007). Definition of a minimal region of deletion of chromosome 7 in uterine leiomyomas by tiling-path microarray-CGH and mutation analysis of known genes in this region. *Genes Chromosomes Cancer* **46**: 451-8.

Wang, R, Titley, JC, Lu, YJ, Summersgill, BM, Bridge, JA, Fisher, C*, et al.* (2003). Loss of 13q14-q21 and gain of 5p14-pter in the progression of leiomyosarcoma. *Mod Pathol* **16**: 778-85, 10.1097/01.MP.0000083648.45923.2B.

Wang, Z, Gerstein, M & Snyder, M (2009). RNA-Seq: a revolutionary tool for transcriptomics. *Nat Rev Genet* **10**: 57-63, 10.1038/nrg2484.

Weitmann, HD, Knocke, TH, Kucera, H & Potter, R (2001). Radiation therapy in the treatment of endometrial stromal sarcoma. *Int J Radiat Oncol Biol Phys* **49**: 739-48.

Wurster-Hill, DH, Noll, WW, Bircher, LY, Pettengill, OS & Grizzle, WA (1986). Cytogenetics of medullary carcinoma of the thyroid. *Cancer Genet Cytogenet* **20**: 247-53.

Ye, L, Santarpia, L, Cote, GJ, El-Naggar, AK & Gagel, RF (2008). High resolution array-comparative genomic hybridization profiling reveals deoxyribonucleic acid copy number alterations associated with medullary thyroid carcinoma. *J Clin Endocrinol Metab* **93**: 4367-72.

Zedenius, J, Wallin, G, Hamberger, B, Nordenskjold, M, Weber, G & Larsson, C (1994). Somatic and MEN 2A de novo mutations identified in the RET proto-oncogene by screening of sporadic MTC:s. *Hum Mol Genet* **3**: 1259-62.